The Intrinsic Network Architecture of the Aging Brain:

How does it relate to Cognition and Behavior?

Thesis (cumulative thesis)

presented to the Faculty of Arts and Social Sciences

of the University of Zurich

for the degree of Doctor of Philosophy

by

Angela Martina Müller

Accepted in the spring semester 2016
on the recommendation of the doctoral committee:
Prof. Dr. rer. Nat. Lutz Jäncke (main advisor)
Prof. Dr. Klaus Oberauer

Zurich, 2016

Acknowledgements

First and foremost, I would like to express my deepest gratitude to Prof. Dr. Lutz Jäncke for his trust, his unique mixture of challenge, enthusiasm and encouragement that motivated me to give my very best and to expand my knowledge and expertise with every new project. Thank you for providing me an environment in which I had the opportunity to follow my ideas but also for giving scientific support in several challenging situations during my Ph.D. At this point, I would also like to thank Professor Klaus Oberauer for his support and co-examination of my dissertation. I will not forget your help and encouragement in the one situation during my dissertation where the whole project really seemed in danger.

Furthermore, I would like to express my thanks to Dr. Susan Mérillat. I am very grateful for your trust, encouraging guidance, support and helpful advice during the three years of my PhD. Thank you for many fruitful discussions and the improvement of my manuscripts.

Further, I would like to thank all my colleagues from the International Normal Aging and Plasticity Imaging Center (INAPIC) and the University Research Priority Program “Dynamics of Healthy Aging” for their friendship, encouraging support, scientific inputs and especially for many happy coffee breaks filled with laugher and many stimulating conversations about everything else but research. Such short digressions into the world of trivia are sometimes the best way to get the head free and ready again for highly focused and efficient scientific work.

Last but not least, I want to thank my family for their tremendous support and love during all my life but especially during these last three years – without your love, encouragement and trust in my abilities, I could not have done it. Thank you with all my heart! Specially warm thanks to my sister – you were so generous with your time, concrete help, and moral support whenever I needed it. You were always here for me as well as believing in me even in my most pusillanimous moments when I was at the brink of giving up.

Summary

Age seems inevitably to be accompanied not only by changes in brain structure and neural functions but also by changes in cognitive performance. However, there exists a huge heterogeneity of how individual brains age. Some older adults seem to be spared from the deleterious effects of age for a long time, while other seem to be earlier and more seriously affected.

Understanding the causes of the different individual aging trajectories and especially understanding the factors that might promote healthy or normal aging and thereby guarantee individual autonomy and wellbeing up into very old age are essential as the proportion of older adults in the population is increasing worldwide.

In this context, one of the most intriguing findings of MRI studies investigating the complex relationship between cognition and brain structure and function is how often one is able to observe still preserved normal cognitive functioning despite clearly manifest structural damage. A possible explanation for this discrepancy between already manifest serious structural damage and seemingly still preserved cognitive functioning could be that the aging brain might possesses functional compensation mechanisms that allow it to maintain cognitive functioning despite structural degeneration.

For some time now, the question whether the aging brain does actually possess functional resources and reserves that enable it to counteract age-related structural decline and other age-related pathological mechanisms is in the center of interest of fMRI studies investigating the brain function-cognition relationship in old adults. Understanding the aging brain's preserved functional plasticity as well as the mechanisms that finally cause the shift from successful compensation to functional dedifferentiation is crucial in order to find interventions that might delay the onset of age-related cognitive decline.

For all three studies presented in the context of this doctoral thesis, the same set of task-free fMRI data from a large cross-sectional sample of 186 older adults (mean age = 70.4, 97 female) was used. The MRI and behavioral data came from the first data acquisition time-point of the Longitudinal Healthy Aging Brain (LHAB) database. The LHAB is a longitudinal database project, which started at the International Normal Aging and Plasticity Imaging Center (INAPIC) of the University of Zurich in 2011 and is currently run at the University Priority Project "Dynamics of Healthy Aging".

First Study

A major contribution to our understanding of the aging brain either comes from studies comparing young with older adults or from studies investigating pathological aging and using the healthy aging older adults as control group. In consequence, we know relatively well, what distinguishes young from old brains or pathological from healthy aging but that does not mean that we really understand the structural and functional transformations characterizing the healthy aging brain. The aim of the first study was therefore to elucidate age-related changes in the intrinsically active functional architecture of the brain in our study group covering an age range from 65 to 85 years. In a first step, we conducted an intrinsic connectivity contrast analysis (ICC) in order to detect the brain regions whose degree of connectedness was significantly correlated with increasing age. Secondly, using connectivity analyses we investigated how the clusters highlighted by the ICC analysis functionally related to the other major resting-state networks. The most important finding was the right anterior insula's loss of connectedness in the older participants of the study group because of the region's causal role in the switching from the task-negative to the task-positive state of the brain. Further, we found a higher functional dedifferentiation of two of the brain's major intrinsic connectivity networks, the default mode network and the cingulo-opercular network, caused by a reduction of functional connection strength, especially in the frontal regions. At last, we showed that all these age-related changes have the potential to impair older adults' performance of working memory tasks.

Second Study

The aim of the second study was to get a better understanding of how this functional baseline configuration of the aging brain may affect cognitive performance, especially the performance of verbal fluency. The successful performance of verbal fluency tasks not only requires the combination of two fundamental cognitive functions, executive-control and language, but the two cognitive functions have also quite different trajectories across the life span. While the perception and production of language are relatively well preserved far into very old age, executive functions are known to suffer from age-related decline earlier in the process. The combination of these two cognitive functions makes verbal fluency, i.e. the ability to fluently produce speech while following some production constraints, ideal to gain a better understanding of the mechanisms that allow the aging brain to perform still at a high level but in a different manner from the young brain. To this end, we computed initially an ICC for the purpose of evaluating the brain regions whose degree of connectedness was significantly correlated with fluency performance. Secondly, using connectivity analyses we investigated how the clusters from the ICC functionally related to the other major resting-state networks. Apart from the importance of intact fronto-parietal long-range connections, the preserved capacity of the default mode network for a finely attuned interaction with the executive-control network and the language network seemed to be crucial for successful verbal fluency

performance in older people. We provided further evidence that the right frontal regions might be more prominently affected by age-related decline.

Third Study

Although differences in fMRI activation patterns between young and old adults have been repeatedly observed, the meaning of such differences remains an open question, with interpretations ranging from them being successful compensation mechanisms to indicators of age-related functional degradation. We speculate that the aging brain's intrinsic network architecture might, at least in part, shape its capacity to compensate for age-related constraints. The aim of the third study was therefore to investigate the functional baseline configuration of the LHAB sample using graph theoretical analyses in order to evaluate the brain's intrinsic potential to compensate for functional and structural reductions occurring with age. We found a clear anterior-posterior dichotomy, with nodes in the posterior part of the brain showing more age-related loss of functional flexibility than nodes in the anterior regions. Additionally, we found an age-related hemispheric asymmetry of the brain's capacity to potentially compensate for functional degradation. Compared to the right hemisphere and especially to the right frontal cortex, the left-sided counterparts might have preserved a higher capacity to compensate for age-related functional degradation. Finally, we found that the cerebellum and subcortical regions, especially the thalamus and the caudate nucleus, exhibit indicators for functional disintegration and dedifferentiation as early as in the intrinsically active baseline configuration.

Zusammenfassung

Altern ist unausweichlich mit strukturellen wie auch funktionellen Veränderungen im Gehirn verbunden, die früher oder später auch zu altersbedingten Veränderungen der kognitiven Leistungsfähigkeit führen. Allerdings ist die Bandbreite gross, innerhalb derer die Alterungsprozesse des Gehirns verlaufen können. So scheinen einige Menschen über lange Zeit von unangenehmen und beeinträchtigenden Folgen des Älterwerdens gleichsam verschont zu bleiben, während andere früher und stärker von altersbedingtem körperlichen und kognitiven Abbau betroffen sind.

Angesichts der Tatsache, dass der Anteil der Betagten und Hochbetagten in der Gesamtbevölkerung stetig zunimmt, ist es von entscheidender Bedeutung, dass möglichst viele ältere Menschen ihr körperliches und seelischen Wohlbefinden, wie auch ihre persönliche Autonomie bis ins hohe Alter bewahren können. Um dafür die Grundlagen zu schaffen, es notwendig, nicht nur die Faktoren zu verstehen, die überhaupt erst zu dieser Heterogenität an Alterungsprozessen führen, sondern auch diejenigen Einflussfaktoren zu identifizieren, die einen möglichst gesunden Alterungsverlauf unterstützen.

In diesem Zusammenhang sind die Befunde von Studien, die Magnetresonanztomographie zur Erforschung der komplexen Zusammenhänge von Struktur und Funktion im alternden Gehirn einsetzen, von besonderem Interesse. Oft finden solche Studien nämlich, dass ältere Menschen trotz deutlich erkennbaren Schädigungen der grauen und weissen Gehirnsubstanz weiterhin eine hohe kognitive Leistungsfähigkeit aufrechterhalten können. Eine mögliche Erklärung für den Widerspruch, dass offensichtliche strukturelle Abbauerscheinungen des Gehirns nicht immer auch mit einer schleichenden Verschlechterung der kognitiven Leistungsfähigkeit verbunden sein müssen, könnte sein, dass das alternde Gehirn noch immer genügend funktionelle Ressourcen besitzt, die es ihm ermöglichen strukturellen Defizite zu kompensieren.

Die Frage, ob das alternde Gehirn tatsächlich noch immer ein so grosses Ausmass an funktioneller Plastizität besitzt, dass es den Folgen von strukturellem Abbau und anderen altersbedingten pathologischen Verläufen über lange Zeit unter Einsatz dieser funktionellen Ressourcen erfolgreich entgegenwirken kann, steht seit einiger Zeit im Fokus des Interesses von Studien, die mit Hilfe von funktioneller Magnetresonanztomographie das komplexe Zusammenspiel von Gehirnfunktion und kognitiver Leistungsfähigkeit im alternden Gehirn untersuchen. Für die Entwicklung erfolgreicher Interventionen, mit deren Hilfe es in Zukunft möglich sein soll, das Auftreten von kognitivem Abbau hinauszuzögern, sind zwei Voraussetzungen zu erfüllen. Nicht nur müssen die Mechanismen genau untersucht und verstanden werden, welche die Grundlage für die funktionelle Plastizität des alternden Gehirns bilden, sondern auch die Prozesse, die letztlich dazu führen, dass aus einst erfolgreichen

Kompensationsmechanismen des alternden Gehirns mit der Zeit Mechanismen werden, die von altersbedingter Dedifferenzierung der funktionalen Netzwerke des Gehirns zeugen.

Für alle drei empirische Studien, die im Kontext dieser Doktorarbeit vorgestellt werden, wurden die fMRT Daten und Verhaltensdaten einer grossen Stichprobe von 186 Erwachsenen im Übergang von Pensionsalter (65 Jahre) ins hohe Alter (85 Jahre und älter) in einem Querschnittsdesign untersucht (Durchschnittalter = 70.4; 97 Frauen, 89 Männer). Alle hier analysierten Daten wurden im Rahmen der ersten Datenerhebungswelle des Longitudinal Healthy Aging Brain (LHAB) Datenbank Projektes erhoben. Das LHAB Projekt startete 2011 unter der Ägide des International Normal Aging and Plasticity Imaging Center (INAPIC) der Universität Zürich und läuft derzeit unter dem Dach des Universitären Schwerpunktes "Dynamik des Gesunden Alterns."

Studie 1

Unser Wissen über das alternde Gehirn ist vor allem von zwei Forschungsbereichen geprägt. In der einen Forschungsrichtung steht das Verstehen pathologischer Alterungsverläufe im Fokus der Bemühungen. Folgerichtig ist das Augenmerk der Forschenden vor allem auf die Patienten gerichtet. Die Kontrollgruppe der gesund alternden Erwachsenen dient primär dem Zweck, pathologisches Altern klar von normalem Altern abzugrenzen, aber nicht dazu, zu untersuchen, was einen normalen Alterungsprozess eigentlich kennzeichnet. Die Erforschung des gesunden Alterungsprozesses steht zwar im Mittelpunkt des Interesses der anderen Forschungsrichtung. Die Mehrheit der in diesem Bereich durchgeführten Studien sind allerdings noch immer Querschnittsstudien, in denen junge mit alten Erwachsenen verglichen werden. Solche Studiendesigns sind zwar geeignet die Unterschiede zwischen Jung und Alt aufzeigen, nicht aber die alterungsspezifischen Veränderung über die Zeit zu erforschen. Aus diesen Besonderheiten der jeweiligen Forschungsdesigns folgt, dass wir derzeit zwar besser verstehen, welche Prozesse pathologisches Altern verursachen, oder worin sich ein altes Gehirn in seiner Funktionsweise von einem jungen Gehirn unterscheidet. Jedoch wissen wir noch immer sehr wenig darüber, was eigentlich ein gesund alterndes Gehirn kennzeichnet, d.h. wie es sich reorganisiert, um die strukturellen und funktionellen Veränderungen, denen es im Verlauf des Alterungsprozesses unweigerlich unterworfen ist, so gut und so lange als möglich auffangen zu können. Ziel der ersten Studie war es darum, in der LHAB Stichprobe allfällige altersbedingte Veränderungen der intrinsisch aktiven funktionalen Netzwerkarchitektur des Gehirns aufzudecken und mögliche Auswirkungen auf die kognitive Leistungsfähigkeit zu verstehen. Um die Gehirnregionen zu bestimmen, die in der LHAB Stichprobe mit ansteigendem Alter von einem zunehmenden Abbau von funktionellen Verbindungen betroffen waren, führten wir zuerst eine rein datengestützte und explorative *Intrinsic Connectivity Contrast* (ICC) Analyse durch. In einem zweiten Schritt versuchten wir mit Hilfe einer Konnektivitätsanalyse auszuleuchten, in welcher Beziehung die Gehirnregionen, die gemässe der Befunde der ICC Analyse bereits von einem altersbedingten Abbau der funktionellen Verbindungen

betroffen waren, zu der intrinsischen Netzwerkstruktur des Gehirns stehen. Der wichtigste Befund dieser ersten Studie war, dass die rechte anteriore Insel von einem altersbedingten Abbau ihrer funktionellen Verbindungen betroffen zu sein schien. Dieser Befund ist darum so wichtig, weil die rechte anteriore Insel nicht nur eine zentrale, sondern auch kausale Rolle spielt, wenn das Gehirn vom reflexiven Modus der nach innen fokussierten Aufmerksamkeit in den aktiven Modus der nach aussen fokussierten Aufmerksamkeit wechseln muss. Weiter stellten wir fest, dass zwei der wichtigsten intrinsischen Netzwerke des Gehirns, das Default Mode Netzwerk und das cingulo-operculäre Netzwerk Anzeichen für funktionelle Ineffizienz zeigten, die durch eine qualitative Abnahme der funktionellen Verbindungsstärken, insbesondere im Frontalkortex, verursacht wurde. Die in dieser ersten Studie gefundenen Veränderungen an der intrinsischen Netzwerkarchitektur könnten unter anderem mitverantwortlich dafür sein, dass die Leistung des Arbeitsgedächtnisses im Alter oft beeinträchtigt ist.

Studie 2

Ziel der zweiten Studie war es, besser zu verstehen, in welchem Mass erhaltene kognitive Leistungsfähigkeit von der intrinsisch aktiven funktionalen Netzwerkarchitektur des alternden Gehirns abhängig ist. Für diese Studie wurde kognitive Leistungsfähigkeit mit der Leistung der LHAB Probanden in Wortflüssigkeitstests operationalisiert. Wortflüssigkeit ist die Fähigkeit unter Einhaltung bestimmter Regeln fliessend Wörter zu produzieren und setzt die Kombination zweier komplexer kognitiven Fähigkeiten voraus: Sprache und exekutive Kontrolle. Diese beiden Funktionen haben über die Lebensspanne verschiedene Entwicklungsverläufe. Während Sprachverstehen und -produktion bis ins hohe Alter recht gut erhalten bleiben, zeigen sich in den exekutiven Funktionen schon relativ früh altersbedingte Einbussen. Da sie die erfolgreiche Kombination dieser beiden kognitiven Fähigkeit voraussetzt, eignet sich Wortflüssigkeit ideal dazu, zu untersuchen, wie das alternde Gehirn dank funktioneller Reorganisation seine Leistungsfähigkeit aufrechterhalten kann. In einem ersten Schritt führten wir wieder eine ICC Analyse durch, dieses Mal mit dem Ziel, die Regionen zu finden, deren Grad an funktioneller Vernetztheit mit erfolgreichem Abschneiden in einem semantischen und phonetischen Wortflüssigkeitstest korreliert war. In einem zweiten Schritt bestimmten wir dann mit Hilfe einer Konnektivitätsanalyse, in welcher Beziehung die von der ICC Analyse als wichtig für Wortflüssigkeit hervorgehoben Regionen zu der intrinsisch aktiven Gesamtnetzwerkstruktur des Gehirns stehen. Der Hauptbefund der zweiten Studie war, dass das komplexe und fein aufeinander abgestimmte Zusammenspiel von Aktivierung und Deaktivierung von drei der wichtigsten intrinsischen Netzwerke, des Default Mode Netzwerks, des Sprachnetzwerks und des exekutiven Kontrollnetzwerkes, im alternden Gehirn erhalten sein muss, um weiterhin eine gute Leistung in semantischer wie auch phonetischer Wortflüssigkeit zu garantieren. Weiter fanden wir Hinweise, dass der Frontalkortex im Vergleich zu posterior gelegenen Hirnregionen von einem höheren Abbau an funktioneller Vernetztheit betroffen zu sein scheint.

Studie 3

Funktionelle MRT Studien, welche die Aktivierungsmuster des Gehirns untersuchten, während die Teilnehmer im Scanner verschiedene kognitive Aufgaben lösten, haben wiederholt gezeigt, dass sich die Aktivierungsmuster älterer Probanden auch dann noch deutlich von jenen der jungen Probanden unterschieden, wenn beide Altersgruppen keine Unterschiede in ihren kognitiven Leistungen aufwiesen. Wie diese unterschiedlichen Aktivierungsmuster zu interpretieren sind, ist bis heute noch immer umstritten. Während einige darin den klaren Beweis sehen, dass das alte Gehirn zu funktioneller Kompensation struktureller Defizite fähig ist, interpretieren andere diese Muster als Hinweis auf eine mit dem Alter zunehmende funktionelle Dedifferenzierung des Gehirns. Man kann argumentieren, dass bei der Interpretation solcher Aktivierungsmuster auch die intrinsisch aktive funktionale Netzwerkarchitektur des Gehirns miteinbezogen werden sollte, denn diese bildet das eigentliche funktionelle Fundament aller Gehirnaktivität und dürfte somit die Fähigkeit des alternden Gehirns zu Kompensationsleistungen bis zu einem gewissen Grad mitbeeinflussen. Ziel der dritten Studie war es deshalb, mit Hilfe von Methoden aus der *Graph Theoretical Analysis* die funktionelle Netzwerkorganisation der LHAB Stichprobe zu beschreiben und auf ihr intrinsisch vorhandenes Potenzial für Kompensationsmechanismen zu untersuchen. Wir fanden eine anterior-posteriore Dichotomie, was das intrinsische Potenzial des Gehirns zu Kompensationsmassnamen anbelangt, denn die posterior gelegenen Gehirnregionen waren deutlich stärker von altersbedingtem Verlust funktioneller Flexibilität betroffen als die Regionen im Frontalkortex. Auch die beiden Hemisphären zeigten verschiedenes intrinsisches Potenzial für eventuelle Kompensation struktureller Defizite. Im Vergleich zur rechten Hemisphäre und insbesondere des rechten Frontalkortex, zeigten die linke Hemisphäre und der linke Frontalkortex ein höheres intrinsisches Potenzial für funktionelle Kompensationsleistungen. Ausserdem konnten wir zeigen, dass von allen Gehirnregionen das Kleinhirn, aber auch subkortikale Regionen wie Thalamus und Basalganglien, die deutlichsten Anzeichen von beginnender funktioneller Desintegration im intrinsisch aktiven Grundzustand des Gehirns zeigen.

Table of Contents

1 Introduction

Age inevitably seems to be accompanied by changes in brain structure and neural functions and - as a result thereof - also by changes in cognitive performance (Steffener, Barulli, Habeck & Stern, 2015). Nevertheless, there exists a huge heterogeneity of how individual brains age. Some older adults seem to be spared from the deleterious effects of age for a long time, while other seem to be earlier and more seriously affected than most of the persons the same age. In the latter case, one of the crucial questions to be answered by the researchers investigating the aging brain becomes apparent: Does there exists a form of purely age-related process of neural and cognitive decline that can be separated from pathological neurodegenerative processes, whose prevalence increases in older populations? Or is the process always the same and the only difference between seemingly healthy aging and pathological aging is the impact and the pace by which the different age-related changes follow each other (Jagust, 2013; Fjell, McEvoy, Holland, Dale, & Walhovd, 2013)?

Understanding the causes of the different individual aging trajectories and especially understanding the factors that might promote healthy aging and thereby guarantee individual autonomy and wellbeing up into very old age are essential as the proportion of older adults in the population is increasing worldwide. This development will even be aggravated as the birth rate will globally decrease while the life expectancy will further increase during the next twenty years (United Nations, 2013). However, the challenge of understanding the causes underlying the heterogeneity of individual brain aging is enormous, because there are so many influences and dimensions (for illustration, please see the figure underneath from Reuter-Lorenz & Park, 2014), which all have to be simultaneously considered by whom who are trying to comprehend the differences between healthy, normal and pathological aging.

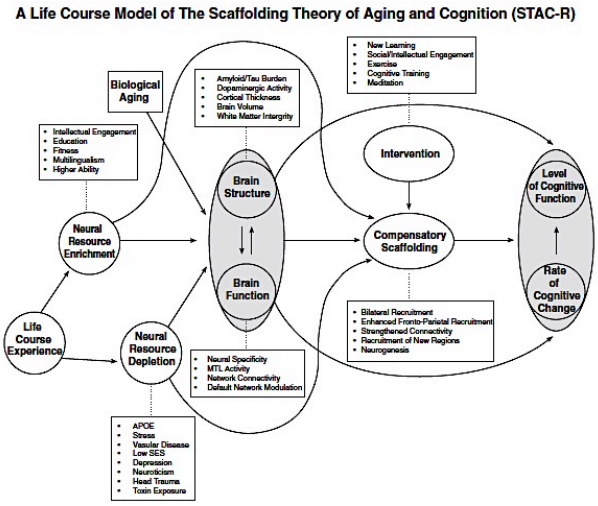

Figure 1.1. Modified from Reuter-Lorenz & Park, 2014

One of the rather counter-intuitive aspects in this context is that preserved cognitive functioning does not unalterably depend on preserved structural integrity (Chételat et al., 2013; Sonnen et al., 2011). Some individuals appear to be not at all affected by the detrimental consequences of age-related structural damage and increasing histopathology on cognition for a long time and the reasons for this cognitive resiliency are still not understood. One possible explanation for this discrepancy between brain structure and cognition could be that even the old brain might still possess functional plasticity so that it is able to compensate for structural deterioration over some time.

For some time now, the question whether the aging brain does indeed possess functional resources and reserves that enable it to counteract age-related structural decline and other age-related pathological mechanisms is in the center of interest of fMRI studies investigating the brain function-cognition relationship in old adults. Understanding the aging brain's preserved functional plasticity as well as the mechanisms that finally cause the shift from successful compensation to functional dedifferentiation is of outmost importance in order to find interventions that might delay the onset of age-related cognitive decline.

In the first section of the next part of the doctoral thesis presented here, a critical review of the findings from task-induced fMRI studies investigating the aging brain and its capacity for compensation will be presented. The following section will treat the origin of the BOLD-signal because the BOLD-signal contrast is the physiological base for functional MRI and should be truly understood in all its features in order to fully comprehend the activation maps generated by this technique. In this context, the relevance of the spontaneous low-frequent fluctuations of the BOLD-signal for the intrinsic functional organization of the brain will be particularly emphasized since the discovery that the intrinsic activity of the brain is organized in spatially synchronized patterns caused a paradigm shift in how we look at brain activity and how we analyze it. A short section resuming the findings from studies investigating the intrinsic network architecture of the aging brain will close this part of the thesis presented here.

In the third part, the aims and research questions motivating this thesis will be described followed by the fourth part that will characterize the study sample and explain the used analysis methods with their advantages and potential pitfalls. The three empirical studies constituting the actual core of the thesis will be presented in detail in part five. In part six, the findings of the three empirical studies will be discussed in the relation to the aims and research questions of part three and further steps will be outlined.

2 Theoretical Background

2.1 What do we know about the functioning of the aging brain – Part One: Findings from task-induced fMRI studies

One of the most intriguing findings of MRI studies investigating the complex relationship between cognition and brain structure and function is how often one is able to observe still preserved normal cognitive functioning despite clearly manifest structural damage sometimes already converging into a preclinical or clinical stage. An excellent example is the study of Sonnen and colleagues (2011) who performed a comprehensive neuropathologic examination of the brains of 336 older adults who all had been found cognitively normal based on a neuropsychological examination in the year before their death. The researchers found moderate or frequent neuritic plaque density in 47% of these cognitive normal older adults (mean age 87; SD 4), and in 6% a neurofibrillary tangle burden of the neocortex severe enough to qualify for the highest degree of Alzheimer pathology, i.e. Braak stage V-VI (Sonnen et al. 2011). One possible explanation for this discrepancy between already manifest serious structural damage and seemingly still preserved cognitive functioning repeatedly observed in older persons could be that the aging brain might possesses functional compensation mechanisms that allow it to maintain cognitive functioning despite structural degeneration.

Evidence that the aging brain might indeed possess such a thing as functional compensation strategies came from activation fMRI studies. Several of them found distinctly different activation patterns in older adults compared to those observed in young when both age groups were performing the same cognitive task roughly at the same level in the scanner. In essence, the observed differences in activation can be described as follows: a) Young and old adults activate the same brain regions, but older adults exhibit less or more activity. Reduced activation patterns are mostly interpreted as evidence for age-related functional degradation in the literature (Grady, 2008). Spatially more extensive activation patterns in contrast are explained as signs of functional dedifferentiation when older adults perform worse than younger adults or as compensation when older and younger adults perform basically at the same level (Grady, 2008). b) Older adults activate additional brain regions in comparison to those activated by the younger. This age-related additional recruitment is mostly observed in brain regions of the frontal cortex. Older adults either activate additional frontal regions in the same hemisphere that is uniquely active in the younger participants or they recruit the homologous areas in the other hemisphere. As long as the performance of the older adults is still at the younger's level this "over-recruitment" is generally also interpreted as compensation strategy in the literature (Grady, 2008). c) Older adults exhibit spatially reduced or temporally delayed deactivation in some

brain regions, mainly in regions belonging to the so-called default mode network in comparison to younger adults. This phenomenon is generally interpreted as functional inefficiency in the literature (Grady, 2008) because it is usually accompanied by worse performance in the older adults. However, the interpretation of these age-related differences in activation patterns in the literature is by no means so unambiguous as the above listed summary might suggest.

a) The interpretation of fMRI activation maps is complex and has its pitfalls

The interpretation of these activation patterns as such is also very complex. Gordon, Tse, Gratton and Fabiani (2014) for example showed that the typically used method of quantification, which is either to measure the height of the peak activation and/or to count the number of significantly activated voxels in the region of interest (ROI) have significant limitations when it comes to capturing the subtleties of age-related changes in activation patterns. For instance, the quantification of activity patterns is usually computed over a number of neighboring voxels on a three-dimensional volume. Because of this, the observed age effects are not just a pure measure of signal amplitude but present a combination of the BOLD-signal peak amplitude and the activation spread of the BOLD-signal thorough the volume (Gordon et al., 2014). The latter for example is heavily influenced by choices for the image processing like the size of the smoothing kernel used during the preprocessing of the data, the chosen size of the ROIs, and so on. But also age-related biological issues like higher anatomical variability due to age-related atrophy for instance have an impact on the BOLD-signal spread and the BOLD-signal amplitude. Higher anatomical variability due to age leads to a higher variability of the distances between individual peak locations in the MNI space in relation to the peak location of the ROI that is defined for both groups in common. The combination of more spatial variability of the individual peak activations due to higher age-related atrophy rate thus affects both parameters: the BOLD-signal amplitude gets flatter and the BOLD-signal spread increases. The relevance of such issues for the interpretation of age-related differences in activation patterns was demonstrated by Gordon and colleagues (2014). They showed that older participants exhibit increased activation in brain regions belonging to the task-positive component in the brain (i.e. dorsal attention network) while no age-related differences were found for the deactivations of the brain regions belonging to the task-negative brain component (i.e. default mode network). More interestingly, there were distinct age-related differences in BOLD-signal spread. Older adults exhibited an increased spread of activation in the task-positive regions, but a strongly reduced signal spread of deactivation in task-negative brain areas (Gordon et al., 2014).

There are other concerns that should be kept in mind when attempting to understand the differences in activation patterns between older and young adults reported in the literature. Many studies reporting additional compensatory activity in older adults relied only on a descriptive assessment of the

significantly activated voxels but did not explicitly test functional asymmetry by means of a laterality index. Berlingeri, Danelli, Bottini, Sherna, and Paulescu (2013) demonstrated for one of the most prominent compensation models, the HAROLD (hemispheric asymmetry reduction in old) model (Cabeza, 2002; Cabeza et al., (2002)) that the apparently more bilaterally distributed activation patterns of older adults in cognitive tasks like episodic-long-term memory, working memory, visual perception, and inhibition might be better explained by other age-related mechanisms than HAROLD. As soon as these alleged HAROLD activation patterns were assessed by computing proper between-group statistical lateralization maps and by quantifying the effect size of the BOLD response in each age group at least some of them revealed themselves as resulting from a lack of activation in the elderly or as activation patterns shared by young and old adults (Berlingeri et al., 2013).

b) Thresholding effects and other factors that have the potential to mislead the interpretation of fMRI activation maps

FMRI activation patterns are dependent on arbitrarily determined statistical thresholds used to differentiate between significant activations and insignificant activations. Therefore, it is very well possible that younger adults recruit exactly the same additional brain region as older adults but the activation in those regions considered to be additionally recruited by older adults does just not reach the threshold for significance in younger adults. This is a crucial point for the interpretation of the underlying brain-behavior association because it is an important difference whether a certain brain region shows activation although a weak one or whether the brain region in question exhibits no activity changes at all in the younger adults. In the former case, younger adults might show the same activation pattern as the older adults as soon as the cognitive load gets higher and this would imply that younger people might possess a higher functional capacity while older adults' brains are less efficient and already at their limit at lower cognitive load (Barulli & Stern, 2013; Reuter-Lorenz & Cappell, 2008).

Furthermore, the majority of studies investigating age-related changes over the lifespan was cross-sectional and typically compared the two opposite ends of the age-spectrum, i.e. young adults with old or even very old adults. This experimental design has its pitfalls. For example, an activation in younger adults that is insignificant when averaged over the group might be significant and meaningful on the individual level when it is possible to account for the individual cognitive performance of the young adult (Morcom & Johnson, 2015). For it is possible that the recruitment of an additional brain region for certain cognitive tasks is not purely age-related but is a characteristic of a behavioral subtype or cognitive strategy that is already present in young age and is just reinforced by the brain's aging process but not caused by it (Morcom & Johnson, 2015). Only longitudinal designs are capable

to disentangle such complex brain-behavior relationships although longitudinal studies also come with their specific problems like retest-effects or biases introduced by attrition (Salthouse, 2011).

Related to the aforementioned problem of cross-sectional studies is the fact that studies investigating the aging brain focus upon cognitive abilities like processing speed, executive functions, working memory, or episodic memory. All these cognitive abilities are highly dependent on the general efficiency of the brain's functional organization, which is mostly genetically determined and stays relatively stable over the lifespan (Nyberg, Lövdén, Riklund, Lindenberger & Bäckman, 2012). Individuals who perform better than most of their peers in youth also tend to perform better than their peers in old age. Furthermore, the difference of individual cognitive abilities in the same age cohort is much larger than the age-related rate of cognitive decline (Morcom & Johnson, 2015). When using a cross-sectional study design and comparing two different age cohorts, it is therefore possible that the differences between old and young might rather be caused by the much larger relative variance of cognitive abilities within the same age group than by the relatively small variance of change in function with age. As a result, the intra-individual cognitive decline might not be as large as the findings of cross-sectional studies often suggest (Morcom & Johnson, 2015).

There exists one final aspect that might be not always duly considered by many studies investigating age-related change in cognition and potential compensation mechanisms. Whether an activation pattern is interpreted as representing compensation or dedifferentiation depends on the cognitive performance that is associated with the pattern. An activation pattern is usually interpreted as compensation as long as the older adults perform roughly at the same level as the young participants though as soon as the older adults' performance is worse than the younger adults' the same activation pattern is interpreted as dedifferentiation. However, there might exist something like a failed compensation in older adults. The recruitment of an additional brain region cannot anymore guarantee a preserved cognitive performance but without the support of that additional brain region the performance would be even worse. In this case the additional activation is still compensatory by nature (Morcom & Johnson, 2015) but would be interpreted as dedifferentiation following the general practice for the interpretation of activation patterns in old brains. Only by the application of transcranial magnetic stimulation TMS or related techniques would it be possible to clearly disentangle dedifferentiation from failed compensation in such cases.

c) Interim conclusion

Taken together, it cannot be denied that despite all their problems and shortcomings activation fMRI studies have provided us with important insights on how the older brain differs from the young brain when performing a specific task. However, in order to really understand why the aging brain shows

these differences it is necessary to understand more about the effect of age on the underlying functional architecture of the brain. In order to understand the activation patterns observed with task-induced fMRI, we need more information about inherent efficiency or degree of preserved functional flexibility of the older brains' functional baseline configuration because this is the starting-point from which the brain generates all the goal-driven behavior.

Until a few years ago, the mapping and quantification of the functional organization of the brain would have been an impossible feat. Due to a paradigm shift in how we look at the brain and thanks to new analysis techniques whose design was prompted by this paradigm shift, it is now possible to evaluate the functional organization of the brain using fMRI. To understand why this progress was possible, one has to look closer at the BOLD-signal, which is the physiological base of fMRI.

2.2 The BOLD-signal in fMRI: From evoked activation to the intrinsic activity of the brain

a) From neuronal to hemodynamic activity

Neurons need energy in form of glucose and oxygen supplied by the cerebral blood flow to process and to transmit information by electrical and chemical signaling. Different levels of brain activity are coupled with different energy demands, which in turn are always coupled with changes in the cerebral blood flow. In the oxygen-rich blood, hemoglobin binds oxygen, which turns into oxyhemoglobin. When the neurons extract the oxygen to support their energy consumption, the oxyhemoglobin is reduced to desoxyhemoglobin. The two forms of hemoglobin possess different magnetic qualities: oxyhemoglobin is diamagnetic and the de-saturated desoxyhemoglobin is paramagnetic because its iron atom possesses an unpaired electron, which realigns its path when an external magnetic field is applied and thereby disturbs the homogeneity of this external magnetic field. This different behavior of oxyhemoglobin and desoxyhemoglobin in an external magnetic field is the physiological base of the Blood Oxygen Level Dependent (BOLD) contrast used in functional magnet resonance imaging in order to visualize brain activity (Raichle & Mintun, 2006).

The energy consumption and consequently also the cerebral blood flow of the brain regions supporting a mental or physical task increase during the task performance. During a quiet state of awake rest, the brain's oxygen consumption is much higher than the glucose consumption but as soon as the brain is engaged in active goal driven behavior, the increase of glucose consumption surpasses the increase of oxygen consumption by far (Fox, Raichle, Mintun, & Dence, 1988; Schölvinck, Leopold, Brookes, & Khader, 2013). This metabolic imbalance leads to a relative excess of oxyhemoglobin in relation

desoxyhemoglobin in the brain regions supporting this behavior. The diamagnetic oxyhemoglobin intensifies the BOLD-signal and thus the increase of cerebral blood flow is followed by a detectable enhancement of the fMRI signal (Raichle & Mintun, 2006). In contrast to the electroencephalogram (EEG) and magnetencephalogram (MEG) technique, which are able to measure direct neural activity, the BOLD-signal is an indirect measure of brain activity because the fMRI technique is only capable to detect the metabolic changes caused by neural activity. The relationship between the hemodynamic signals and the underlying neural signals of the brain is still not fully understood despite a number of studies trying to shed light on the mechanisms. Nevertheless, Logothetis and colleagues (2001) were able to show that the BOLD-signal correlates best with the changes in the local field potentials (LFP) and not– as was intuitively assumed - with the spiking activity of the neurons. The LPFs are a complex measure of neuroelectric activity composed of subthreshold signals arising from the integrated electrical activity in pre- and postsynaptic terminals of the brain (Schölvinck et al., 2013; Raichle, 2015a).

b) Task-induced fMRI

As a consequence of the metabolic nature of the BOLD-signal contrast, the first ten years of fMRI were focused on the brain regions, whose hemodynamic activity time courses significantly changed as the result of the temporal structure inherent to the task the participant was performing in the scanner. The results of such task-induced fMRI experiments are activation maps displaying the brain regions significantly involved in the task. The experimental paradigms, by which these activation maps were generated, strongly influenced the manner of how the functioning of the brain was interpreted (Raichle, 2009). The brain was understood as reacting reflexively on external demands in terms of individual regions, i.e. an area exhibiting a significant increase in activity during the task had to be the brain region subserving just that specific function (Raichle, 2009). This interpretative approach illustrates very well the brain's ability for segregated information processing but fails to explain its capability for global information integration, which is the other principal feature of the brain's functional organization (Bullmore & Sporns, 2012).

c) The spontaneous low-frequent fluctuations of the BOLD-signal reveal the intrinsic network architecture of the brain

Then, about twenty years ago, there was a paradigm shift in the way how to look at the brain in general and how to interpret the observed fMRI activity patterns (Raichle, 2009). That shift was initiated by two different discoveries, but both had in common that they draw attention to the fact that the BOLD-signal always exhibits low-frequent spontaneous fluctuations (< 0.1 Hz) (Raichle, 2009). These slow fluctuations of the BOLD-signal can be observed not only in the absence of an external

stimulus when the participant is lying relaxed and awake in the scanner and performing no overt task but also during active task engagement. Although the brain's intrinsic activity and its relevance for the functional network architecture has now been in the focus of intensive research for some time, the neuronal origin of this slow intrinsic activity is still not fully understood (Keilholz, 2014).

The first of these two seminal discoveries was made by Biswal, Yektin, Haughton and Hyde (1995). They showed that the spontaneous BOLD-signal fluctuations of the brain were forming non-random patterns of synchronized intrinsic activity within the somato-motor system even when the participant was doing nothing else but lying awake and relaxed in the scanner. Biswal and colleagues' (1995) discovery of the somato-motor system inspired other researchers to use their approach to identify other intrinsic brain sub-systems. Today, we distinguish 7 – 17 different intrinsic sub-systems (Yeo et al., 2011) that are all defined by their individual patterns of spatial synchronized spontaneous BOLD-signal fluctuations, which are not just highly reproducible across subjects and time but also very similar to configurations observed during active goal-driven behavior (Cordes et al., 2000; Damoiseaux et al., 2006; De Luca, Beckmann, De Stefano, Matthews & Smith, 2006). Their synchronized intrinsic activity is now referred to as functional connectivity and the topology of the spatio-temporal patterns of such synchronized BOLD-signal fluctuations are called resting state networks (RSN) or intrinsic connectivity networks (ICN), which is the more appropriate term as the brain is never truly at rest (Sadaghiani, Hesselmann, Friston, & Kleinschmidt, 2010).

d) The outstanding role of the default mode network

The second discovery causing a change of perspective in fMRI neuroimaging was the formal characterization of the so called default mode network (DMN), a distinct set of brain regions (posterior cingulate cortex/precuneus, lateral parietal cortex, ventral medial prefrontal cortex, and dorsal medial cortex) that is always showing a high level of spontaneous synchronized activity during task-free conditions but deactivates during tasks with an attentional focus on the external environment (Shulman et al., 1997; Raichle et al., 2001; Greicius, Krasnow, Reiss & Menon, 2003).

In contrast to the other ICNs, which generally show higher functional connectivity when the brain is actively engaged in a task, the DMN regions are more functionally connected during a task-free rest state than during goal-driven behavior. Because of this, the DMN is also called the task-negative ICN while the other ICNs are subsumed under the term task-positive ICNs (Fox et al., 2005). The DMN seems to have an exceptional position in relation to the other ICNs. While the functional relevance of the task-positive ICNs is probably related to the functionality of their counter-parts during goal-driven behavior, the DMN's functionality is still not completely understood. Some researchers (Hanna-Andrews, Smallwood, & Spreng 2014; Doucet et al., 2012) associate its function with mental

activities that commonly accompany the relaxed state of quiet repose typical for the task-free condition during fMRI data acquisition like day-dreaming, mind wandering, self-consciousness, and remembering past experiences or planning future events.

However, there are some aspects of the DMN, which indicate that this understanding of the functionality of the DMN might fall short (Raichle, 2015a). For a start, the possible functions of the DMN listed in the previous paragraph are all higher order cognitive states and highly specific for humans. However, the DMN or at least DMN-like patterns of intrinsic brain activity can also be detected in monkeys (Vincent et al., 2007), rats (Lu et al., 2012) and mice (Stafford et al. 2012), which suggests a more fundamental purpose of the DMN. Another important aspect when speculating about the functionality of the DMN is the fact that the task-free state of the brain is energetically an extremely costly condition. The human brain represents roughly 2% of the total body weight but consumes 20% of the total energy supply at rest when the DMN is most active (Raichle & Mintun, 2006). In contrast, the regional increases in metabolic activity associated with the brain's goal-driven performance are generally quite small, often less than 5% of the baseline activity (Raichle & Mintun, 2006; Raichle, 2015a). Regarding the functionality of the DMN, there exists no reasonable argument why activities like mind wandering or other forms of stimulus independent thought that are commonly associated with the DMN activity should consume more additional energy than any other goal-driven behavior or demanding cognitive task (Raichle, 2015a). Consequently, there is a huge percentage of energy consumed by the brain that is not accounted for.

There are other interesting energetic/metabolic characteristics of the DMN that should be considered when speculating about its potential function. Neurons use two different processes for energy consumption: 1. (An)aerobic glycolysis, which is faster but generates only two moles of adenosine triphosphate (ATP) per molecule of glucose and also produces lactate and pyruvate 2. Oxidative phosphorylation which is slower but more efficient, and uses lactate and pyruvate to produce roughly 30 ATP. As the more efficient process, oxidative phosphorylation is the source of most of the energy needed by the neurons of the brain nevertheless aerobic glycolysis is present in the adult brain even at rest and metabolizing roughly 12-15% of the total of glucose (Raichle & Mintun, 2006). However, not all brain regions exhibit the same level of aerobic glycolysis. The DMN and areas in the dorsolateral prefrontal cortex do not just exhibit the highest levels of aerobic glycolysis in the brain but are also characterized by a high variance in the task-free fMRI BOLD-signal (Raichle, 2015a). The high metabolic activity of the DMN seems to come at the cost of a higher vulnerability because the DMN is prone to an augmented amyloid deposition even in cognitive normal older adults (Jagust, 2013).

Finally, there is a last intriguing characteristic of the DMN that should be considered when one wants to understand its role in the functional organization of the brain. The state of quiet awake rest, during

which the DMN is most active, seems to be a particular dynamic and explorative state of the brain. By defining two measures to describe the dynamics of the brain, i.e. synchrony quantifying the spatial coherence of the BOLD-signal across regions of the brain and metastability quantifying the variance of synchrony over time, Hellyer and colleagues (2014) showed that metastability is primarily associated with high intrinsic activity in the DMN during rest, while synchrony is associated with activity in the executive control network (ECN) and the dorsal attention network (DAN) during goal-driven behavior. Brain states of high metastability can be characterized as highly exploratory states facilitating the dynamic transition between a large repertoire of brain configurations and allowing for an efficient response to changing external challenges (Hellyer et al., 2014). In contrast, when external events demand high external attention and focused behavior the brain responds to this by a global increase in spatial synchrony and a reduction of global metastability thereby allowing for more stable neural dynamics necessary to maintain consistent and focused behavior. The brain's dynamic switching between the externally focused and attentive state and the internally focused and explorative state are the typical features of self-organized criticality, which allows a system to naturally exist in a stable yet adaptable state allowing the system to switch quickly between different configuration in order to adjust to new external demands (Bullmore, Barnes, Bassett, Fornito, Kitzbichler, et al., 2009; Leech & Sharp, 2014).

To close the arguments presented here: While it is undoubtedly possible to detect the BOLD-signal time-series specifically associated with mind-wandering or self-conscious thoughts in task-free fMRI data and even analyze the specific contents of these thoughts (Doucet et al., 2012), the functionality of the DMN is more wide-ranging and more fundamental for the functioning of brain than these activities.

e) The dynamic nature of the ICNs

Although everyone who had looked at the sequence of the single volumes constituting a task-free time-series on subject level once (please, see the figure 2 adapted from Raichle 2010) knew about the dynamic nature of the intrinsic brain activity, during the first years of task-free fMRI researchers were explicitly interested to understand the spatial patterns of the synchronized intrinsic activity but not their temporal fluctuations.

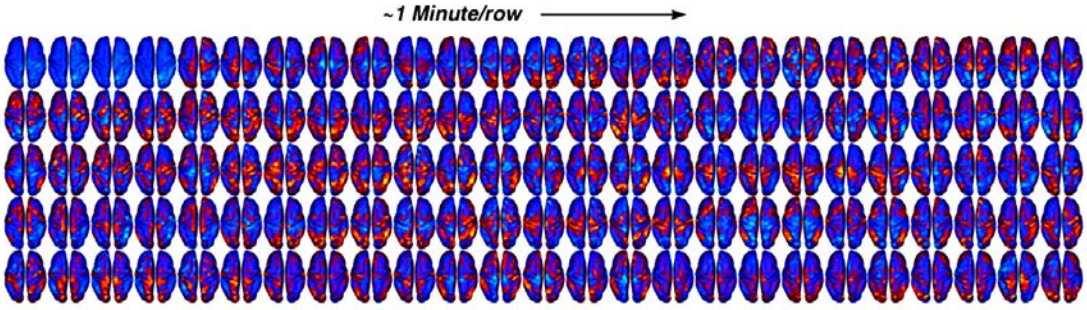

Figure 2.1. The fluctuating patterns of intrinsic activity seen in the brain of a single subject with fMRI. The data were obtained over a period of 5 min (TR = 2,3 sec) and illustrate the slow dynamics of the intrinsic brain activity (adapted from Raichle, 2010).

As a result, the generally used duration of a task-free fMRI data acquisition was and still is 5 – 7 min because that is the minimum of time needed to make sure that the correlations of the ICNs plateau and are stable (Van Djick et al., 2010) and the statistical methods most standardly used to analyze task-free fMRI data all assume temporal stationarity of the investigated ICNs. This assumption can be justified in as much as the ICNs known in the literature indeed represent an average and therefore in some way static pictures of the synchronized intrinsic activity as the measured fluctuations are averaged over the entire scan duration. However, ICNs are not stationary but are dynamically activating and deactivating and the brain regions constituting them might belong to different ICNs at different time-points during the scanning time.

f) Interim conclusions

The discovery of the relevance of the low-frequent spontaneous BOLD-signal fluctuations was not just the base for a more in-depth understanding of the spatio-temporal functional organization of the brain. Likewise, the brain is nowadays no longer understood as passively reacting to external demands, which was the predominant conviction during the first years of fMRI, but as always intrinsically active and thereby proactively predicting future demands (Fox & Raichle, 2007; Deco, Jirsa & McIntosh, 2011) in order to be able to act immediately and energetically highly efficient as soon as it is required by the situation.

Furthermore, the brain's intrinsic activity is not just the starting-point from which the brain generates the actual goal-driven behavior but it is still going on while the brain performs that behavior and thereby influencing its outcome (Hesselmann, Kell, Eger & Kleinschmidt, 2008a, Hesselmann, Kell, & Kleinschmidt, 2008b, Sadaghiani, Hesselmann, Friston & Kleinschmidt, 2010, Sadaghiani, Poline, Kleinschmidt, & D'Esposito, 2015). Finally, there is still another shift in how we interpret the brain's activity and activation pattern that was inspired by the discovery of the DMN and the other ICNs. Nowadays, the individual brain region showing a significant activity increase during task-induced fMRI experiments is no longer interpreted as a distinct generator for a specific cognitive function. On

the contrary, it is now understood as a part of an underlying network that dynamically interacts with many other network configurations in order to support not just one but many different functions of the brain (Pessoa, 2014).

2.3 What do we know about the functioning of the aging brain – Part Two: Findings from task-free fMRI studies

a) Age effects on the default mode network

The effects of age on the intrinsic activity of the DMN have been of significant interest to investigators studying the aging brain as evidenced by a large number of studies on this topic (Ferreira & Busato 2013; Sala-Llonch, Bartés-Faz & Junqué, 2015). However, aging is not the only field of research that is fascinated by the DMN. As the numbers derived from PubMed listing (please see figure 2.2) show the number of publications concerning the DMN has increased exponentially over the last twenty years and encompasses not only studies in the healthy brain but also studies investigating brain diseases, for example Alzheimer's dementia or Parkinson's disease, schizophrenia, autism, attention deficit hyperactivity disorder, and depression (Leech & Sharp, 2014) just to name a few. Considering the remarks about the functionality of the DMN from the previous section, the prominent role of the DMN in almost everything brain-related is hardly surprising.

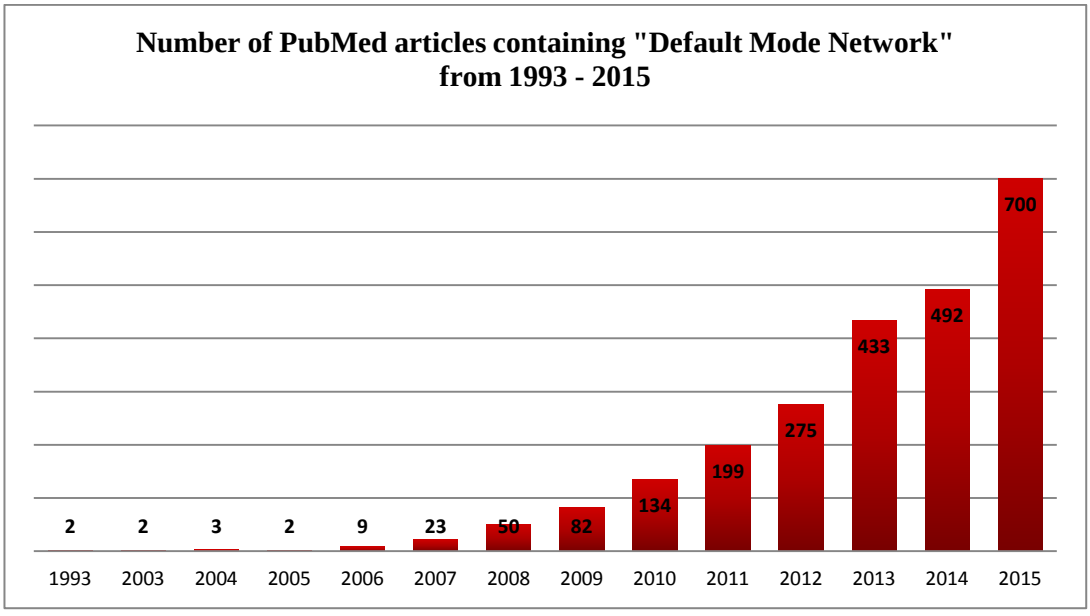

Figure 2.2

With regard to the aging brain, the most consisting findings are a functional disconnection of parts of the DMN or a decrease of the within-network connectivity (Andrews-Hanna et al., 2007; Betzel et al.,

2014; Cao et al., 2014; Geerligs, Renken, Saliasi, Maurits & Lorits, 2014; Onoda, Ishihara, & Yamaguchi, 2012), which are frequently accompanied by findings of an increase of the between-networks connectivity resulting in a functional dedifferentiation, respective a loss of functional segregation of the DMN (Betzel et al., 2014, Chan, Park, Savalia, Petersen & Wig, 2014). These observations are often interpreted as evidence that the DMN is more vulnerable to age-related functional dedifferentiation than other ICNs.

However, a closer look at the studies supporting this conclusion suggests that the way in which they were conducted could have introduced a bias favoring this conclusion. Firstly, many researchers investigating the healthy aging brain focused on the DMN because of its central role in the Alzheimer pathology (Buckner et al., 2009; Jagust & Mormino, 2011) and as a result age-effects on the other ICNs are rather understudied. Secondly, the majority of studies investigating the aging brain used a cross-sectional design. By comparing very young adults with older adults, these researchers appear to make the implicit assumption that all characteristics unique for the older group are solely caused by the aging process and thereby neglecting other factors like cohort-effects, education, life-experience (Morcom & Johnson, 2015) or unknown preclinical AD status (Brier et al., 2014). That such confounding influences could indeed have biased our understanding of the DMN in old age was shown by a study of Persson, Pudas, Nilsson and Nyberg (2014). The authors investigated the longitudinal change in DMN activity and connectivity in a sample of healthy middle-aged and old-aged adults (49 – 79 years) over a time period of 6 years. They found no overall longitudinal changes in within-network connectivity of the DMN, while within-region DMN analyses showed reduced deactivation between baseline and follow-up (Persson et al., 2014). Although the DMN showed stable connectivity over the whole group, individual differences in memory were associated with a decrease in within-connectivity of the DMN (Persson et al., 2014).

As just demonstrated, a longitudinal approach might alter our understanding of the aging brain and for that reason there is a caveat for the now following outline of the age-effects on the other ICNs. The majority of the studies reporting age-changes in other ICNs had likewise used a cross-sectional design; therefore it might very well possible that their findings have to be accommodated as soon as there is more longitudinal evidence.

b) Age effects on other ICNs

Studies investigating the influence of aging on ICNs supporting higher cognitive functions like the fronto-parietal or executive-control network (Geerligs, Renken, Saliasi, Maurits, & Lorits 2015; Shaw, Schultz, Sperling & Hedden, 2015; Zhang et al., 2014) the cingulo-opercular or salience network (Geerligs et al., 2015; Voss et al., 2013), the dorsal attention network (Tomasi & Volkow, 2012;

Zhang et al., 2014) consistently found an age-related decline of within-network connectivity. Some studies (Betzel et al., 2014; Chan et al., 2014; Ferreira et al., 2015) also reported that the degradation of the within-network connectivity was associated with an increase of between-networks connectivity. Thus, the task-active higher order ICNs seem to undergo largely the same process of progressive functional dedifferentiation as their task-negative counter-part, the DMN, with the only difference that these findings are not so consistently reported in the literature while age-related dedifferentiation of the DMN is always found.

The findings for the sensory and motor networks are not so coherent though. Some studies reported that the ICNs implicated in primary information processing or motion seemed to show no age-related changes (Geerligs et al., 2015) while others studies even found an increase of the within-network connectivity in the motor and sensory networks (Tomasi & Volkow, 2012). Furthermore, some studies suggested that the age-related trajectory of functional degradation in primary ICNs differs from that in the higher order cognitive ICNs. But the findings were not unequivocal. Chan and colleagues (2014) for instance found that the aging process of the sensory-motor networks is fitted best with a linear curve and that the dedifferentiation progress of the higher order ICNs can be fitted with a linear but also with a quadratic model. Betzel et al., 2014 however came to the exact opposite conclusion, they found that the dedifferentiation process of the higher cognitive networks is fitted best with a linear model, while the somato-motoric network, the primary visual network and the salience network is fitted best with a quadratic model.

The divergent findings these two studies highlight an issue that currently complicates a comparison between different task-free fMRI studies investigating the aging brain. Already during the preprocessing but even more so during the main analysis of the data there are many methodical decisions to be made; for example, how to handle noise sources, selection of the appropriate smoothing kernel of the fMRI data, the definition of a seed or the number of components to extract from the data and so on. Every single of these decisions influences the findings of the study and currently there exist no consensus regarding the different preprocessing options or regarding the question which methods should be used for which research question. Because of this methodological heterogeneity, the comparison of the results from different studies is almost impossible and this applies even when the same analysis method, e.g. graph theoretical analysis or independent component analysis, were used.

With that said and to sum up this section: The one finding the studies using task-free fMRI in order to investigate the aging brain all seem to agree on is the observation that the intrinsic network architecture of the aging brain is affected by a progressive functional dedifferentiation caused by the

decrease of within-network connectivity in combination with an increase of inter-network connectivity.

3. Aims and research questions

The proportion of adults aged 65 years and older increased in the general population worldwide over the last decades and the end of that demographic trend is not yet in sight (United Nations, 2013). Most but not all older persons experience cognitive decline, which significantly reduces quality of life (Abrahamson, Clark, Perkins & Greg, 2012), life satisfaction (St John & Montgomery, 2010) and last but not least individual autonomy. Understanding the processes causing the cognitive decline is of outmost importance to identify means to delay the onset of deleterious age-effects.

As outlined in the previous sections of this thesis, findings of task-induced fMRI studies suggest that the aging brain has the functional plasticity to counteract the consequences of structural degeneration for some time. However, the majority of the fMRI studies claiming to have discovered compensation mechanisms in the aging brain were cross-sectional. The cross-sectional design is not ideal to clearly separate between-group differences caused by confounding factors as high within-group variability, cohort-effects or education from the differences caused by a function of age. Only longitudinal study designs are able to disentangle these two sorts of differences in an unambiguous way. Additionally, there exist good arguments against the interpretation that these activation patterns represent indeed compensation mechanisms of the aging brain but to interpret them as evidence for the aging brain's progressive functional dedifferentiation. A better understanding of the specifics of the baseline intrinsic network architecture of the aging brain might therefore help to more clearly differentiate between compensation and dedifferentiation.

The three studies presented in the fifth part of this thesis were all conducted within the scope of the Longitudinal Healthy Aging Brain (LHAB) database project that started 2011 at the International Normal Aging and Plasticity Imaging Center (INAPIC) at the University of Zurich and is currently run at the University Priority Project "Dynamics of Healthy Aging". The LHAB project aims to investigate the complex relationships between cognitive and motor performance and structural and functional correlates of the aging brain (Zöllig et al., 2011).

Within the scope of the LHAB database project, different types of structural MRI and task-free fMRI are acquired from a large sample of older adults in the transition from old age (> 65 years) to very old age (> 85) on an annual or bi-annual basis. The LHAB provides therefore the ideal means to investigate if the aging brain altogether possesses the capacity for functional compensation of its structural decline, how this capacity for compensation relates to the intrinsic network architecture and finally to determine which age-related alterations of the network architecture of the aging brain are ultimately responsible for the shift from compensation to dedifferentiation.

So far the experience with longitudinal analysis of task-free fMRI data is very limited and that is not just true for the research field focusing on the aging and developing brain but for all research branches. Besides, the majority of projects that have already published longitudinal task-free fMRI data analyzed the data from two measurement time-points only. One of the big challenges in the context of the LHAB is therefore to find robust methods to detect even subtle changes in functional connectivity on group as well as on individual level over the time and to disentangle the different aging trajectories.

Accordingly, **the first research question** was of technical nature and related to the above mentioned methodical challenge of finding a reliable analysis method able to detect even small changes in functional connectivity. The age-distribution of the LHAB study sample is exceptional in that it is characterized by relative over-representation of older adults belonging to the leftward end of the age-spectrum. Because the majority of the participants were between 65 and 70 years old at the beginning of the LHAB project, we expected just very small age-related alterations in cognition and brain structure and function during the first years for these participants as long as they stayed healthy. We therefore hypothesized that a purely data-driven approach at the voxel-level might be most suitable to detect the subtle age-related changes in intrinsic connectivity expected in this population of healthy older adults within a year. After a thorough review of the currently existing analysis techniques designed to analyze task-free fMRI data we found that the Intrinsic Connectivity Contrast analysis fulfilled best our criteria as defined above.

The Intrinsic Connectivity Contrast power (ICCp) index (Martuzzi et al., 2011) is a whole brain voxel based measure of connectivity related to the graph theory analysis (GTA) measure "*degree*" (Rubinov & Sporns, 2010). In GTA, a node can be defined on a single voxel level, i.e. every single voxel is a node, or on a coarser resolution level, e.g. on ROI level as a macro-anatomical region or a functionally delineated cluster of voxels. The degree of a node corresponds to the number of this node's connections with all other nodes in the network. Compared to a seed correlation analysis or a standard GTA the ICCp analysis has two advantages: 1. The ICCp analysis is data driven and free of any need to define a seed based on a priori assumptions about regions of interest. 2. An ICCp analysis can be computed without the need of defining a threshold. Since the brain is a highly complex and extremely densely connected structure, every node is functionally connected to every other node in some way, i.e. either by a direct or by a mediated relationship. Thus, a commonly used, but also critical procedure is to define an arbitrary threshold that the connections have to surpass in order to separate the strong and supposedly important links from weak links and noise. To date, there exists no consensus about what constitutes a neurophysiologically meaningful threshold. Instead of using a threshold to determine the most important connections, the ICCp works by weighting the connections of a voxel with the other voxels by the strength of these connections, i.e. by their r^2 value. Consequently, the

voxel-based connectivity maps produced by this approach reflect not only the number of connections of an individual voxel but also how strong these connections are (Martuzzi et al., 2011).

Currently, the ICC index is not widely used in the field; the PubMed database lists only a handful of studies using this analysis method. For that reason, the aim of the first study conducted for this thesis was to evaluate the suitability of the ICC analysis for our purposes. In the first study, which had the character of a pilot study in this regard, we used a cross-sectional within-group design and associated the age of the participants with the ICCp index that was computed of the task-free fMRI data from the first measurement time-point.

The **second research question** was related to the first one insofar, as we wanted to evaluate the potential of the ICC analysis to elucidate the complex relationship of cognitive performance/behavior and intrinsic network architecture of the brain. This goal is by no means trivial as the true effect size of the relationship between network connectivity and cognition is likely to be in the range of $r = 0.25$ or even less. The detection of such a small to moderate effect sizes needs large study samples of ideally over 200 participants (Biswal et al., 2010; Shaw et al., 2015) and very sensitive analysis methods. In order to evaluate if the ICC analysis has the potential to detect these small associations between intrinsic network architecture and cognition, we conducted the second cross-sectional study presented in the context of this thesis.

The **third research question** aimed to elucidate the characteristics of the intrinsic network architecture of healthy older adults in general. Currently, the largest part of our knowledge about the aging brain either comes from studies comparing healthy young adults with older adults or from studies investigating pathological aging that used a group of the healthy aging older adults as controls. As a result, we know relatively well, how young brains differ from old brains and what distinguishes pathological aging from healthy aging. However, that does not mean that we are able to accurately describe the specific impact of healthy aging on the intrinsic network architecture of the brain. The third study presented in the context of this thesis aimed to map out the functional organization of the LHAB study population and to evaluate if it exhibits some sort of intrinsic potential that might allow it to compensate for structural decline and already present functional during active goal-driven behavior.

4 Methods

4.1 Participants

In order to qualify for the participation in the LHAB project, the candidates had to be 65 years or older, right-handed, native Swiss-German or native German speakers, and healthy. To assess physical and mental health, the 12-Item Short-Form Health Survey (SF-12) was administered. The self-reported mean physical health composite score in the LHAB sample was 50.8 (SD = 7.2), which is well above the US norm mean of 43.9 (age group between 65 and 74 years). The self-reported mean mental health composite score was 55.0 (SD = 6.0), which is slightly above the US norm mean of 51.6 points (age group between 65 and 74 years).

Besides the standard safety criteria relevant for MRI assessments the participants had to fulfill the following inclusion criteria: no history or current diagnosis of psychiatric or neurologic diseases, e.g. Parkinson's disease, Alzheimer's dementia, multiple sclerosis, migraine, a MMSE score > 26, and no medical conditions such as diabetes, tinnitus, and diseases of the hematopoietic system. All participants gave written informed consent to their participation in this longitudinal project under the approval of the local ethics committee and in accordance with the Helsinki declaration.

For the three studies within the scope of the thesis presented here we analyzed the data of the 230 persons who participated in the first wave of the LHAB project in 2011. The data of 186 participants (mean age = 70.4; SD = 4.8; 89 men and 97 women) were finally utilized in the three studies as they fulfilled the study-specific inclusion criteria such as completeness of the MRI data (a complete MRI data set consisted of structural images (T1 and T2 weighted) and functional images (blood oxygenation level-dependent signals (BOLD) single shot whole brain EPI)) and motion parameters < 2mm.

4.2 Experimental Design

The LHAB is a longitudinal project that started in 2011. The first three measurements were all acquired within a one-year-interval; the remaining measurements will be acquired in two-year intervals. In general, each measurement point has three different parts. The first part consists of an intensive assessment of the participants' cognitive and motoric performance. The LHAB test-battery is composed of 33 different neuropsychological tests that cover reasoning (3), verbal intelligence (3),

verbal fluency (2), executive functions (3), processing speed (3), attention (3), working memory (3), memory (3), spatial orientation (3), spatial reasoning (4) and motoric and fine motoric coordination (3). The cognitive testing session takes approximately four hours and is conducted in two parts in order to minimize testing fatigue in the participants, i.e. the first half of the tests takes place in the morning, the second half in the afternoon after a lunch break. When needed, additional breaks can be administered.

Apart from the cognitive assessment the participants also undergo a MRI exam of 1h at every measurement point. As a general rule, behavioral assessment and the MRI exam are completed within the same week but at different days of the week. After these two parts, the participants are expected to complete a number of surveys (on line or in writing) covering different topics as psychological and physiological health, medication, sleep, depression, nutrition, and leisure-time activities at home.

4.3 The specifics of acquiring task-free fMRI data

FMRI data – task-induced as well as task-free data – are acquired as a series of volumetric images over time. Different temporal resolutions and scanning lengths are possible. Usually, an individual whole brain image is acquired all 2 – 3 sec depending on the length of the entire scan and the requested spatial resolution, i.e. voxel size. When optimizing a scanning sequence for task-free fMRI data, the goal should be to find an optimal trade-off between a reasonable scan length, usually 5 – 15 min, while allowing for an as large as possible number of single time-points and a high spatial resolution, i.e. voxel size of 2-3mm^3 (Birn et al., 2013). With reference to reasonable acquisition duration, Van Dijk and colleagues (2010) demonstrated that scan lengths as short as of 5 – 7 min are adequate for the connectivity strength of the ICNs to become stable. However, longer acquisitions durations of 9 – 16 min seem to be preferable as soon as one wants to accurately and reliably distinguish individual differences in connectivity strength or changes in ICN's due to age or neurodegenerative processes (Birn et al., 2013).

In contrast to the task-induced fMRI paradigm during which the participant lying in the scanner is required to perform specific and more or less complex tasks at exactly predefined time-points, the standard task-free fMRI paradigms impose just minimal requirements on the person in the scanner. For an acquisition of task-free fMRI data the participants are generally instructed to lie as motionless as possible in scanner and to think on nothing particular. On one hand this specific feature makes the task-free paradigm ideal for participants who are not or not anymore able to comply with the complex instructions of a task-induced fMRI experiment due to age or disease. On the other hand, the participant might begin to get bored and finally fall asleep due to under-stimulation during the scan.

This last scenario should be avoided at all costs because sleep related state changes affect the intrinsic connectivity patterns.

The problem of changing states of awareness during task-free fMRI exams seems quite serious and was just recently brought to the attention of the community investigating intrinsic connectivity with MRI. Using an analysis technique designed to decode different wakefulness levels from task-free fMRI data, Tagliazucchi and Laufs (2014) reanalyzed a large number of publicly available task-free fMRI data sets and found that the data of an impressive portion of participants were confounded by various stages of awareness (30% of the participants were already asleep after the first three minutes of data acquisition). However, the reanalysis of Tagliazucchi and Laufs (2014) also showed that the risk of the participants falling asleep can be reduced by instructing them to hold their eyes open and to fixate a cross during the entire duration of the scan. Other methods to control for varying states of awareness are concurrent acquisition of heart rate variability, or EGG recordings, or to use a MRI-scanner compatible eye-tracker, which allows to control whether the participant's eyes are open and fixating the cross during the scan (Power, Schlaggar & Petersen, 2014).

The term "task-free" suggests that the participant lying in the scanner is not exposed to any external stimulation. However, this is obviously not true because the participant is exposed to the heavy acoustic noise produced by the scanner equipment. Furthermore, depending on the specific instruction during the task-free fMRI data acquisition, i.e. eyes open/eyes open while fixating or eyes closed the participant is passively or even actively processing visual input. While it has been shown that scanner noise influences the temporal coupling between different ICNs (Rondinoni, Amaro, Cendres, dos Santos, & Salmon, 2013), the effect of the eyes open/eyes closed condition is comparatively small (Patriat et al., 2013).

4.4 Pre-processing of task-free fMRI data

One of the major challenges of fMRI is the fact that the meaningful BOLD signal, i.e. the increase of metabolic activity due to a task actively performed in the scanner or due to the spontaneous BOLD-signal fluctuations, is small in relation to the numerous and complex sources of noise. Even after advanced denoising procedures only 23 of the roughly 200 signals identified in a single subject reflect neural activity (Power et al., 2014). There are three main sources of noise: a) Thermal noise describes fluctuations in MR signal intensity caused by the thermal motion of electrons within the subjects in the scanner and scanner hardware (Huettel, Song, & McCarthy, 2014). b) System noise is induced by imperfections of the scanner hardware like static or dynamically changing variability of the magnetic field (Huettel et al., 2014). c) Physiological noise is generated by head motion, heart rate and

respiration (Huettel et al., 2014). In contrast to task-induced fMRI, where the signal to noise ratio can be increased by the a priori knowledge of the timing and intensity of the task and by combining the numerous trials acquired during a single fMRI experiment (Huettel et al., 2014), the optimal removal of all these different noise sources in task-free fMRI is one of most challenging aspects of this technique.

The biological basis of ICNs is the synchrony of the very small low-frequent BOLD-signal fluctuations between different entities of the brain, which might be defined on voxel-level or on the level of individual brain regions. The simplest and most commonly used measure to quantify the similarity of these spontaneous fluctuations in intrinsic activity is the Pearson correlation coefficient. Therefore, the most important priority during the different pre-processing steps of task-free fMRI data is to remove all sources of possible spurious correlations while avoiding pre-processing approaches that might produce additional noise or spurious correlations on top of the unpreventable noise from physiological sources and the scanner equipment.

Motion artifacts can seriously compromise the data quality of all types of fMRI analyses because even small head movements can cause a spatial displacement of the voxel with the result that the now acquired BOLD-signal is generated by another neuron population than the BOLD-signal captured by that voxel before the head movement (Murphy, Birn & Bandettini, 2013). Likewise, as soon as a head movement causes a voxel to be moved in the next acquisition slice in the relation to its original slice, the interval is changed between the excitations and this transiently changes the intensity of the BOLD-signal in that voxel (Murphy et al., 2013). Finally, every head motion during the exam reduces the homogeneity of the magnetic field that has been optimized at the beginning of the exam and has a critical influence on the quality of the imaging data (Murphy et al., 2013). Consequently, the removal or correction of noise caused by subject movement has a high priority in the analysis of fMRI data. Apart from the standard procedure by which the translational and rotational displacements of the single volumes constituting a subject's fMRI time series are computed in relation to a reference volume and these motion parameters regressed out of the fMRI data during one of the following analysis steps, there are more rigorous methods to amend motion artifacts like different scrubbing techniques, i.e. an approach that either completely withholds motion contaminated images from the analysis (Power et al., 2014) or replaces the outliers with dummy variables to be used during the standard motion correction procedure.

Physiological noise, for instance breathing (0.3 Hz) and heart rate (1Hz), is characterized by a higher frequency than the very slow intrinsic fluctuations of the BOLD-signal (< 0.1 Hz), but because of the repetition times used for task-free fMRI data acquisition are relatively long (2 – 3 sec), cardiac and respiratory noise are prone to be aliased into the low frequent BOLD-signal and therefore should be

removed during pre-processing (Murphy et al., 2013). There exist essentially two different options to accomplish the removal of these physiological confounds. During one approach, heart rate and respiration are recorded simultaneously during the scan. The other approaches like the CompCor method (Bezahdi, Restom, Liau & Liu, 2007) work by extracting the signals from white matter and cerebral spinal fluid. These signals are definitively of non-neural origin but are also influenced by physiological noise or motion. Both methods use the thus extracted information about the physiological noise to regress it out during the denoising step implanted in standard pre-processing procedure of every fMRI data analysis. However, the downsides of the removal of these artifacts are reduced between-session variability in the same subject and significant reduced inter-subject variability (Birn et al., 2014).

Global signal regression is an approach to deal with spurious BOLD-signals, and was routinely used in early task-free fMRI studies. This has changed after it was detected that global signal regression can induce spurious anticorrelations or inflate actually existing neurobiological anticorrelations between the networks (Murphy, Birn, Handwerker, Jones, & Bandettini, 2009). Because of this, the discovery that the intrinsic network organization of the brain is almost as much shaped by anticorrelations between the single brain units as it is by positive correlations (Fox et al., 2005; Fox, Zhang, Snyder, & Raichle, 2009), was initially doubted (Murphy et al., 2009). Since then, a number of studies (Chai, Nieto-Castanon, Öngür, & Whitefield-Gabrieli, 2012) were able to demonstrate that anticorrelations are not just an image pre-processing artifact but have a neurobiological correlate. Recently, McAvoy, Mitra, Coalson, d'Avossa, Keidel, and colleagues (2015) raised additional concerns regarding global signal regression by showing that the global signal has neurological significance because it is asymmetrically distributed. On the left hemisphere the global signal is stronger over the language regions and on the right hemisphere stronger over regions known to be involved in attention processes.

As illustrated in this section, there exist quite a number of different methods to deal with noise and spuriously induced correlations and the decision for one method or a specific combination of denoising techniques can heavily influence the outcome of the analyses. Even twenty years after the landmark study of Biswal (Biswal et al., 1995), there exists still no consensus about a standard protocol for noise reduction and pre-processing of task-free fMRI data. The lack of a generally accepted best practice to deal with noise in task-free fMRI prevents an easy comparison of findings from different studies and reduces the test-retest reliability.

4.5 Methods used to identify ICNs and to analyze and describe the intrinsic network architecture of the brain

The three most commonly used analysis methods for task-free fMRI data are seed based correlation analysis (SCA), group-independent component analysis (ICA) and graph theoretical analysis (GTA). While SCA and ICA mainly serve for the identification of ICNs, GTA is an analysis technique that is especially well suited to describe the intrinsically active network architecture of the brain.

4.5.1 Seed correlation analysis

SCA was the method used by Biswal and colleagues (1995) to describe the first ICN ever. In many ways, SCA is a very straightforward analysis approach as one defines a single voxel or a cluster of voxels or even an entire brain region as seed, extracts the time-series of the seed's BOLD-signal and then separately correlates it with the time-series of every other gray matter voxel in the whole brain. All voxels, whose time-series correlations with the original seed surpass a predefined statistical threshold after correction for multiple comparisons build an intrinsic connectivity cluster map exhibiting the brain regions that are significantly connected to the seed (Cole, Smith & Beckmann, 2010).

However, this method has some potential weaknesses. Already the first step of an SCA, the selection of a suitable seed, has its risks as the neurobiological relevance of an SCA based intrinsic connectivity map depends on an optimal localization and an optimal size of the seed (Cole et al., 2010). Consequently, the selection of a suitable seed requires sound a priori knowledge about which area of the brain is the most representative for the ICN or cognitive function of interest. The selection of an unsuitable seed bears the risk that the seed taps into a mixture of BOLD-signals coming from different networks than just from the ICN under consideration (Cole et al., 2010). The risk that a seed's time course is the reflection of more than just one network is higher for a seed located in one of the association cortices than for seeds localized in the primary motor cortex or sensory cortices. The same restriction holds true for the size of the seed – spatially more expansive seeds are more likely to contain voxels belonging to different functional networks. However, a spatially very constricted seed might also not be ideal as it might not be equally representative for the investigated function in all subjects due to individual differences in the functional organization of the brain. Finally, the intrinsic connectivity maps computed from an SCA on voxel-level are more prone to be confounded by structured noise like head movement, physiological noise or scanner produced artifacts than ICNs computed on a coarser spatial resolution level (Cole et al., 2010).

4.5.2 Group independent component analysis

In contrast to an SCA, which is a univariate approach, an ICA is a multivariate analysis approach and works by decomposing the multidimensional fMRI data into single components. Such a component is characterized by a spatial pattern that can be partially overlapping with the patterns of other components but is independent by its unique combination of different brain regions and by its unique time course. As the approach does not preclude spatial overlap, a specific voxel might belong to more than one component, but at different time-points during the whole length of the scan.

An ICA computed on the group level usually starts with temporal concatenation of the single subject fMRI data. Sometimes, a PCA is performed before the data concatenation for each subject individually to reduce the complex, high-dimensional fMRI data into a smaller set of components that retains most of the variation of the data (Calhoun, Adali, Pearlson, & Pekar, 2001). After these preparatory steps the actual ICA is computed. However, components reflecting the group average functional brain organization may not match very well the actual components in individual subjects. For that reason and because the researchers' focus of interest is usually on these subtle differences of brain organization between subjects, the group average components have to be back-projected on the subject space. One method to accomplish this is the dual regression method by which one first regresses the group average spatial maps on the data of each individual subject in order to identify the patterns of signal changes over the time that fit those of the group best. In a second step, those time courses are in turn regressed on the individual subject data with the goal to estimate how well these components contribute to the time series of each voxel. The results of these two regressions are statistical parameter maps that can be used for further analyses like identifying group differences etc. (Huettel et al., 2014). In the cases where an additional PCA for data reduction had been used, (Calhoun et al., 2001), the original single-subject data is projected onto projection matrices which are generated by combining the group-level unmixing matrix created during the ICA with the subject-level matrices derived during the PCA (Calhoun et al., 2001; Cole et al., 2010).

In comparison to the SCA, that requires sound a priori knowledge to define a neurobiologically meaningful seed, the ICA is purely data-driven and exploratory. However, an ICA comes with its own challenges and risks. Firstly, the researcher using an ICA approach has to decide how many components he/she wants to extract from the fMRI data, i.e. whether she/he wants to compute a low- or high-dimensional ICA. The range of extracted components varies between 20 to over 100 components in the literature (Kiviniemi et al., 2009). Second, in a high-dimensional ICA there is always the risk that an ICN is not represented by one single ICA component but is split in different ICA components, each of them representing just a subpart of the ICN in question. In contrast, a low dimensional ICA bears the risk that the components might represent a combination of two or more

ICNs, for example the executive-control network and the cingulo-opercular network are represented in the same component. The splitting as well as the mixing of components complicates the necessary selection between the components that will be used for the further analysis and the components that will have to be discharged because they represent noise. Finally, every ICA results in a number of neurobiologically meaningful components but also in a certain number of components representing noise like motion artifacts, physiological noise signals or scanner-induced artifacts. Identifying the neurologically meaningful components and separating them from the noise components requires considerable expertise on the part of the researcher. The selection process is essential, because the quality of all further analyzes heavily depends on whether all noise components were discharged and the remaining components were correctly identified.

4.5.3 Graph Theoretical Analysis

GTA is a mathematical branch that allows creating comprehensive network representations, so-called graphs, and has become a very popular tool in the neuroimaging community because it is ideally suited to describe complex large network structures like the human brain. Some abstractions are needed to apply GTA to the brain. Structurally, i.e. macro-anatomically, functionally determined brain regions or even single voxel are defined as nodes/vertices and structural connections like the white matter fibre tracts or statistical dependencies like the correlation of the BOLD-signals between different regions/nodes of the brain are defined as links/edges. These two elements, nodes and links, provide all information needed to compute a connectivity matrix in which the nodes are represented in the columns and rows of the matrix and the connections between them are entered in the respective fields of the matrix. Based on the connectivity matrix different graph theory measures can be computed, each describing another aspect or characteristic of a node in respect to the whole brain and as well as in respect to every other single node of the network.

Originally, GTA had been developed to model pairwise relations between different objects constituting complex systems like computer networks, communication networks, social networks but also molecules with the atoms as nodes and bonds as links. Nevertheless, the application of GTA to intrinsic connectivity data is by no means straightforward but associated with many difficulties and open questions like the definition of functionally homogeneous nodes and adequate links that fully meet the assumptions underlying GTA, or the practice of thresholding the networks in order to separate insignificant from strong significant or the interpretation of some GTA measures.

a) Possible methods to partition the brain for node definition

Already the choice of the best method to partition the brain into functional meaningful nodes for GTA is a highly debated question. At the moment of the writing this synopsis, none of the three most commonly used approaches for node definition qualifies as gold standard because each comes with its own set of weaknesses (Stanley, Moussa, Paolini, Lyday, Burdette & Laurienti, 2013). The most fine-grained method to partition the brain is to define every single voxel as a node. Apart from the fact that the computation of a network build from several thousands of voxels is computationally expensive and time-consuming, the interpretation of the different graph measures becomes very complex. However, the most serious argument against this parcellation scheme is that a voxel is functionally an arbitrary unit without neurobiological meaning, because a single voxel still comprises several 100'000 of neurons. Another potentially problematic issue of a voxel-based-partition is that the connectivity between the neighbor nodes may be overestimated because of the inevitable blurring and smoothing of the data during pre-processing. For these reasons, one does not necessarily gain a deeper understanding of the functional organization of the brain by using the most fine-grained parcellation.

Another commonly used approach is to partition the brain into nodes defined by macro-anatomical or cyto-architectonical borders by applying anatomical templates like the AAL-atlas (Tzourio-Mazoyer et al., 2002) or the cyto-architectonically defined Brodmann areas. If one is investigating the relationship between function and anatomical structure and using multimodal methods, this may be the best or even only way to partition the brain. However, an ideal node for a functional GTA should be in itself as intra-nodal homogeneous and inter-nodal heterogeneous as possible (Fornito, Harrison, Zalesky, & Simmons, 2013). A macro-anatomically or cyto-architectonically defined region as for example the inferior parietal gyrus or middle temporal gyrus is functionally highly heterogeneous and does therefore not fulfill those criteria.

Purely data-driven statistical methods like clustering analysis techniques or independent component analysis (ICA) on the BOLD-time-series of the fMRI data might therefore be more suited to provide the functional homogeneity that is a necessary prerequisite for the correct application of GTA to intrinsic connectivity data. However, the data-driven parcellation approaches have their own set of limitations that influences the results of a GTA. One of the most important limitations is that the researcher who wants to use these statistical methods has to make some crucial preliminary decisions such as defining the number of clusters or components to extract. In addition, ICA-based partitions usually do not cover the whole brain and the degree of functional homogeneity of the so defined nodes might still be unsatisfactory (Gordon, Laumann, Adeyemo, Huckins, Kelley & Petersen, 2016; Shen, Tokoglu, Papademetris, & Constable, 2013).

Just recently, a fourth method to functionally partition the brain has become more widely used. The technique of functional border mapping identifies abrupt transitions in task-free intrinsic connectivity patterns and uses the so generated pattern of transition activity to parcellate the brain. Nodes generated by this technique are functionally highly homogeneous and overlap with known cyto-architectonic areas (Gordon et al., 2014).

b) The Pearson correlation – advantages and pitfalls

Not so intensively debated as the correct definition of functional nodes but nonetheless extremely important is the appropriate definition of links in task-free fMRI data. Because its meaning is intuitively understood and it is easily computed even for large networks, the Pearson correlation coefficient is most widely used to define links. However, correlations computed for intrinsic connectivity data do not represent direct links between the nodes but are generally interdependent of each other due to transitivity (Zalesky, Fornito & Bullmore, 2012; Petersen & Sporns, 2015). Therefore, they rather represent a mixture of the direct and indirect associations of a node (Power et al., 2014), which additionally reflects the synaptic efficiency of these connections (Petersen & Sporns, 2015). That is a problem insofar as one of the assumptions of some of the commonly used GTA measures is violated by the nature of the correlation coefficient. GTA measures like path, path length and degree and all GTA measures derived from these two metrics are based on the assumption that a link represents just one discrete connection between two nodes, as it is the case for structural brain connections that represent direct anatomical linkages. As a result, those metrics might not be appropriate for intrinsic connectivity data and should be interpreted very carefully when used (Petersen & Sporns, 2015).

c) Thresholding the networks – advantages and pitfalls

Related to the accurate definition of a link for task-free fMRI data is another problematic issue, i.e. the widely used practice to define a threshold that the connections have to surpass in order to separate the strongest and supposedly most important links from weak links. Despite the relevance of anticorrelations for a structured network architecture characterized by integrated, i.e. positive correlations, as well as clearly segregated, i.e. anticorrelations, network dynamics, anticorrelations are generally dismissed as a result of the thresholding procedure and just the positive correlations retained to build the graph. Consequently, important information about network differentiation or age- or disease- related degree of dedifferentiation is lost. Likewise, based on the assumption that only very strong connections reliably convey information about the functional organization of the brain, researchers working with GTA usually prefer high thresholds resulting in sparse networks. By doing so, they might again forfeit important information (Pessoa, 2014). Santarnecchi, Galli, Polizzotto,

Rossi and Rossi (2014) for example could show that a two-level connectivity structure, which combines the information of very strong but also moderately weak connections was better suited to explain inter-individual differences in IQ in a sample of young to middle aged adults (mean age = 34 years). They demonstrated that strong connections carried the information about the general functional organization of intelligence in the human brain, and weaker connections explained the inter-individual variability in intelligence (Santarnecchi et al., 2014).

d) Interim conclusion

This quite critical summary shows that the most common methods used to analyze task-free fMRI data are far from perfect and leave many important questions open. However, open questions and not ideal analysis approaches are by no means confined to task-free fMRI but inhere within all other neuroimaging techniques. Nevertheless, these concerns should not prevent researchers from using these techniques and analysis methods as long as there do not exist better ones and as long as they are well aware of the problems inherent in these methods and are interpreting their findings with the necessary caution.

5.1 First Study

Small changes, but huge impact? The right anterior insula's loss of connection strength during the transition of old to very old age[1]

5.1.1 Introduction

Growing old is not only associated with the aging brain's structural degeneration like progressive gray matter atrophy or loss of white matter integrity as evidenced by structural neuroimaging methods (Fjell et al., 2009; Good et al., 2001; Jäncke et al., 2015; Raz et al., 1997; Salat et al., 2004; Sowell et al., 2003) but also with cognitive and behavioral changes. Functional neuroimaging methods like PET or fMRI, on the other hand, were able to provide a slightly different point of view: Despite manifest structural decline, there is evidence for functional reorganization of the aging brain. It has been repeatedly observed that activation patterns of older brains are spatially more extensive in comparison to the activation patterns of younger participants even though young and old still perform at the same level. In addition, older adults seem to recruit additional brain regions. However, while task-induced fMRI studies investigating the aging brain generally observe roughly the same age-typical changes in the BOLD-signal patterns, the interpretations of these age-related patterns can be quite different, ranging from functional dedifferentiation (Berlingeri et al., 2013, Meinzer et al., 2012, Persson et al., 2007) to successful compensation (Cabeza et al., 2002, Davis et al., 2008).

About a decade ago, there was a paradigm shift in how these activation patterns are interpreted; away from a rather localization-oriented understanding that an area showing a significant increase in activity during the task has to be the brain region subserving just that specific function to a more network-oriented perspective. Thus, not a single brain area is thought to be responsible for a specific function but rather a coordinated interaction of a group of brain regions forming a network or even a cooperation of different functional networks; all interacting with each other in a fine-tuned concerted manner. Studies using different forms of connectivity analyses, analyzing task-induced as well as task-free fMRI data, were able to show that the aging brain can generally be characterized by reduced functional connection strengths in comparison to the brain of younger adults. This impacts the entire functional architecture of the brain. Not only the within-network connections decrease but also the between-network connections of the brain are affected and the different networks eventually seem to merge into each other and become more and more functionally dedifferentiated with age (Betzel et al., 2014; Geerligs et al., 2014; Meunier et al., 2009).

[1] A similar version of this paper was published as Muller, A.M., Mérillat, S., & Jäncke, L., (2016). Small changes, but huge impact? The right anterior insula's loss of connection strength during the transition of old to very old age. Front. Aging Neurosci. doi: 10.3389/fnagi.2016.00086.

Up to now, the knowledge about age-related alterations of the brain mainly comes from two branches of research. Firstly, there are a quite impressive number of cross-sectional studies comparing young with older adults. However, a limitation of the cross-sectional study design is that one is looking at both age groups as two quite homogeneous entities, i.e. young vs. old, and thereby neglecting the inner-group variance. Especially in groups of older subjects inter-individual differences can be large and people develop along different trajectories ranging from pathologically aging to healthy aging. Therefore, although we now have gained some knowledge about the differences between young and older brains, we still do not very well understand how age-related structural, functional and cognitive changes are related to each other and producing such a variety of aging trajectories even in the healthy aging older adults. The second line of research focuses on understanding the mechanism that underlie pathological aging. Here, the brain and behavioral data of healthy older adults are used in order to highlight the differences between disease and health, but the processes of healthy aging are not in the main interest. Consequently, one might consider understanding the mechanisms characterizing the healthy aging brain, i.e. understanding the changes of the aging brain from old to very old age and the implications for behavior and cognition, as a field of research still deserving more interest and effort.

The aim of the current study was to elucidate the age-related differences of the brain's functional architecture in a study group covering the age range from healthy old age (> 65 years) to very old healthy age (> 80 years) and to relate these functional differences to actual cognitive performance. We used task-free fMRI data because we wanted to eliminate all possible confounding factors, including the generally higher testing anxiety in older participants in a MRI scanner, the difficulty for older participants to gain familiarity with the artificial testing designs that are often unavoidable in fMRI experiments, the increased variation in the problem-solving strategies of older participants, the testing fatigue that usually occurs more quickly in older participants, and many other factors, all of which can heavily influence the findings of task-induced fMRI paradigms in older adults.

In order to be as unbiased as possible for the question at hand, we also decided in favor of a purely data driven analysis. Therefore, in a first step, we performed an Intrinsic Connectivity Contrast (ICC) analysis (Martuzzi et al., 2011). The ICC analysis is a whole-brain analysis method on the voxel-level that is able to identify the brain regions whose degree of connectedness with other brain regions is associated with increasing age without the need to determine a priori regions of interest. In a second step, we partitioned the brain into functionally defined clusters and then computed a connectivity analysis with the ICC clusters as source regions in order to specify their most relevant target regions. In a third step we correlated the resulting connectivity profile of each ICC cluster with age and with the participants' performance in working memory for the purpose of elucidating how the age-related alterations in the intrinsically active baseline configuration are associated with performance in a

cognitive function, which is very well established to be affected by the aging process (Draganski et al., 2014).

5.1.2 Methods

I. Participants

All MRI and behavioral data used in the study presented here were acquired in the context of the first data collection time point of the Longitudinal Healthy Aging Brain (LHAB) project. The LHAB is a longitudinal database project that started in 2011 at the International Normal Aging and Plasticity Imaging Center (INAPIC) of the University of Zurich and is currently run at the University Research Priority Program (URPP) "Dynamics of Healthy Aging" (Zöllig et al., 2011). By combining extensive cognitive testing with thorough MRI exams, the LHAB project aspires to investigate and understand the cognitive and neural mechanisms that promote healthy aging of the brain.

To qualify for participation in the LHAB project, interested persons had to fulfill the following criteria: Suitability for MRI assessments, 65 years or older, right handed, native Swiss-German or native German speakers and healthy, i.e. no history or current diagnosis of psychiatric or neurologic diseases, e.g. Parkinson's disease, Alzheimer's dementia, multiple sclerosis, migraine, further a MMSE score of > 26 and no chronic or acute medical conditions such as diabetes, tinnitus, and diseases of the hematopoietic system. All participants gave informed consent to the participation of the longitudinal project under the approval of the local ethics committee and in accordance with the declaration of Helsinki.

The data of 230 participants were acquired for the LHAB baseline measurement in 2011, but we had to exclude the data of 9 participants because of incompleteness of the MRI data, 32 due to motion artifacts over 2mm, one because of pathological high white matter lesion load, and one due to a diagnosis of type II diabetes shortly after the first time of assessment. Finally, the data of two other participants were not analyzed because they fulfilled the defined outlier criteria for the cognitive tests by scoring significantly lower ($\geq$ 3 SD) than the rest of the study sample in 10% of the overall 115 cognitive tests and subtests. As a consequence, we were able to use the data of 186 subjects (mean age = 70.4; SD = 4.8; 89 men and 97 women) for the study presented here. A two sample t test confirmed that there was no significant age difference between the remaining 186 participants and the excluded 44 subjects. However, as the LHAB database was especially designed to fulfill the specific requirements of a longitudinal analysis approach, the age distribution of the 186 subjects might be not so ideal for a cross-sectional approach that was used for the study presented here. The age

distributions showed a distinct predominance of participants (105 of the 186) covering a relatively small age range from 65 to 70 years. As a result, subjects aged 75 or older (= 32 participants) might be relatively underrepresented in the study sample (Figure 5.1.1).

Figure 5.1.1 The age-distribution of the study sample

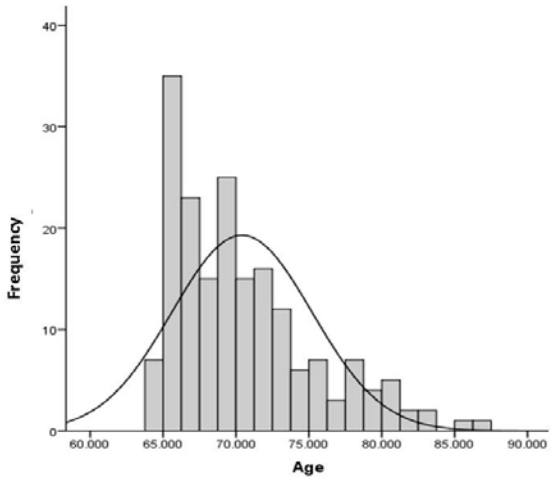

The figure 5.1.1 shows the age distribution for the 186 participants whose data were used in this study

II MRI-data acquisition

All MRI-data were acquired on the same Philips 3T Ingenia Medical Scanner with a Philips 15 channel head-coil at the University Hospital Zurich.

From the LHAB MRI protocol, the following images were used: 1. A T1 weighted TFE- SENSE sequence with TR = 8.2ms, TE = 3.7ms, Flip Angle = 90 (FOV = 240 × 160 × 240mm^3, matrix size = 256 × 256, isotropic voxel size = 0.94 × 0.94 × 1mm) 160 slices per volume. 2. A task-free blood oxygenation level-dependent signals (BOLD) single shot whole brain EPI with a TR = 2000ms, TE = 21ms, Flip Angle = 76; 43 transverse slices (FOV = 220 × 150 × 220mm^3, matrix size = 64 × 64, ascending acquisition without gap, anisotropic voxel size = 1.72/ 1.72/ 3.50mm, aligned to the AC-PC line), acquisition time 7.39min, 225 volumes.

For this part of the data acquisition, the participants were instructed to lay as motionless as possible, stay awake and think of nothing in particular while fixating a cross that was displayed on a screen outside the scanner and was visible for the participant by means of a mirror system attached to the receiver coil. Immediately after the task-free scan, each participant had to confirm that he/she had not fallen asleep during that part of the MRI exams.

III. Pre-processing of the fMRI data

All pre-processing steps of the MRI data listed below were performed using the SPM12 software (http://www.fil.ion.ucl.ac.uk/spm) implemented in Matlab (MATLAB R2014b, The Math Works Inc.). First, the first six volumes of the task-free fMRI data were discarded allowing for T1 saturation effects, leaving 219 volumes for the analysis and then realigned in a two-pass procedure to correct for potential head movements during the task-free scan. Second, the fMRI time series were slice time corrected for the ascending acquisition. Third, the T1 weighted anatomical image was coregistered to the mean functional image generated during the aligment step. Fourth, the T1 weighted anatomical images were segmented into the three tissue classes, gray matter, white matter and cerebrospinal fluid in native space. Fifth, a study-population specific GM template was generated using the DARTEL routine (Ashburner, 2007) implemented in SPM12 that allows for a high dimensional and nonlinear registration of the anatomical and functional images and their subsequent normalization to the MNI-template. The functional and the anatomical data subsequently used for the functional analyses were resampled to a 2mm isotropic voxel-size during this step. While the functional images for the ICC analysis were only minimally smoothed using an isotropic Gaussian kernel (FWHM 1mm) in order to minimize possible spurious correlations, the functional images used in ICA were smoothed using an isotropic Gaussian kernel (FWHM 6mm).

IV First analysis step: Intrinsic Connectivity Contrast (ICC) analyses on the pre-processed task free fMRI data

All following intrinsic connectivity (IC) analyses were performed using the Conn Toolbox (version 15a; http://www.nitrc.org/projects/conn) for SPM (Whitfield-Gabrieli & Nieto-Castanon, 2012).

Band-pass filtering and denoising of the data: The BOLD signal time-series for each participant was extracted and band-pass-filtered (0.008 – 0.09 Hz), as well as despiked and detrended. Non-neural low frequent (< 0.1 Hz) signals such as heart rate or respiration are able to modulate the intrinsic low frequent fluctuations of the BOLD-signal, which are the substructure investigated in task-free fMRI analysis. Therefore, it is important to correct for these physiological confounding signals. The Conn Toolbox accomplishes this by means of the CompCor method (Behzadi et al., 2007). As the final step during the denoising procedure implemented in the Conn Toolbox the motion parameters as well as the confounding signals calculated by the CompCor method are regressed out.

First level analyses: The Intrinsic Connectivity Contrast Power (ICCp) index (Martuzzi et al., 2011) is a whole brain voxel based measure of connectivity related to the graph theory analysis (GTA) measure "*degree*" (Rubinov & Sporns, 2010). Compared to the standard GTA methods an ICC analysis has two advantages: 1. An ICCp analysis is data driven and free of any need to define a seed based on a priori

assumptions about regions of interest. 2. The ICCp analysis does not depend on arbitrarily thresholding the network because the index works by weighting the connections of a voxel with the other voxels by the strength of these connections, respectively by the square number of its correlation strength, and therefore producing voxel based connectivity maps reflecting the existence as well as the strength of the connections of every individual voxel (Martuzzi et al., 2011).

On the second level or group level, the Conn Toolbox computes a GLM over all participants. To compute the connectivity maps illustrating the voxel level ICCp index and its correlation with age on group level, a high threshold for the peak voxels of $p < 0.01$ uncorrected, and an extension threshold for the clusters of $p < 0.05$ FWE corrected was used.

V Second analysis step: Seed correlation analyses to identify the functional network affiliation of the ICCp clusters

The ICCp maps of the first analysis step identified the clusters whose ICCp index was significantly correlated with age. The next step was to establish the intrinsic connectivity network (ICN) affiliation of each of these regions highlighted by the ICCp analysis by means of a subsequent seed correlation analysis (SCA).

To this end, correlation maps on voxel-level were computed by correlating the BOLD-signal time-course, averaged over all voxels constituting an ICCp cluster, with the BOLD-signal time-course of every other single voxel over the duration of the task-free scan for each participant.

For the group-level analysis the toolbox Conn implements contrasts for analyses at the voxel level as repeated-measures analyses by using ReML estimation of covariance components that are evaluated through F-statistical parameter maps. A height threshold for the peak voxel: $p < 0.001$ FDR corrected and an extension threshold for the clusters: $p < 0.001$ FWE corrected were used for the computing of the intrinsic connectivity map for the ICCp cluster.

VI Third analysis steps: Independent component analysis (ICA) to partition the brain into functionally relevant networks and ROIs

Results of an ICCp analysis can only highlight regions that demonstrate an association of connectedness with a specific feature like different states of consciousness, cognitive performance, or, as in this case, with increasing age. To identify which of the numerous connections a given ICCp cluster maintains with other brain regions have exactly triggered the ICCp findings additional analyses are necessary. Therefore, to get an understanding of how the ICCp clusters relate beyond their own

network to other ICN's of the brain, we performed an ICA in order to partition the brain into functionally meaningful networks and ROIs that are associated with these networks.

For this step, the functional images already smoothed with an isotropic Gaussian kernel of 6 mm (FWHM) during the preprocessing were additionally band-pass-filtered (0.008 – 0.09 Hz) and linearly detrended using the DPARS-F Toolbox (Chao-Gan & Yu-Feng, 2010).

For the ICA we used the MATLAB based Group ICA of fMRI Toolbox (GIFT) v3.0a (http://mialab.mrn.org/software/gift/). ICA is a statistical method of blind signal source separation. Assuming a generative model and a linear mixture of independent sources, it works with higher order statistics in order to maximize the spatial or temporal independence of the data and to identify the independent components hidden in the signal (Calhoun et al., 2001). In order to get components preferably representing whole networks instead of single ROIs or sub-networks we used a low dimensional approach and extracted 30 components using the Infomax algorithm. Of the extracted 30 components, 13 components could be identified as neurophysiologically relevant ICNs by visual inspection and by comparing them with the results of previous studies that likewise used a low-dimensional ICA approach to parcellate the brain into ICNs (Damoiseaux et al., 2006; Shirer et al, 2012). In the next step, we thresholded the ICA components at a z-value = 5 for the purpose of getting a sensible number of ROIs as well as reasonable sized ROIs and separated the components into their constituent single clusters using mricron (http://www.mccauslandcenter.sc.edu/mricro/index.html).

At last, we additionally computed the association of each of the 13 networks with the age of the participants in order to test for potential age-effects on the within network architecture of these networks.

VII Fourth analysis step: Connectivity analyses to investigate the relationship of the ICCp clusters among the other functional intrinsic connectivity networks (ICN)

To elucidate how the ICCp clusters relate to the other 13 ICNs identified by the ICA, the former were defined as source ROIs while the 93 ICA-derived clusters were defined as target ROIs.

VIIa Age Effects in the functional connection profile of the ICC clusters showing age-related alterations in connectedness

In a first step we computed the connection profile of each ICCp cluster for the purpose of understanding how the ICCp clusters generally relate to the 13 networks and 93 network ROIs identified by the previous ICA. In a next step, we repeated the analyses and correlated the connection

profile of each ICCp cluster with age in order to bring out the connections specifically affected by age-related differences in connectedness.

VIIb Additional steps to ensure the independency between search and test

We are well aware of the fact that we computed circular analyses by correlating the connection profiles of the ICCp clusters with the participants' age a second time. The reasons of this course of action were as follows: 1. As mentioned before in the method section, the age distribution of the study sample used in this paper was characterized by a majority of participants representing a relatively small age range from 65 to 70 years. Because of this predominance of 65 to 70 year olds in the age distribution, every existing age-effect in our study sample is reduced even though the effect is highly reliable and stable. To be able to detect such small effects, one needs statistical power, i.e. an appropriate large sample size. 2. Especially when associated with cognitive, behavioral, or other data collected outside the MRI scanner, connectivity analyses on task-free data are very power-sensitive. In order to be able to present results that also survive the correction for multiple comparisons, we have to use the whole sample of 186 participants. In order to prove our stand that we are dealing with a pure power-problem and not presenting results representing noise inflated to a pseudo effect by double dipping, we repeated all steps from the ICCp analysis to the two versions of connectivity analyses. To ensure the independency of our analyses this time, we blindly divided the sample of 186 participants in two equal halves, confirmed with a t test that the two sub-samples showed no significant age difference, and then used the first half of the sample for the ICCp analysis and the other half of the sample for the connectivity analyses. The results of these additional analyses are presented in an appendix and demonstrate that we did find almost identical results as presented in the main manuscript when using the divided data sets, but a more lenient statistical threshold ($p < 0.05$ uncorrected for multiple comparisons) on the level of the connectivity analyses.

VIIc Association of the age-related functional loss of connectedness with cognitive performance

The results of the ICCp analysis had highlighted three regions as exhibiting age-related alterations of functional connectedness. To test our hypothesis that these age-effects might as well be related to cognitive functions of our study population, we associated the connection profiles of the three ICCp clusters with the participants' performance scores in the LHAB test-battery.

In order to determine cognitive functions preferably associated with all three regions exhibiting age-related connectedness-effects alike; we used the NeuroSynth database (http://neurosynth.org; Yarkoni et al., 2011).

NeuroSynth is an internet based platform for large-scale, automated synthesis of functional magnetic resonance imaging (fMRI) data extracted from 10'903 published articles, which cover over 386'455 activations (status 23.04.2014). One of the advantages of this platform is its ability to compute posterior probabilities and therefore to quantify the probability that an activated voxel is associated with a particular cognitive function (Yarkoni et al., 2011). We used the NeuroSynth framework to compute the posterior probabilities for the three ICCp clusters' peak voxels of being involved in executive-control (search term: "executive"), working memory (search terms: "wm task" and "working memory"), attention (search term: "attention"), reasoning (search term: "reasoning"), memory (search term: "memory"), and processing speed (search term: "speed"). In combination, the posterior probabilities of all three ICCp peak coordinates loaded highest on working memory (Table 1). Based on this result, we used the participants' performance scores of the Corsi Block Tapping Test as implemented in the Wiener Testsystem (WTS) and the Two-Back Test as implemented in the Testbatterie Aufmerksamkeitspruefung (TAP) to relate them to the connection profile of the ICCp clusters. As both working memory tests showed significant gender effects, we computed the correlations while controlling for gender.

Table 5.1.1 Results of the NeuroSynth meta-analysis: Posterior probabilities for different higher cognitive functions

ICCp cluster & coordinates	Executive Control	Working Memory	Attention	Reasoning	Memory	Processing Speed
	"executive"	"wm task" & "working memory"	"attention"	"reasoning"	"memory"	"speed"
Right SFG (+02 +40 +54)	0.56	**0.70**	0.37	**0.78**	0.54	0.52
Right Insula (+34 + 28 +00)	**0.64**	**0.68**	0.57	0.52	0.59	0.58
Left SFG (-20 +32 +52)	0.36	**0.54**	**0.57**	0	**0.54**	0.35

The table 5.1.1 lists the posterior probabilities of the coordinates of the peak voxels of the three ICCp clusters to be involved in executive control, in working memory, attention, memory, and processing speed. The posterior probability quantifies the probability that an activated voxel is associated with a particular cognitive function. In the study presented here, we computed the posterior probabilities for the most important cognitive domains, which are standardly assessed by the LHAB-test battery. The highest posterior probabilities are marked in dark gray; the second highest values are highlighted by a light gray.

5.1.3 Results

I Results of the ICCp analysis

The ICCp analysis revealed three brain regions that exhibited a negative correlation of the ICCp index with the age of the participants, older subjects showed significantly lower ICCp index values in comparison to the younger subjects: The right superior frontal gyrus, the right insula, the left superior frontal gyrus (Figure 5.1.2a-c; for cluster size and peak voxels, please see Table 5.1.2). Interestingly, the ICCp analysis primarily stressed anterior brain regions as exhibiting age-related differences in connectedness.

Figure 5.1.2 Location of the three ICCp clusters and their corresponding SCA cluster maps

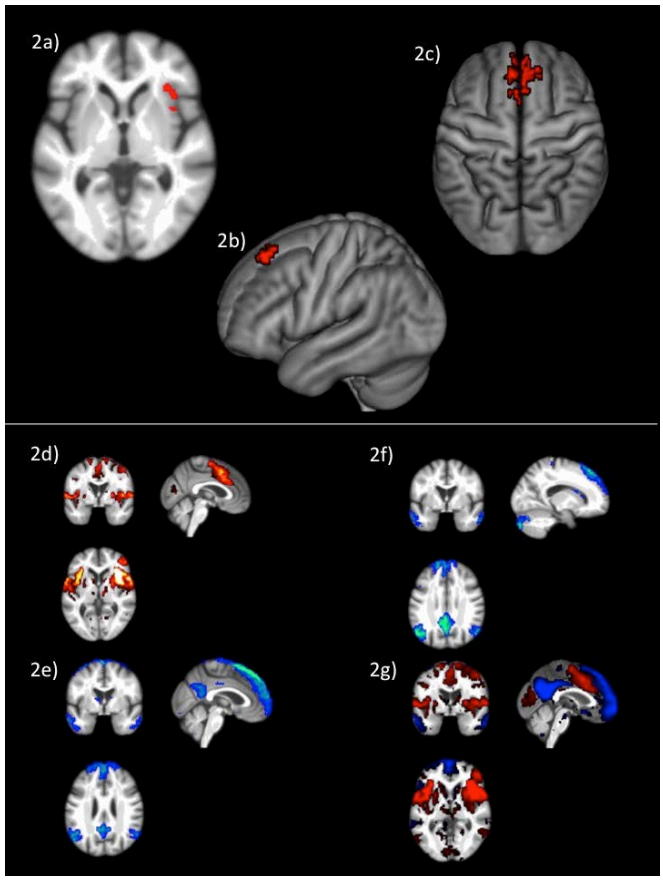

The superior part of the figure 5.1.2 shows the three brain regions exhibiting age-related loss of connectedness in the right and left superior frontal gyri, and the right anterior insula: 2a) ICCp cluster in the right anterior insula; 2b) ICCp cluster in the left superior frontal gyrus; 2c) ICCp cluster in the in the right midline part of the superior frontal gyrus (high threshold on voxel-level: $p < 0.01$ uncorrected; cluster threshold: $p < 0.05$ FWE corrected). The inferior part of the figure displays the corresponding SCA cluster maps computed with the ICCp clusters as seed-ROIs (high threshold on voxel-level: $p < 0.001$ FDR corrected; cluster threshold: $p < 0.001$ FWE corrected). 2d) The SCA cluster map of the ICCp cluster in the right insula shows the typical pattern of the cingulo-opercular network belonging to the task-positive system of the brain as symbolized by the warm color. 2e) and 2f) The SCA cluster maps of the two ICCp clusters in the superior frontal gyrus identifies them as a part of the DMN, the cool colors symbolize the task-negative system of the brain. 2g) The SCA cluster maps combined illustrates that the clear spatial separation of the DMN and the cingulo-opercular network.

Table 5.1.2 Results of the ICCp analysis

Coordinates of the Peak Voxel	Number of Voxels	Cluster p-FWE	Peak p-FWE	Peak p-uncorr	Location
+02 +40 +54	184	< 0.001	0.9999	< 0.001	Bilateral medial superior frontal gyrus
+34 +28 +00	68	0.0106	0.0390	< 0.001	Anterior right insula
-20 +32 +52	62	0.0209	1.00	< 0.001	Left superior frontal gyrus

The table 5.1.2 displays the coordinates of the peak voxels, the number of voxels covered by the ICCp cluster and their location in the brain (high threshold on voxel-level: $p < 0.01$ uncorrected; cluster threshold: $p < 0.05$ FWE corrected, only the negative correlation of the ICCp index with age was computed).

II Results of the subsequent SCA with the ICCp clusters as seed

To better understand the functional relevance of the ICCp clusters and to determine their network affiliation, we computed three SCAs.

a) The SCA map for the right superior frontal gyrus ICCp cluster characterized that cluster as belonging to the default mode network (DMN); the SCA map exhibited the classical DMN pattern (Gusnard et al., 2001; Raichle et al., 2001; Greicius et al., 2003) with clusters in the frontal midline reaching into the middle cingulate cortex, in the posterior cingulate cortex as well as in bilateral lateral parietal regions and temporal cortex (Figure 2f).

b) The SCA map computed for the ICCp cluster in the right anterior insula (Figure 2d) displayed clusters covering the bilateral thalami and basal ganglia, the bilateral insulae and reaching into the inferior frontal gyri; further clusters were located in the bilateral middle frontal gyri, the bilateral anterior cingulate cortices, the bilateral supramarginal gyrus/inferior parietal lobe regions extending into the superior temporal gyri, and the bilateral calcarine gyri. This specific cluster pattern corresponds to the cingulo-opercular network (CON) (Dosenbach et al. 2007, Sadaghiani & D'Esposito, 2014).

c) The intrinsic connectivity map for the ICCp cluster in the left superior frontal gyrus likewise showed the characteristic DMN pattern (Figure 2e) with clusters in the bilateral medial part of the superior frontal gyrus, in the bilateral posterior cingulate cortices, the bilateral angular gyri, and the temporal cortices as well as in the hippocampi.

III Results of the low dimensional ICA

We extracted 30 components and 13 of these could be identified as functional meaningful and well established ICNs: C02 cingulo-opercular network (CON); C04 ventral attention network (VAN); C05 auditory network (AUD); C13 anterior default mode network (antDMN); C14 visual network (VIS); C16 left executive control network (LECN); C18 language network (LANG); C20 limbic network (LIMB); C21 sensorimotor network (SMN); C23 higher visual network (highVIS); C25 right executive control network (RECN); C26 dorsal attention network (DAN); C28 posterior default mode network (postDMN).

To test for potential within-network age-effects of the 13 ICA components identified as biologically relevant ICNs, we computed the association of each network with age. None of the 13 networks defined by the ICA showed significant age-related degradation of within-network connectivity.

IV Results of the connectivity analyses: The connection profiles of the ICCp clusters

a) ICCp cluster in the right SFG: The SCA had highlighted this cluster as a part of the DMN and its connection profile confirmed this network affiliation since the clusters showed the strongest positive connections with target ROISs of the anterior DMN followed by ROIs of the language network and the LECN. As to be expected for a DMN region, the cluster exhibited significant anti-correlations with the DAN, the SMN, the AUD and both visual networks (Table 5.1.3; Figure 5.1.3a).

Table 5.1.3 General connection profile of the right SFG ICCp cluster

Targets	Effect Size	T(185)	p-uncorr	p-FDR		
C13_antDMN_rMedSFG	0.6	36.6	< 0.001	< 0.001		
C13_antDMN_lMedSFG	0.6	35.84	< 0.001	< 0.001		
All_ICCpCluster_LeftSFG	0.52	30.14	< 0.001	< 0.001		
C02_CON_lACC	0.42	25.33	< 0.001	< 0.001		
C13_antDMN_rCrus1	0.43	24.9	< 0.001	< 0.001	Long Distance	Cerebellum
C18_LANG_rCrus2	0.38	22.45	< 0.001	< 0.001	Long Distance	Cerebellum
C18_LANG_lMTG	0.35	21.71	< 0.001	< 0.001	Long Distance	Temporal
C13_antDMN_lANG	0.34	21.49	< 0.001	< 0.001	Long Distance	Parietal
C13_antDMN_lCrus2	0.34	20.46	< 0.001	< 0.001	Long Distance	Cerebellum
C18_LANG_lTriang	0.31	20.38	< 0.001	< 0.001		
C18_LANG_lCrus2	0.3	18.29	< 0.001	< 0.001	Long Distance	Cerebellum
C13_antDMN_lMTG	0.26	18.23	< 0.001	< 0.001	Long Distance	Temporal
C18_LANG_lITG	0.25	17.84	< 0.001	< 0.001	Long Distance	Temporal
C13_antDMN_lPCC	0.27	17.81	< 0.001	< 0.001	Long Distance	Parietal

C13_antDMN_rANG	0.27	16.74	< 0.001	< 0.001	Long Distance	Parietal
C18_LANG_rOrbit	0.25	16.71	< 0.001	< 0.001		
C18_LANG_lPrecun	0.25	16.11	< 0.001	< 0.001	Long Distance	Parietal
C13_antDMN_rPCC	0.24	16.04	< 0.001	< 0.001	Long Distance	Parietal
C02_CON_rACC	0.26	15.95	< 0.001	< 0.001		
C26_DAN_lIPL	-0.21	-15.5	< 0.001	< 0.001	Long Distance	Parietal

The table 5.1.3 lists the 20 target ROIs exhibiting the strongest connections with the source ROI located in the in the right midline of the superior frontal gyrus, the effect sizes, and the t-values. All connections to regions beyond the frontal cortex are defined as long-distance connections and the corresponding target region is specified in the last column of the table.

Figure 5.1.3 The general connection profile of the ICCp cluster in the right SFG and the connection profile associated with the participants' scores in the WM task

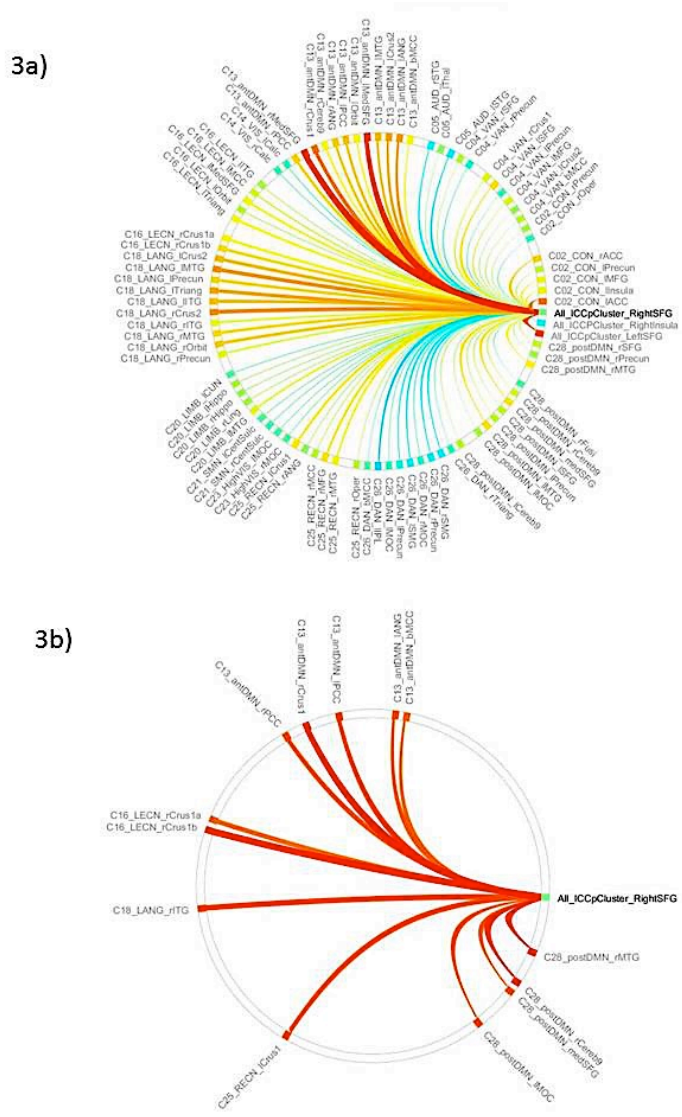

The figure 5.1.3a shows the general connection profile of the ICCp cluster located in the right superior frontal region ($p < 0.05$ FDR corrected (two-sided)). Figure 5.1.3b emphasizes the connections and corresponding target ROIs essential for successful performance in the

Corsi Block Tapping Test ($p < 0.05$ FDR corrected (two-sided)). The blue color range indicates negative connections, the red color range indicates positive connections, dark shades of blue/red indicate strong connections, and light shades of blue/red indicate weaker connections

b) ICCp cluster in the right anterior insula: The SCA results had assigned this ICCp cluster as a constituent region of the CON and its connection profile corroborated this network affiliation. The cluster in the right anterior insula exhibited the strongest positive correlations with the ROIs of the CON followed by ROIs of the DAN, VAN and AUD. As typical for a CON region, the right anterior insula showed significant anti-correlations with the anterior and posterior DMNs and the LANG (Table 5.1.4; Figure 5.1.4a).

Table 5.1.4 General connection profile of the right anterior insula ICCp cluster

Targets	Effect Size	T(185)	p-uncorr	p-FDR		
C02_CON_rInsula	0.74	47.95	< 0.001	< 0.001		
C05_AUD_rSTG	0.43	32.41	< 0.001	< 0.001	Long Distance	Temporal
C05_AUD_lSTG	0.38	26.24	< 0.001	< 0.001	Long Distance	Temporal
C04_VAN_bMCC	0.37	26.24	< 0.001	< 0.001		
C02_CON_rACC	0.41	25.62	< 0.001	< 0.001		
C13_antDMN_rPCC	-0.34	-25.2	< 0.001	< 0.001	Long Distance	Parietal
C26_DAN_rSMG	0.39	24.88	< 0.001	< 0.001	Long Distance	Parietal
C13_antDMN_lPCC	-0.36	-24.7	< 0.001	< 0.001	Long Distance	Parietal
C25_RECN_rOper	0.41	24.64	< 0.001	< 0.001		
C26_DAN_lSMG	0.34	22.9	< 0.001	< 0.001	Long Distance	Parietal
C13_antDMN_lANG	-0.34	-22	< 0.001	< 0.001	Long Distance	Parietal
C13_antDMN_rCrus1	-0.3	-21.7	< 0.001	< 0.001	Long Distance	Cerebellum
C04_VAN_rMFG	0.32	21.32	< 0.001	< 0.001		
C02_CON_lInsula	0.3	20.7	< 0.001	< 0.001		
C18_LANG_lPrecun	-0.3	-20.2	< 0.001	< 0.001	Long Distance	Parietal
C13_antDMN_lMTG	-0.27	-19.8	< 0.001	< 0.001	Long Distance	Temporal
All_ICCpCluster_LeftSFG	-0.27	-19.7	< 0.001	< 0.001		
C02_CON_rOper	0.28	18.9	< 0.001	< 0.001		
C18_LANG_rCrus2	-0.23	-18	< 0.001	< 0.001	Long Distance	Cerebellum
C13_antDMN_lMedSFG	-0.25	-17.1	< 0.001	< 0.001		

The table 5.1.4 lists the 20 target ROIs exhibiting the strongest connections with the source ROI located in the in the right anterior insula, the effect sizes, and the t-values. All connections to regions beyond the frontal cortex are defined as long-distance connections and the corresponding target region is specified in the last column of the table.

Figure 5.1.4 The general connection profile of the ICCp cluster in the right insula and the connection profiles associated with age and with the participants' scores in the WM task.

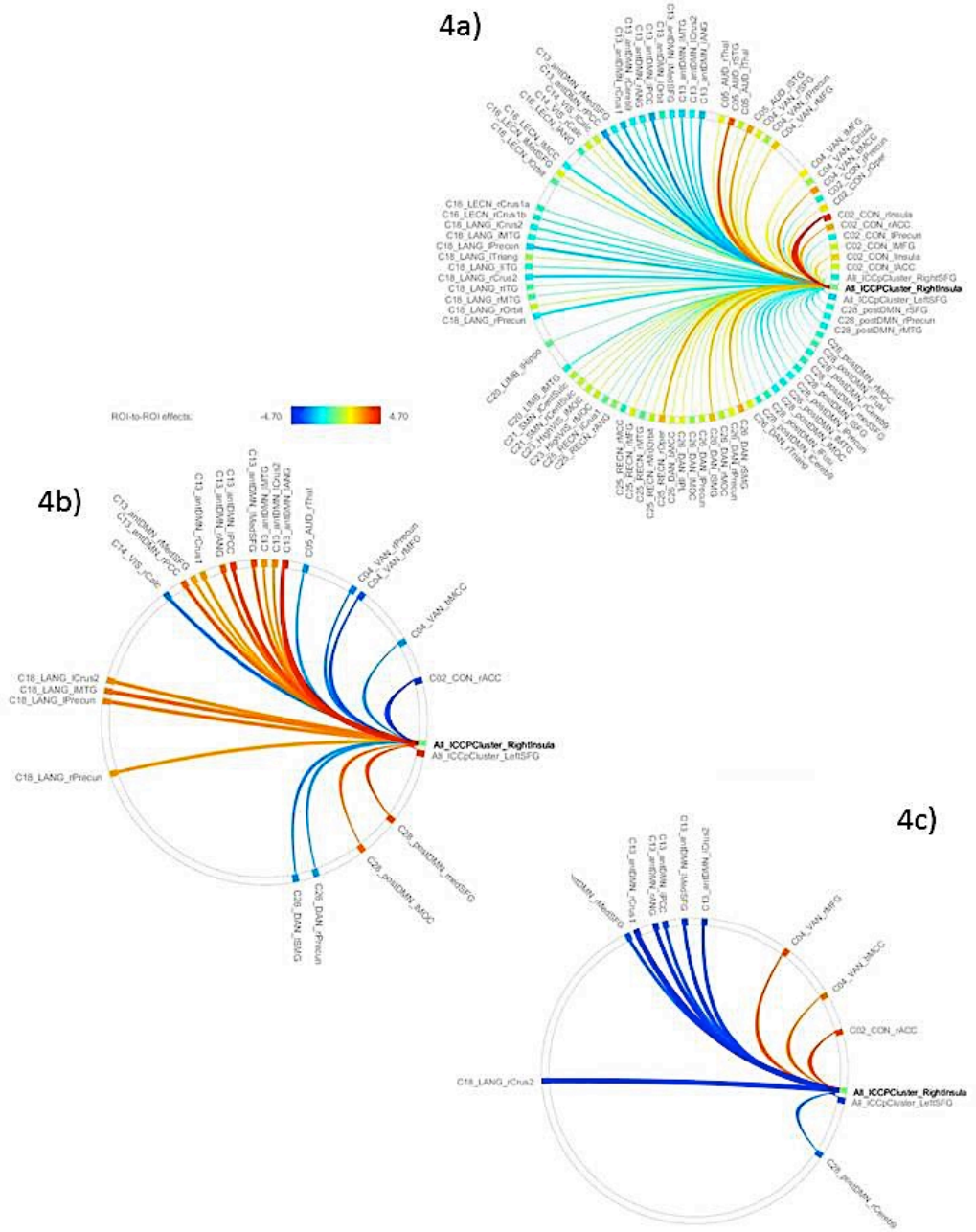

The figure 5.1.4a shows the general connection profile of the ICCp cluster located in the right anterior insula ($p < 0.05$ FDR corrected (two-sided)). Figure 5.1.4b highlights the connections and corresponding target ROIs showing a significant reduction of strength with increasing age ($p < 0.05$ FDR corrected (two-sided)). Figure 5.1.4c emphasizes the connections and corresponding target ROIs essential for successful performance in the Corsi Block Tapping Test ($p < 0.05$ FDR corrected (two-sided)). Color code for 5.1.4a and 5.1.4c: The blue color range indicates negative connections, the red color range indicates positive connections, dark shades of blue/red indicate strong connections, and light shades of blue/red indicate weaker connections. Color code for 5.1.4b: The blue color range highlights connections with a tendency to become more anti-correlated with increasing age, the red color range highlights connections showing a trend to become more positively correlated with age. The intensity of the colors used indicates the significance of the strength reductions.

c) ICCp cluster in the left SFG: The SCA identified this cluster as functionally belonging to the DMN. Consistent with that affiliation the cluster exhibited the strongest positive connections to the ROIs of the anterior DMN, followed by the ROIs of the LANG, LECN and postDMN (Table 5.1.5; Figure 5.1.5a).

Table 5.1.5 General connection profile of the left SFG ICCp cluster

Targets	Effect Size	T(185)	p-uncorr	p-FDR		
C13_antDMN_lMedSFG	0.88	41.79	< 0.001	< 0.001		
C13_antDMN_rMedSFG	0.57	35.24	< 0.001	< 0.001		
C13_antDMN_lANG	0.61	32.02	< 0.001	< 0.001	Long Distance	Parietal
All_ICCpCluster_RightSFG	0.52	30.14	< 0.001	< 0.001		
C13_antDMN_rCrus1	0.52	26.85	< 0.001	< 0.001	Long Distance	Cerebellum
C13_antDMN_lPCC	0.54	26.33	< 0.001	< 0.001	Long Distance	Parietal
C13_antDMN_rPCC	0.43	23.49	< 0.001	< 0.001	Long Distance	Parietal
C13_antDMN_lMTG	0.4	22.84	< 0.001	< 0.001	Long Distance	Temporal
C18_LANG_lPrecun	0.42	22.32	< 0.001	< 0.001	Long Distance	Parietal
C16_LECN_lMCC	0.34	21.96	< 0.001	< 0.001		
C18_LANG_lMTG	0.37	21.3	< 0.001	< 0.001	Long Distance	Temporal
C16_LECN_rCrus1b	0.35	21.17	< 0.001	< 0.001	Long Distance	Cerebellum
C28_postDMN_medSFG	0.39	21.02	< 0.001	< 0.001		
C18_LANG_rCrus2	0.36	20.99	< 0.001	< 0.001	Long Distance	Cerebellum
C13_antDMN_rANG	0.36	20.36	< 0.001	< 0.001	Long Distance	Parietal
All_ICCPCluster_RightInsula	-0.27	-19.73	< 0.001	< 0.001		
C26_DAN_rSMG	-0.31	-19.71	< 0.001	< 0.001	Long Distance	Parietal
C16_LECN_lTriang	0.34	19.28	< 0.001	< 0.001		
C04_VAN_lSFG	0.32	19.01	< 0.001	< 0.001		
C13_antDMN_rCereb9	0.25	18.43	< 0.001	< 0.001	Long Distance	Cerebellum

The table 5.1.5 lists the 20 target ROIs exhibiting the strongest connections with the source ROI located in the in the left superior frontal gyrus, the effect sizes, and the t-values. All connections to regions beyond the frontal cortex are defined as long-distance connections and the corresponding target region is specified in the last column of the table.

Figure 5.1.5 The general connection profile of the ICCp cluster in the left superior frontal gyrus and the connection profiles associated with age and with the participants' scores in the WM task.

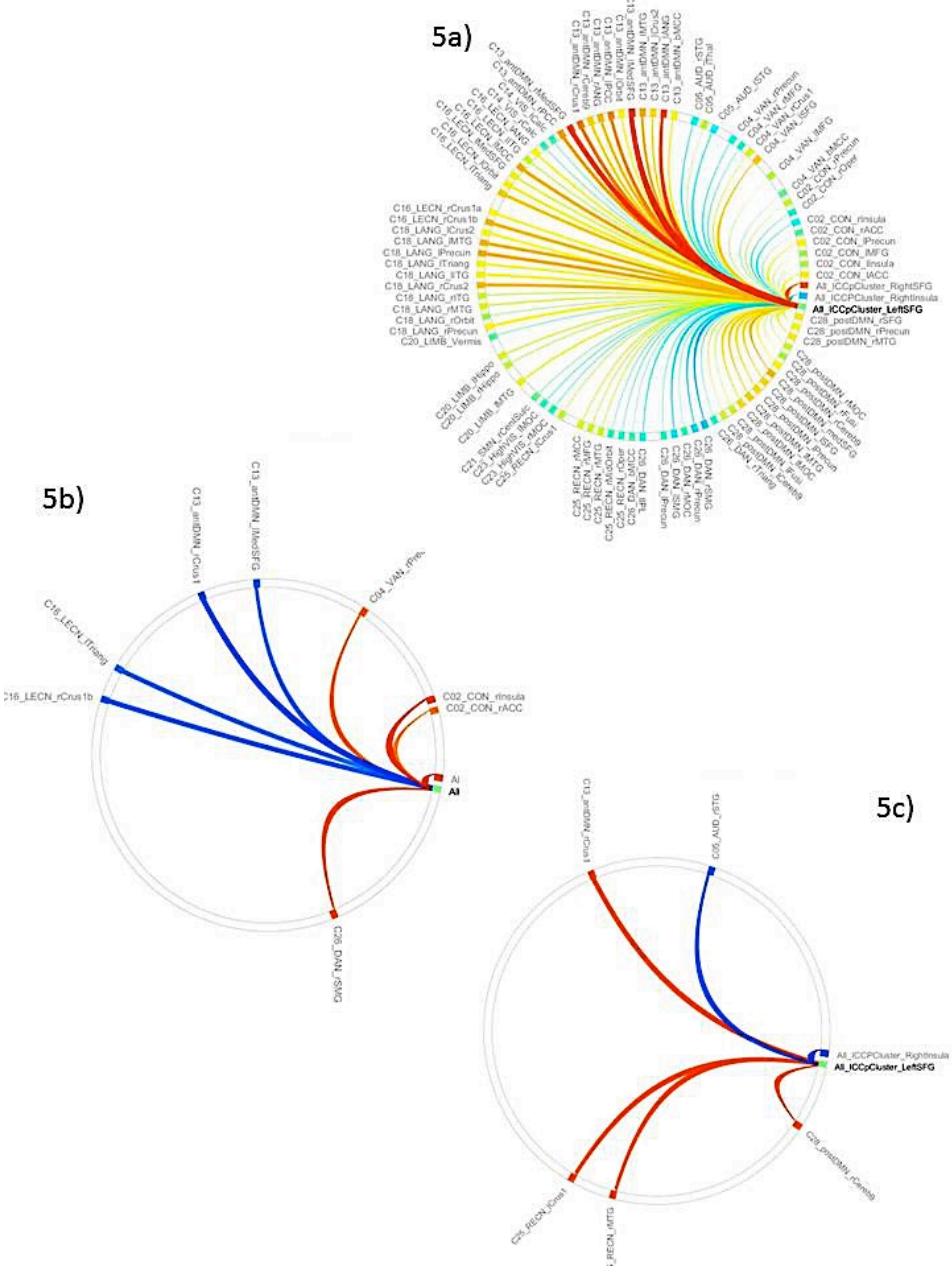

Figure 5.1.5a shows the general connection profile of the ICCp cluster located in the left superior frontal gyrus ($p < 0.05$ FDR corrected (two-sided)). Figure 5.1.5b highlights the connections and corresponding target ROIs showing a significant reduction of strength with increasing age ($p < 0.05$ FDR corrected (two-sided)). Figure 5.1.5c emphasizes the connections and corresponding target ROIs essential for successful performance in the Corsi Block Tapping Test ($p < 0.05$ FDR corrected (two-sided)). Color code for 5.1.5a and 5.1.5c: The blue color range indicates negative connections, the red color range indicates positive connections, dark shades of blue/red indicate strong connections, and light shades of blue/red indicate weaker connections. Color code for 5.1.5b: The blue color range highlights connections with a tendency to become more anti-correlated with increasing age, the red color range highlights connections showing a trend to became more positively correlated with age. The intensity of the colors used indicates the significance of the strength reductions.

V Age-related alterations of the connection-profiles

The ICC analysis had shown that some brain regions exhibited a loss of connectedness with increasing age. In order to get a better understanding of which target regions were most affected, we performed a second connectivity analysis with the aim to elucidate the age-specific association of the connectivity strengths of the ICC source ROIs to the ICA target ROI's.

In contrast to the fine-grained ICC analysis on single voxel level, only two of the ICCp clusters showed significant age effects in their connection profiles on ROI-level that also survived the correction for multiple comparisons. In short, the observed age-effects on the connection profiles can be summarized as follows: Age and connection strength showed an inverse relationship.

a) With increasing age, the ICCp cluster in the right anterior insula exhibited an overall decrease of connection strength. Both connection types, positively as well as negatively correlated networks or single ROIs were affected by this decrease. Therefore, originally anti-correlated regions like ROI's of the anterior and posterior DMNs now showed a reduction in anti-correlation and therefore a trend to become positively connected with age, while the connection strengths of originally positively correlated ROIs of the CON and the VAN decreased and showed a tendency to become anti-correlated. From the 24 source ROI - target ROI connections showing age-effects, 17 connections were long-distance connections to the temporal (2), parietal (9), and occipital (2) regions of the brain as well as to the cerebellum (3) (Table 5.1.6; Figure 5.1.4b).

Table 5.1.6 Connection profile of the right anterior insula ICCp cluster associated with age

Targets	Effect Size	T(184)	p-unc	p-FDR		
C13_antDMN_lANG	0.07	4.7	< 0.001	< 0.001	Long Distance	Parietal
All_ICCpCluster_LeftSFG	0.06	4.25	< 0.001	0.002		
C02_CON_rACC	-0.06	-3.98	< 0.001	0.003		
C13_antDMN_lPCC	0.05	3.73	< 0.001	0.006	Long Distance	Parietal
C28_postDMN_medSFG	0.05	3.44	< 0.001	0.014		
C13_antDMN_lMedSFG	0.05	3.31	0.001	0.017		
C04_VAN_rMFG	-0.05	-3.24	0.001	0.017		
C13_antDMN_rPCC	0.04	3.24	0.001	0.017	Long Distance	Parietal
C13_antDMN_rANG	0.05	3.2	0.002	0.017	Long Distance	Parietal
C18_LANG_lMTG	0.04	3.15	0.002	0.018	Long Distance	Temporal
C28_postDMN_lMOC	0.05	3.07	0.002	0.021	Long Distance	Occipital
C18_LANG_lPrecun	0.04	2.93	0.004	0.03	Long Distance	Parietal
C13_antDMN_lCrus2	0.04	2.91	0.004	0.03	Long Distance	Cerebellum

C14_VIS_rCalc	-0.04	-2.84	0.005	0.033	Long Distance	Occipital
C18_LANG_lCrus2	0.04	2.83	0.005	0.033	Long Distance	Cerebellum
C04_VAN_rPrecun	-0.04	-2.8	0.006	0.034	Long Distance	Parietal
C13_antDMN_lMTG	0.04	2.71	0.007	0.04	Long Distance	Temporal
C26_DAN_lSMG	-0.04	-2.68	0.008	0.04	Long Distance	Parietal
C13_antDMN_rCrus1	0.04	2.68	0.008	0.04	Long Distance	Cerebellum
C18_LANG_rPrecun	0.04	2.67	0.008	0.04	Long Distance	Parietal
C04_VAN_bMCC	-0.04	-2.64	0.009	0.041		
C13_antDMN_rMedSFG	0.04	2.6	0.01	0.044		
C05_AUD_rThal	-0.03	-2.57	0.011	0.044	Long Distance	Subcortical
C26_DAN_rPrecun	-0.03	-2.57	0.011	0.044	Long Distance	Parietal

The table 5.1.6 lists the connections of the right insula ICCp cluster and the corresponding target ROIs that exhibit an age-related reduction in connection strength or an anti-correlation of age and connection strength ($p < 0.05$ FDR corrected (two-sided)), the effect sizes, and the t-values. All connections to regions beyond the frontal cortex are defined as long-distance connections and the corresponding target region is specified in the last column of the table.

b) The same reverse relationship between increasing age and connection strength could be observed for the ICCp cluster in the left SFG: Originally positively connected networks/ROIs now showed a trend to become anti-correlated with increasing age and vice versa, originally anti-correlated networks/ROI's exhibited a trend to become positively correlated. Thus, the originally anti-correlated left SFG became more positively connected with ROIs of the CON, DAN and VAN in association with age. In contrast, ROIs of the LECN and anterior DMN that originally had showed a clear positive correlation with the ICCp cluster now exhibited an decrease in connections strength, i.e. they became more anti-correlated with increasing age. Of the eight source ROI – target ROI connections affected by age four connections were long-distance connections to parietal brain regions (2) and the cerebellum (2) (Table 5.1.7; Figure 5.1.5b).

Table 5.1.7 Connection profile of the left SFG ICCp cluster associated with age

Targets	Effect Size	T(184)	p-uncorr	p-FDR		
All_ICCpCluster_RightInsula	0.06	4.25	0.000033	0.002603		
C02_CON_rInsula	0.06	4.13	0.000054	0.002603		
C13_antDMN_rCrus1	-0.07	-3.72	0.000263	0.007199	Long Distance	Cerebellum
C26_DAN_rSMG	0.06	3.69	0.0003	0.007199	Long Distance	Parietal
C04_VAN_rPrecun	0.04	3.15	0.001881	0.036084	Long Distance	Parietal
C16_LECN_rCrus1b	-0.05	-3.1	0.002255	0.036084	Long Distance	Cerebellum
C13_antDMN_lMedSFG	-0.06	-3.03	0.002802	0.038421		
C16_LECN_lTriang	-0.05	-2.94	0.003689	0.040121		
C02_CON_rACC	0.05	2.93	0.003761	0.040121		

The table 5.1.7 lists the connections of the left SFG ICCp cluster and the corresponding target ROIs that exhibit an age-related reduction in connection strength or an anti-correlation of age and connection strength ($p < 0.05$ FDR corrected (two-sided)), the effect sizes, and the t-values. All connections to regions beyond the frontal cortex are defined as long-distance connections and the corresponding target region is specified in the last column of the table.

VI Results of the connectivity analysis investigating the association of the three ICCp clusters' connection profiles and working memory performance

We computed the main effect of the participants' performance in two working memory tests (2-back Test and Corsi Block Tapping Test) and the connection profiles of the three ICCp clusters while controlling for gender effects. After correction for multiple comparisons, only the Corsi Block Tapping Test exhibited significant associations with the following connection profiles:

a) Right superior frontal gyrus: The connection profile of the right SFG associated with the participants' performance in the Corsi Block Tapping Test highlighted only positive long-distance connections with target ROIs primarily belonging to the anterior and posterior DMN and located in the right temporal cortex, the bilateral parietal cortex and the cerebellum. After controlling for age, four positive long-distance connections to the cerebellum (antDMN_rCrus1, LECN_rCrus1b, postDMN_rCereb9) and to the right middle temporal gyrus (postDMN_rMTG) still seemed to be essential for a successful performance (Table 5.1.8; Figure 5.1.3b).

Table 5.1.8 Connection profile of the right SFG ICCp cluster associated with working memory performance

Targets	Effect Size	T(182)	p-uncorr	p-FDR		
C13_antDMN_rCrus1	0.07	3.87	0.000152	0.00627	Long Distance	Cerebellum
C28_postDMN_rMTG	0.05	3.81	0.000187	0.00627	Long Distance	Temporal
C28_postDMN_rCereb9	0.05	3.8	0.000198	0.00627	Long Distance	Cerebellum
C16_LECN_rCrus1b	0.06	3.72	0.000261	0.00627	Long Distance	Cerebellum
C13_antDMN_lPCC	0.05	3.22	0.001495	0.028691	Long Distance	Parietal
C18_LANG_rITG	0.04	3.13	0.00205	0.028691	Long Distance	Temporal
C25_RECN_lCrus1	0.05	3.12	0.002092	0.028691	Long Distance	Cerebellum
C28_postDMN_lMOC	0.05	3.04	0.002687	0.032242	Long Distance	Occipital
C13_antDMN_rPCC	0.05	2.93	0.003837	0.036335	Long Distance	Parietal
C13_antDMN_lANG	0.05	2.92	0.003925	0.036335	Long Distance	Parietal
C28_postDMN_medSFG	0.05	2.9	0.004163	0.036335		
C13_antDMN_bMCC	0.04	2.78	0.006062	0.046418		
C16_LECN_rCrus1a	0.04	2.76	0.006286	0.046418	Long Distance	Cerebellum

The table 5.1.8 lists the connections and the corresponding target ROIs that have exhibited a significant association ($p < 0.05$ FDR corrected (two-sided)) with the participants' performance in working memory, operationalized by the number of correct sequences in the Corsi Block Tapping Test. All connections to regions beyond the frontal cortex are defined as long-distance connections and the corresponding target region is specified in the last column of the table.

b) Right anterior insula: The number of correct trials in Corsi Block Tapping Test depended on the right anterior insula's preserved negative correlations with ROIs in the frontal cortex, the middle cingulate cortex, the parietal cortex, and the cerebellum. When we repeated the connectivity analysis and additionally controlled for age effects, only a negative correlated connection to a ROI of the antDMN in the right cerebellum crus I showed a significant association with number of correct trials in the Corsi Block Tapping Test (Table 5.1.9; Figure 5.1.4c).

Table 5.1.9 Connection profile of the right anterior insula ICCp cluster associated with working memory performance

Targets	Effect Size	T(182)	p-uncorr	p-FDR		
C13_antDMN_rCrus1*	-0.06	-4.49	< 0.001	0.001	Long Distance	Cerebellum
All_ICCpCluster_LeftSFG*	-0.05	-3.85	< 0.001	0.006		
C18_LANG_rCrus2	-0.05	-3.81	< 0.001	0.006	Long Distance	Cerebellum
C13_antDMN_rANG*	-0.05	-3.65	< 0.001	0.008	Long Distance	Parietal
C13_antDMN_lMedSFG*	-0.05	-3.58	< 0.001	0.008		
C13_antDMN_lCrus2*	-0.05	-3.4	< 0.001	0.012	Long Distance	Cerebellum
C02_CON_rACC*	0.05	3.38	< 0.001	0.012		
C04_VAN_rMFG*	0.05	3.2	0.002	0.019		
C13_antDMN_lPCC*	-0.05	-3.15	0.002	0.02	Long Distance	Parietal
C13_antDMN_rMedSFG*	-0.04	-3.01	0.003	0.027		
C04_VAN_bMCC*	0.04	3	0.003	0.027		
C28_postDMN_rCereb9	-0.04	-2.83	0.005	0.041	Long Distance	Cerebellum

The table 5.1.9 lists the connections and the corresponding target ROIs that have exhibited a significant association ($p < 0.05$ FDR corrected (two-sided)) with the participant's performance in working memory, operationalized by the number of correct sequences in the Corsi Block Tapping Test. All connections to regions beyond the frontal cortex are defined as long-distance connections and the corresponding target region is specified in the last column of the table. The asterisks indicate connections that had also showed significant age-effects.

c) Left superior frontal gyrus: Preserved positive long-distance connections to the right middle temporal gyrus and to the bilateral cerebellum (postDMN_rCereb9, antDMN_rCrus1, RECN_lCrus1) as well as preserved negative connections to target ROIs in the right superior temporal gyrus (AUD_rSTG) and to the ICCp cluster located in the right anterior insula were correlated with a

successful performance in the Corsi Block Tapping test. After controlling for age, none of these connections survived the correction for multiple comparisons (Table 5.1.10; Figure 5.1.5c).

Table 5.1.10 Connection profile of the left SFG ICCp cluster associated with working memory performance

Targets	Effect Size	T(182)	p-uncorr	p-FDR		
All_ICCpCluster_RightInsula*	-0.05	-3.85	0.000164	0.015782		
C28_postDMN_rCereb9	0.05	3.26	0.001316	0.039922	Long Distance	Cerebellum
C13_antDMN_rCrus1*	0.06	3.17	0.001772	0.039922	Long Distance	Cerebellum
C25_RECN_rMTG	0.05	3.1	0.002208	0.039922	Long Distance	Temporal
C25_RECN_lCrus1	0.04	3.1	0.002227	0.039922	Long Distance	Cerebellum
C05_AUD_rSTG	-0.04	-3.07	0.002495	0.039922	Long Distance	Temporal

The table 5.1.10 lists the connections and the corresponding target ROIs that have exhibited a significant association ($p < 0.05$ FDR corrected (two-sided)) with the participants' performance in working memory, operationalized by the number of correct sequences in the Corsi Block Tapping Test. All connections to regions beyond the frontal cortex are defined as long-distance connections and the corresponding target region is specified in the last column of the table. The asterisks indicate connections that had also showed significant age-effects.

5.1.4 Discussion

Increasing age is accompanied by structural and functional brain alterations, which have the potential to affect functions across all cognitive, emotional, and behavioral domains. Previous studies had demonstrated a degradation of the functional architecture of the aging brain as early as in the intrinsically active functional baseline configuration. Based on the assumption that this intrinsically active functional network structure is at least to some degree related to actual goal driven behavior and cognition, our study aimed to investigate which brain regions already exhibit age-related loss of regional inter-connectedness in a task-free condition and how that loss of connectivity might impair behavior and cognition in a large sample of 186 adults in the transition from old to very old age.

In a first step, we performed a purely data-driven ICCp analysis on voxel level with the aim of finding brain regions exhibiting differences of connectedness with increasing age. The ICCp analysis highlighted three regions, all located in the anterior part of the brain.

To determine the ICN affiliation of these regions we then computed a SCA for each of these ICCp clusters. The combination of ICCp analysis and SCA marked two ICNs, the DMN and the cingulo-opercular network, as showing age-related differences, more specifically a decrease of connectedness

of their specific constituent regions in the left and right superior frontal gyri, and in the right anterior insula respectively.

In a third step, we wanted to understand how these ICCp regions were embedded in the functional baseline architecture of the whole brain and which of their target regions were especially affected by these age-related connection changes. For that purpose, we computed three different connectivity analyses, a first analysis to establish the general functional connection profile of each of these ICCp clusters, a second to investigate the influence of higher age on these connection profiles and a third to investigate the possible effects of these age-related alterations on working memory. The results of the first two connectivity analyses can be summed up as follows: Age and connection strength exhibited an anti-correlation: In participants of higher age, the connection profiles of the ICCp clusters showed signs of functional dedifferentiation on the ROI-to-ROI level due to a reduction in connections strength. Especially long-range connections were affected by these reductions in connection strength. The third connectivity analysis demonstrated that these age-effects might have consequences for cognition: The same connections emphasized by the prior connectivity analysis as showing age-related decrease were also stressed as relevant for working memory. Especially preserved long-distance connections from the frontal cortex into the cerebellum, the lateral and medial parts of the parietal cortex to temporal regions seemed to be essential for a successful working memory performance. In the next sections, we will discuss the relevance of our findings in more detail.

a) Frontal regions seem more affected by age-related alterations of connectedness than regions in the posterior part of the brain

The ICCp analysis on voxel-level mainly highlighted frontal regions as affected in connectedness by increasing age. This finding is remarkable even more because it seems quite paradoxical when combined with the subsequent connectivity analyses that revealed long-distance connections from these frontal regions into the posterior part of the brain as affected by age. This observation inevitably triggers the question: When the source region is affected by a decrease in connectedness should the corresponding target region not also show a decrease in connectedness? To understand the paradox that the ICCp analysis stressed the frontal regions but not their respective target ROIs located in the posterior parts of the brain, one has to look closer at the ICCp index. The value of the ICCp index is determined by the existence of a connection and by the strength of this connection. When only frontal source ROIs show a decrease in the ICCp index but not their posterior target regions then this unilateral phenomenon can only be explained by a decrease in connection strength of the frontal regions while the posterior regions do not show such degradation. Therefore, one might conclude that the results of the ICCp analyses could indicate that the anterior frontal regions of the brain show a

different trajectory for connection strength, respectively a faster decrease in connection strength than the posterior parts of the brain with increasing age.

b) The role of the right dorsal anterior insula

The most important finding of our study is the right anterior insula's age-related decrease of connectedness observed for the older participants of the study sample that covered an age range from 65 to 85 years.

The right anterior insula is one of the most influential output hubs of the brain (Sridaharan et al., 2008) because it is causally initiating the switching from the brain's internal modus operandi to the external modus operandi vital for all successful goal-directed behavior (Goulden et al., 2014; Menon & Uddin, 2010; Sridaharan et al., 2008). The internal modus operandi of the brain is characterized by high activity of the default mode network. Although the default mode network's role in the brain is still not fully understood, the so called "default mode" of the brain can be described as a highly dynamic and exploratory state of the brain characterized by a high variance of synchrony over time (Hellyer et al., 2014). However, for successfully performing goal-directed behavior the brain has to change from the rather unconstrained default mode state into a functionally focused state, which is characterized by increased global synchrony and by a coordinated activity of the control and attention networks of the brain (Hellyer et al., 2014). The right anterior insula initiates this switching from one brain state into the other by signaling the DMN to deactivate and the ECN to activate. A dysfunction of the right anterior insula and as a consequence a disturbed dynamic interplay of ECN and DMN in order to generate and maintain successful goal-directed behavior is associated with schizophrenia, autism and AHDS (Menon & Uddin, 2010; Moran et al., 2013; Sheffield et al., 2015; Uddin 2015) but also with cognitive impairments after traumatic brain injury (Bonelle et al., 2012, Jilka et al., 2014).

The SCA demonstrated the ICCp cluster of the right anterior insula as belonging to the cingulo-opercular network, i.e. to one of the prominent control networks constituting the task-positive system of the brain, which has an antagonistic relation to the task-negative system of the brain as presented by the DMN. Bearing this antagonistic intrinsic architecture of the brain in mind, one would expect the anterior insula to show positive correlations with all other networks of the task-positive component while exhibiting negative correlations with the DMN. Nevertheless, we found first indicators of age-related functional degradation in our study sample as early as in the general connection profile of the right anterior insula ICCp cluster because it showed preserved negative correlations with the target-ROIs of both default mode networks but only partially the expected positive correlations with the RECN and LECN (Cohen et al., 2014). When we associated the connection profile of the right anterior insula with age there was clear evidence, that the seemingly preserved negative correlations with the

anterior and the posterior DMN exhibited a tendency to become weaker, respectively a trend to become more positively correlated with increasing age in our study sample.

Age-related alterations of the functioning of the DMN, especially a failure of the DMN to timely deactivate during cognitive demanding tasks is not a new finding but was already demonstrated by a number of previous studies investigating the aging brain (Gordon et al., 2014, Grady et al., 2006, Grady et al., 2010, Meinzer et al., 2012, Persson et al., 2007). However, the potential causal implication of the right anterior insula in this age-related dysfunctional deactivation of the DMN might present a new insight for the understanding of the disturbed dynamic interaction between DMN and ECN so frequently observed in the aging brain.

c. The ICCp clusters in the left and the right superior frontal gyrus: Same network affiliation but different functional roles and age-effects

Although the SCA and their general connection profiles identified the ICCp clusters in the right and left SFG as belonging to the same network, the anterior DMN, we found two small but interesting differences between the functional characteristics of these two clusters. The first of these differences might indicate that the DMN does not always act as a functional entity, but that sub-parts of the DMN might have quite different roles depending on the demands of the situation. The right insula and the left SFG ICCp clusters' general connection profiles but also the connection profiles associated with the performance scores in working memory emphasized the importance of strong anti-correlations between these two regions. Likewise, the negative association between the right anterior insula and the left superior frontal gyrus belonged to the connections exhibiting the strongest age-effects, i.e. showing a decrease in anti-correlation. On the other hand, the second DMN cluster in the midline of the superior frontal gyrus, i.e. ICCp cluster in the right SFG, did not exhibit this clear and functionally important anti-correlation with the ICCp cluster in the right anterior insula. When associated with the working memory scores, its connection profile primarily underlined the importance of preserved strong intra-network connections of the DMN for successful task performance, especially to one of the core hubs of the DMN, the posterior cingulate cortex.

Besides their distinct functional roles for working memory, the two SFG ICCp clusters showed spatially different age effects. When associated with age, the connection profile of the left SFG ICCp cluster primarily showed the typical finding of affected long-range connections. In contrast, although the general connection profile for the right SFG ICCp cluster showed a number of long distance connections into the parietal and temporal cortices as well as into the cerebellum, the subsequent association of the connection profile revealed that none of these long-range connections seemed to be significantly affected by age. In the case of the right SFG ICCp cluster the age-related loss of

connectedness seems to be a rather local phenomenon.

d. Cognitive relevance of the findings: Implications for the aging brain's working memory performance

Previous studies have already associated the successful performance of working memory with the dynamic interaction of three different main ICNs. While the ECN and the cingulo-opercular network activate together and integrate partially during working memory tasks (Cohen et al., 2014), the DMN deactivates (Gordon et al., 2012, Liang et al., 2015).

When associated with the scores for the Corsi Block Tapping Test, the connection profile of the right anterior insula stressed the importance of a clear temporal separation of the DMN and the ECN activity for working memory. Successful performance of working memory was correlated with a high integration of the right anterior insula ICCp cluster into the cingulo-opercular network and the VAN, respectively positive connections with the right dorsolateral prefrontal cortex) and the anterior to middle part of the cingulate cortex and negative correlations with the antDMN and postDMN. The two DMN ICCp clusters showed the reverse relationship: High performance in working memory correlated with high within-network correlation of the DMN, especially with a high positive correlation between the two-midline hubs of the DMN, the ICCp cluster in the right SFG and the target-ROIs in the PCC. This specific network constellation replicated the findings of previous studies, which already demonstrated the relevance of this posterior-anterior midline connection of the DMN for successful behavioral and cognitive performance (Andrews-Hanna et al., 2007).

However, Piccoli and colleagues (2015) were able to show that the anti-correlated network configuration of the DMN and the two task-positive networks has to be dynamic to a certain degree during working memory tasks. By separating the three different stages during working memory, i.e. encoding of the stimulus – maintaining the stimulus during the delay phase – and retrieval, the authors (Piccoli et al., 2015) demonstrated that the DMN is only fully anti-correlated during the delay phase but shows partial positive correlations with regions of the other two networks during the encoding and retrieval step.

We found that working memory performance in our study group was associated with preserved anti-correlation between the DMN and the cingulo-opercular network. Very cautiously, one might speculate that the aging brain has to preserve this antagonistic network configuration of the three networks that characterizes the delay phase as early as in the intrinsically active functional baseline-configuration in order to be still able to successfully shield the to be maintained stimulus from confounding influences of a not sufficiently deactivated DMN during an actual working memory task.

When comparing the working memory performance correlated connection profiles of the three ICCp clusters, there is another interesting feature that should be discussed: The number of long-range connections to the posterior parts of the cerebellum, i.e. the cerebellum crus I and II, which seem relevant for working memory. The relevance of the cerebellum, particularly of the cerebellum lobule VII and the crus I for working memory performance was already established by previous studies (Luis et al., 2015; Stoodley et al., 2012). Luis and colleagues showed that the active involvement of a fronto-parietal-cerebellar network, i.e. the involvement of the right and left ECN with its cerebellar nodes, is important for supporting working memory. Our data seem to complement the findings of Luis et al. (2015) in so far as they indicate that also the timely deactivation of cerebellar regions functionally belonging to the DMN is critical for successful working memory performance.

Limitations

There are some limitations of our study: Within the scope of the LHAB protocol, we only acquire task-free but no task-induced fMRI data, all actual cognitive and behavioral measurements are collected outside the scanner and therefore not directly linked to the brain data from the MRI data acquisition. This fact sets some constraints to the range within which we can elucidate how the aging brain actually performs a certain cognitive task or behavior. However, the aim of the study presented here was not to investigate how the aging brain performs working memory tasks but to investigate which brain regions may exhibit an age-related loss of connectedness in the life-period from old age to very old age and how these age-effects might relate to actual cognition and behavior. This is a valuable research question in itself given the fact that most of the knowledge about the specifics of the aging brain is gained from cross-sectional studies investigating the differences between young adults, usually college students aged from 20 to 30 years, and older adults. Due to these studies, we might better know which age-related differences characterize the older brain in comparison to young brains but understanding age differences on a relatively coarse level does not also imply that we understand the aging processes of the brain that cause these differences. Albeit also cross-sectional, our study aimed to elucidate the age related differences in connectivity on a much more fine-grained level by looking at the intrinsically active baseline configuration in a study sample of healthy older participants aged between 65 to 85 years.

A discussion point still unanswered by the discussion of our findings might be the fact that our data-driven analyses detected age-related alterations in the right anterior insula and in the cingulo-opercular network. We are well aware of the still-ongoing debate about the cingulo-opercular network and its relation to another ICN, the salience network, about the respective functions of these two ICNs and the relation of the anterior insula to them (Dosenbach et al., 2008; Power et al., 2011; Sadaghiani & D'Esposito, 2014; Seeley et al., 2007; Sridaharan et al., 2008; Uddin 2015). Because of analyzing

task-free fMRI data and behavioral data only indirectly related to the brain data, we were not able to elucidate the question or to take a stand on the debate. However, the main finding of our study, the age-related functional degradation of the right anterior insula, and its interpretation should not be questioned by this open debate since the influence of the right anterior insula in the brain's switching from the internal to the external modus operandi and the role of the DMN and ECN in this process are insights generally agreed on in the discussion.

Conclusions

A major contribution of our knowledge of the aging brain either comes from studies comparing young with older adults or from studies investigating pathological aging and using the healthy aging older just as a control group, which is used to highlight the differences between health and disease but is not in the focus of the research interest. The study presented here aimed to understand better which functional changes characterize the healthy aging brain's transition from old age to very old age. We assumed that the state of the intrinsically active functional baseline configuration of the brain might be at least to some degree a limiting factor that determines goal-directed behavior. Therefore, we investigated task-free fMRI data from a large sample of older adults in the transition from old to very old age in order to understand how the intrinsically active functional architecture changes during this transition.

Because of its role as one of the most important output hubs of the brain and its causal influence in the switching from the task-negative into the task-active modus operandi of the brain, the most important finding was the age-related loss of connectedness of the right anterior insula in our study group. Previous studies have already demonstrated that the aging brain shows a reduced capacity to timely deactivate the DMN in comparison to younger adults. Our study might be able to contribute to the understanding of this observation by showing that this phenomenon is not merely caused by the DMN exhibiting age-related functional degradation but that the cingulo-opercular network as well might be responsible for the impaired dynamic switching from the task-negative state to the task-positive state.

Additionally, our further results supported the findings of previous studies by showing that the reduction of connection strength and the ICN's merging into each other because of that reduction are not just a characteristic that differentiates young from older brains but an ongoing process still characteristic for the aging brain's transition from old age to very old age.

Acknowledgements

The current analysis incorporates data from the Longitudinal Healthy Aging Brain (LHAB) database project, which is carried out as one of the core projects at the International Normal Aging and Plasticity Imaging Center / INAPIC and the University Research Priority Program “Dynamics of Healthy Aging” of the University of Zurich. The following members of the core INAPIC team were involved in the design, set-up, maintenance and support of the LHAB database: Anne Eschen, Lutz Jäncke, Mike Martin, Susan Mérillat, Christina Röcke, and Jacqueline Zöllig.

5.2 Second Study
Older but still fluent? Insights from the intrinsically active baseline configuration of the aging brain using a data driven graph-theoretical approach[2]

5.2.1 Introduction

The process of growing old is characterized by changes in cognitive performance (Hedden & Gabrieli, 2004; Reuter-Lorenz et al., 2000; Park & Reuter-Lorenz, 2009; Salthouse, 1996; Singer et al., 2003; Spreng et al., 2010a; Turner & Spreng, 2012), which are preceded or accompanied by structural alterations in the brain like progressive gray matter atrophy or loss of white matter integrity (Fjell et al., 2009; Good et al., 2001; Raz et al., 1997; Raz et al., 2005; Salat et al., 2004; Sowell et al., 2003). Functional neuroimaging methods like PET or fMRI were able to introduce another and potentially more optimistic aspect. A number of studies using task-induced fMRI reliably found that older adults often showed different, mainly spatially extended activation patterns but were still able to perform at the same high level as young adults. This observation was interpreted as demonstrating that the aging brain has still preserved a certain degree of functional plasticity. Because of that plasticity it may be able to functionally compensate for already manifest age-related gray matter and white matter degeneration and thus retain the performance level for a time. There exists already a number of theories (HAROLD Cabeza et al., 2002; PASA Davis et al., 2008; CRUNCH Reuter-Lorenz & Cappell, 2008; STAC Reuter-Lorenz & Park, 2014) that all try to subsume these age-related differences in brain activity observed in a large number of task-induced fMRI studies under an overarching principle.

The majority of studies exploring the activation pattern of the aging brain have used fMRI or PET in the context of task-induced activation paradigms. In this study, we will use task-free fMRI data instead of task-related fMRI because of the following reasons. First, to thoroughly comprehend the meaning of an activation pattern of a brain actively engaged in a demanding task, one has likewise to apprehend the functional starting base of that activity, since our brain is never truly at rest. Even when a person is lying relaxed in the scanner and thinking of nothing in particular, her/his brain is intrinsically highly active, systematically and highly dynamically creating different activity patterns that look very similar to the activation patterns we see in task-induced fMRI paradigms (Cordes et al., 2000; Damoiseaux et

[2] A similar version of this paper was published as Muller, A.M., Mérillat, S, & Jäncke, L., (2016). Older but still fluent? Insights from the intrinsically active baseline configuration of the aging brain using a data-driven graph-theoretical approach. Neuroimage, 127:346-62. doi: 10.1016/j.neuroimage.2015.12.027.

al., 2006; De Luca et al., 2006). This dynamic spontaneous connectivity is the functional foundation from which the brain generates goal-oriented behavior and the efficiency of its intrinsic organization may be a limiting factor that determines the outcome of an actual behavior (Sadaghiani & Kleinschmidt, 2013). Comprehending the specific characteristics of the aging brain's intrinsically active functional baseline might therefore help us to get a better understanding of how it is still able to perform a cognitive demanding task despite structural loss. Second, a further advantage of task-free fMRI is that it allows to avoid potential confounds and limitations encountered in task-based approaches like practice effects or performance anxiety (Simpson et al., 2001). Thirdly, several papers have shown that intrinsic connectivity networks (ICN) are a good predictor for the underlying anatomical network organization (Collin et al., 2014; Kolchinsky et al., 2014; van den Heuvel & Sporns, 2013). Taken together, task-free fMRI provides promising opportunities for investigating the functional topology of the brain and has been widely used to study differences between populations.

Given that healthy aging is associated with a substantial change in verbal fluency, we are interested to examine the potential relationship between the intrinsic functional network structure and verbal fluency proficiency in the aging brain. In particular, we are interested to identify potential compensation or adaption strategies of the aging brain. To that aim we analyzed task-free fMRI data of a large sample of 186 older adults in combination with their verbal fluency data. Several studies have been published so far employing task-induced MRI studying age- and performance-related associations between verbal fluency performance and brain activation patterns (Birn et al., 2010; Destrieux et al., 2012, Fu et al., 2006; Marsolais et al., 2014; Meinzer et al., 2009, Meinzer et al., 2012a; Nagels et al., 2012; Persson et al., 2004, Persson et al., 2007). In these studies young adults generally show a clear leftward activation pattern, encompassing frontal regions like the inferior and middle frontal gyrus, medial frontal gyrus, cingulate cortex and superior temporal gyrus during the performance of verbal fluency tasks (Meinzer et al., 2009). In contrast, older participants recruit not only the right-sided homologs in the middle and inferior frontal gyrus, but additionally activate the left superior frontal gyrus, the right lingual gyrus, and the right precentral gyrus (Meinzer et al., 2009).

Successful performance of tasks of verbal fluency requires the combination of two fundamental cognitive functions, executive-control and language (Shao et al., 2014). The two cognitive functions have quite different trajectories across the life span. While the perception and production of language are relatively well preserved far into very old age, executive functions are known to suffer from age-related decline earlier in the process (Glisky, 2007). Therefore, the combination of these two cognitive functions makes verbal fluency, i.e. the ability to fluently produce speech while following some production constraints, ideal to gain a better understanding of the mechanisms that allow the aging brain to perform still at a high level but in a different manner from the young brain.

There exist two different forms of verbal fluency: Semantic fluency demands that one fluently names as many words as possible from the same semantic category, e.g. animals or fruits, during a fixed time period. On the other hand, phonemic or lexical fluency requires the tested person to name as many words as possible beginning with the same letter during a fixed period of time. Older participants tend to show significantly worse performance in semantic fluency compared to young adults (Clark et al., 2009). Concerning phonemic fluency, the age-related differences are much less pronounced (Meinzer et al., 2009, Meinzer et al., 2012a; Persson et al., 2004, Persson et al., 2007) although phonemic fluency is always rated as the more difficult task regardless of the participant's age.

In order to be unbiased and receptive to unexpected discoveries, we pursued a purely data driven approach. From previous studies using intrinsic connectivity data we know that one of the aging brain's characteristic features is a general reduction of connectedness, especially the decline or even disruption of long-range connections among regions situated in different brain lobes (Andrews-Hanna et al., 2007; Meunier et al., 2009). Based on these findings we hypothesized that the preserved degree of connectedness of the brain regions genuinely involved in such a demanding cognitive task like verbal fluency has to be a limiting factor that determines the performance of the old brain. For that reason we performed an Intrinsic Connectivity Contrast (ICC) analysis (Martuzzi et al., 2011). The ICC analysis is based on the graph theoretical concept of "degree" and therefore apt to measure the connectedness of regions. In comparison to other graph theoretical analyses (GTA) it has the advantage that it does not require a priori assumptions about possible regions or networks of interest and works on the single voxel-level so that it is apt to detect very small and unexpected effects. To the best of our knowledge, this study is the first to apply the ICC approach in correlation with cognitive performance in a population of older adults. Finally, for the purpose of relating the regions highlighted by the ICC analysis to other major intrinsic connectivity networks (ICN) and to better understand their meaning in the context of the underlying functional baseline configuration we computed a connectivity analysis.

5.2.2 Methods

I Participants

Behavioral and MRI data from 186 older adults (mean age = 70.4; SD = 4.8; 97 females) were taken from the first wave of the LHAB (Longitudinal Healthy Aging Brain) database, which is currently being built at the International Normal Aging and Plasticity Imaging Center (INAPIC, University of Zurich, Switzerland) (Zöllig et al., 2011). Participants were right-handed and native Swiss-German or German speakers. The 12-Item Short-Form Health Survey (SF-12) was administered to assess physical

and mental health. The self-reported mean physical health composite score in our sample was 50.8 (SD = 7.2), which is well above the US norm mean of 43.9 (age group between 65 and 74 years). The self-reported mean mental health composite score in our sample was 55.0 (SD = 6.0), which is slightly above the US norm mean of 51.6 points (age group between 65 and 74 years).

Besides the standard exclusion criteria relevant in the context of MRI assessments, the following exclusion criteria were applicable for the current study: (a) history or current diagnosis of psychiatric or neurologic diseases (e.g. Parkinson's disease, Alzheimer's dementia, multiple sclerosis, migraine), (b) an MMSE score of 26 or lower, (c) medical conditions such as diabetes, tinnitus, and diseases of the hematopoietic system.

All participants gave informed consent for participation of the longitudinal project under the approval of the local ethics committee and in accordance with the declaration of Helsinki.

At the first time-point of data collection in 2011, 230 older adults were enrolled in the LHAB project, but only the data of 186 subjects (mean age = 70.4; SD = 4.8; 89 men and 97 women) could be used in this study: The MRI datasets of 9 participants were incomplete, 31 subjects had to be excluded because of motion artifacts over 2mm, and one participant showed a pathological high white matter lesion load. Another participant was excluded because of a diagnosis of type II diabetes shortly after the first time of assessment. Finally, the data of two other participants were not analyzed because they scored in 15% of all tests significantly lower (> 3 SD) than the rest of the study sample.

II Neuropsychological data

The LHAB database project comprises annual assessments of brain structure and resting-state function and a broad testing battery to probe cognitive and motor functions. The assessment of semantic and phonemic fluency performance is part of the regular LHAB cognitive testing battery.

a) Semantic fluency: The semantic fluency performance was examined using a standard German word fluency test (RWT: Regenburger Wortflüssigkeitstest, Aschenbrenner et al., 2000). In this test, participants have two minutes to write down as many words as possible for a predefined semantic word category. They were instructed to avoid words with the same word roots or of using singular and plural forms of the same word. The number of correctly produced words was counted for the first and the second minute separately and also the total sum of words for the whole two minutes of the test was calculated. The present study uses data from the first LHAB measurement time-point and the specified category for this time-point was "animals".

b) Phonemic fluency: A sub-test of the Leistungsprüfsystem (LPS) of Horn (Horn, 1983) was used to assess phonemic fluency. In this task, participants have to write down as many words as possible beginning with the same predetermined letter during three consecutive one-minute runs. After each run a new letter is given for the next one-minute period. Participants were reminded not to use words with the same word root and to not vary between the singular and plural forms of the same word. The number of correctly produced words was aggregated across the three runs. The letters used for the first LHAB measurement time-point were *f*, *k* and *r*.

c) Covariates: It has been previously shown that high blood pressure but also the medication against high blood pressure influences the BOLD-signal (Lindauer et al., 2010). Within the LHAB testing regime, the participants' blood pressure is measured three times within the six-hour cognitive assessment session (in the morning before the assessment begins, before the lunch break, and at the end of the assessment in the afternoon). For this study, these three measurements of the diastolic and systolic blood pressure were averaged and the mean arterial blood pressure (MABP) was computed based on the formula of Salat and colleagues (Salat et al. 2012). The MABP was used as a second-level covariate in the analyses to control for the effects of high blood pressure.

For all the subsequent analyses, the scores in semantic and phonemic fluency, as well as all the data that were used to control for possibly confounding effects, like chronological age, years of education, MABP, and intracranial volume (ICV) were transformed to z scores. We performed two sample t-tests to assess potential gender differences in the demographic and physiological data, and in the fluency scores.

III MRI-data acquisition

All MRI-data were acquired on the same Philips 3T Ingenia Medical Scanner with a Philips 15 channel head-coil at the University Hospital in Zurich.

From the LHAB MRI protocol the following images were used: 1. A T1 weighted TFE- SENSE sequence with TR = 8.2ms, TE = 3.7ms, Flip Angle = 90 (FOV = 240 × 160 × 240mm^3, matrix size = 256 × 256, isotropic voxel size = 0.94 × 0.94 × 1mm) 160 slices per volume. 2. A T2 weighted TSE-SENSE sequence with TR = 3000ms; TE = 80ms Flip Angle = 90 (FOV 512 x 28 x 512mm^3; matrix size = 488 x 309, anisotropic voxel size 0.45/ 5/ 0.45mm) 28 slices per volume. 3. A task-free blood oxygenation level-dependent signals (BOLD) single shot whole brain EPI with a TR = 2000ms, TE = 21ms, Flip Angle = 76; 43 transverse slices (FOV = 220 × 150 × 220mm^3, matrix size = 64 × 64, ascending acquisition without gap, anisotropic voxel size = 1.72/ 1.72/ 3.50mm, aligned to the AC-PC line), acquisition time 7,39 min, 225 volumes.

For this part of the data acquisition, the participants were instructed to relax but also to lie as motionless as possible, to keep the eyes open while fixating on a cross that was displayed on a screen outside the scanner and was visible for the participant by means of a mirror system attached to the receiver coil. Immediately after the task-free scan, each participant was asked if he/she had fallen asleep. All participants confirmed that they were fully awake during the exam.

IV Pre-processing of the MRI data

All pre-processing steps were performed with the SPM8 software (http://www.fil.ion.ucl.ac.uk/spm) and the VBM8 toolbox for SPM8 (http://dbm.neuro.uni-jena.de/vbm) implemented in Matlab (MATLAB R2011B, The Math Works Inc.).

Before the actual pre-processing two additional preparatory steps were executed: First, the first six volumes of the EPI data were discarded allowing for T1 saturation effects, leaving 219 volumes for the analysis, and then a first aligment of the EPI-data was performed: Only the «mean-image» and the «motion-parameter-file» of this step were used in the further pre-processing steps. Second, a study population specific gray matter template was generated in order to be used in the DARTEL procedure implemented in SPM8 (Ashburner, 2007) that allows for a high dimensional and non-linear registration of the anatomical and functional images and their subsequent normalization.

The actual pre-processing consisted of the following steps: 1.The T2-weighted images were coregistered to the T1-weighted images as a reference. 2. The mean-images from the first preparatory step were coregistered to the T2-weighted images. 3. The final realignment of the functional images was done in two steps. During the first run the functional images were aligned to the first image; the mean-images now indirectly also coregistered to theT1-weighted images were used as firsts in this run. In the second run, all functional images were aligned to the new mean EPI images produced during the first run of the actual aligment. 4. The fMRI time-series were slice time corrected for the ascending acquisition. 5. The T1-weighted images were anew segmented into gray matter, white matter and CSF tissue maps using the segmentation procedure implemented in VBM8. 6. The DARTEL procedure was run using the GM study group template generated in the second preparatory step. 7. The functional and structural images were normalized to the MNI-space. During this step the functional as well as the structural images were resampled to a 2x2x2mm voxel size and only minimally smoothed using an isotropic Gaussian kernel (FWHM 1mm) in order minimize possible spurious correlations for the following GTAs on voxel level.

V First analysis step: Intrinsic connectivity contrast (ICC) analyses on the pre-processed task free fMRI data

To perform the ICC analysis the Conn Toolbox (version14i; http://www.nitrc.org/projects/conn) for SPM (Whitfield-Gabrieli & Nieto-Castanon, 2012) was used.

Band-pass filtering and denoising of the data: Since the spontaneous, coherent, and low frequent fluctuations of the BOLD-signal are used for the IC analyses, the BOLD time-series for each participant was extracted and band-pass-filtered (0.008 – 0.09 Hz), as well as despiked and detrended. As non-neural low frequent (< 0.1 Hz) signals such as heart rate or respiration are able to modulate the BOLD-signal, they may likewise influence the IC maps. Hence, a further important step is to correct for these physiological confounding signals. The Conn Toolbox accomplishes this by means of the CompCor method (Behzadi et al., 2007). As a last procedure during the denoising step implemented in the Conn Toolbox the motion parameters as well as the confounding signals calculated by the CompCor method are regressed out.

First level analyses: The Intrinsic Contrast Connectivity power (ICCp) index (Martuzzi et al., 2011) is a whole brain voxel based measure of connectivity related to the graph theory analysis (GTA) measure "*degree*" (Rubinov & Sporns, 2010). In GTA, a node can be defined on a single voxel level, i.e. every single voxel is a node, or on a coarser resolution level, e.g. on ROI level as a macro-anatomical region or a functionally delineated cluster of voxels. The degree of a node corresponds to the number of this node's connections with all other nodes in the network. Compared to a seed correlation analysis or a standard GTA an ICCp analysis has two advantages: 1. An ICCp analysis is data driven and free of any need to define a seed based on a priori assumptions about regions of interest. 2. An ICCp analysis can be computed without the need of defining a threshold. Since the brain is a highly complex structure and its constituent units on every level are extremely densely interconnected, every node is generally connected to every other node to some degree. Thus, a commonly used, but also critical procedure is to define arbitrarily a threshold that the connections have to surpass in order to separate the strong and supposedly important links from weak links and noise. To date, there exists no consensus about what constitutes a neurophysiologically meaningful threshold. While most researchers only look at the strongest connections and therefore at the most sparse network configurations, there is evidence that weaker connections may also convey important information (Santarnecchi et al., 2014). Instead of using a threshold in order to determine the most important connections, the ICCp works by weighting the connections of a voxel with the other voxels by the strength of these connections, i.e. by their r^2 value, and so producing voxel-based connectivity maps reflecting the existence as well as the strength of the connections of every individual voxel (Martuzzi et al., 2011).

On the second level or group level, the Conn Toolbox computes a GLM over all participants with the semantic, or the phonemic fluency scores as predictors in the design matrix and the ICCp values for every single voxel as the dependent variables. To compute the connectivity maps illustrating the voxel-level ICCp index and its positive correlation with the fluency performance on group level, a high threshold for the peak voxels of $p < 0.01$ uncorrected, and an extension threshold for the clusters of $p < 0.001$ FDR corrected was used. At this point, we want to emphasize that we are not interpreting the results of the ICCp analyses in terms of statistical significance, but we are interpreting the p-values as a measure of an effect, i.e. as a sort of threshold for defining sensible seized ROIs, which can be used in the following connectivity analyses. By doing this, we refer to J. Krauth (1988), who recommended using "the p-value as the lowest significance level at which someone would still have obtained a significant result for a given data set, a given significance test, and a given test problem. This has the advantage that other researchers can decide for themselves whether the results are significant at the significance level they may find acceptable."

VI Second analysis step: Connectivity analyses

The analyses described in the following section were performed separately for the semantic and phonemic ICCp results.

The ICCp maps of the first analysis step identified the voxels or voxel clusters whose ICCp index was positively correlated with verbal fluency performance. The next steps were to investigate whether these ICCp clusters are just locally very densely connected, form long-range connections, e.g. between the frontal and the parietal lobe or the cerebellum, or show a mixture between local and long-distance connections. Additionally we wanted to establish the network affiliations of the ICCp clusters in order to understand in general their function in relation to the intrinsic architecture of the whole brain. For these purposes we computed two connectivity analyses one for the ten combined semantic, and one for the five combined phonemic ICCp clusters as source ROIs.

In contrast to the more fine-grained voxel level resolution, results on the coarser level of ROIs are more intuitively interpretable, because they can be more easily associated with already well-established intrinsic connectivity networks (ICN) like the default mode network (DMN) or the executive-control network (ECN). Firstly, we extracted each single cluster of the ICCp maps separately and transformed it into a binary ROI to be used as a source ROI for the connectivity analysis. In order to define functionally relevant target ROIs for the connectivity analyses we used the already existing and commonly used parcellation of Shirer and colleagues (Shirer et al., 2012). That parcellation was computed by means of an independent component analysis (ICA) on task free fMRI

data of a sample of 15 healthy young adults. It consists of 90 nodes, representing 14 well-established functional ICNs.

The connectivity analyses were again performed using the Conn Toolbox (version 14k). On the group level of the connectivity analyses, we controlled this time for confounding factors by defining the chronological age, the years of education, the MABP, and the ICV as covariates in the GLM.

To control for the family-wise error rate caused by the mass-univariate testing between every connection of the 90 nodes of the analyzed connectome, the NBS approach of Zalesky and colleagues (Zalesky et al., 2010) as implemented in Conn was used. In contrast to the link-based FWE control for multiple comparisons, the NBS approach identifies potential connected structures formed by links that exceed a set of chosen thresholds. For the here presented connectivity analyses the chosen threshold set was as follows: ROI-to-ROI connections p-FDR 0.05 (seed-level); Seed-ROI (NBS, by size), p-FDR 0.05 (one-sided positive).

5.2.3 Results

I Neuropsychological and physiological data

The performed t-tests to assess potential gender differences revealed no significant difference between male and female participants with the exception of the educational level, quite common for that age cohort. On average, the men of our study sample have a higher level of education than the women. Despite the difference in their educational background we decided against gender separated analyses based on the fact that there was no gender difference in the verbal fluency performance (Table 5.2.1).

Table 5.2.1 The participants: Age, MMSE scores in phonemic and semantic fluency, and covariates

	Mean (Men/Women)	SD	T	p
Age	70.46/70.45	4.99/4.76	.019	.985
MMSE	28.78/28.84	1.06//0.97	- .385	.701
Phonemic Fluency	33.95/32.74	7.79/7.244	1.096	.275
Semantic Fluency	26.43/24.95	6.98/5.89	1.551	.123
Education (in years)	12.55/13.79	3.41/3.33	3.591	**0.000***
Middle arterial blood pressure (MABP)	102.99/100.14	10.06/10.93	1.836	.068

The table 5.2.1 shows the participants' age, MMSE and scores in phonemic and semantic fluency as well as covariates: The men (n = 89) and the women (n = 97) of the LHAB study sample (n = 186) showed no significant differences in verbal fluency or the other covariates except for the education level ($p < 0.001$).

II Results for the intrinsic connectivity contrast (ICC) analyses

a) Semantic fluency

The ICCp map for semantic fluency showed ten mostly frontal clusters, six in the language dominant left hemisphere, and four clusters in the right hemisphere; two of these right lateralized clusters had their cluster peak-voxel on the right side but were located in the medial line of the brain and extending into both hemispheres. Two clusters were found outside the frontal cortex; one was located in the left temporal cortex extending into the rolandic operculum and the other one in the left angular gyrus (Figure 5.2.1 and Table 5.5.2).

. Figure 5.2.1 Illustration of the 10 ICC clusters for semantic fluency

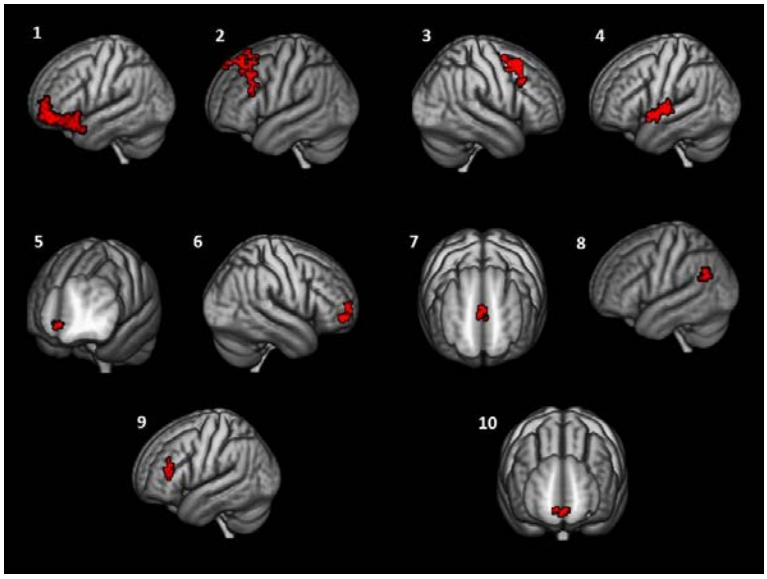

The figure 5.2.1 shows the 10 ICC cluster for semantic fluency, arranged from the most extensive ICC cluster to the smallest: 1. Semantic_l_parsorb; 2. Semantic_l_medsfg; 3. Sematic_r_parsoper; 4. Semantic_l_rolop; 5. Semantic_l_medsfg_2; 6. Semantic_r_midorbit; 7. Semantic_r_medsfg, 8. Semantic_l_ang; 9. Semantic_l_parstriang; 10. Semantic_r_medsfg_2 (High threshold peak voxels: $p < 0.01$ uncorr.; cluster threshold: Cluster $p < 0.001$ FDR corr.). For the cluster sizes, coordinates of the peak voxels and the locations of the clusters please see table 5.2.2.

Table 5.2.2 The 10 clusters of the ICC analysis for semantic fluency

	ICC Cluster Name	Cluster Size	Location of the Peak Voxel and MNI Coordinates	Regions
1	Semantic_l_parsorb	467	left inferior frontal gyrus/pars orbitalis (-44 +44 -8)	anterior prefrontal cortex (BA 10), inferior frontal gyrus (BA 47)
2	Semantic_l_medsfg	382	left medial superior frontal gyrus (-4 +40 +54)	premotor cortex (BA 6), dorsal frontal cortex (BA 8)
3	Semantic_r_parsoper	217	right inferior frontal gyrus/pars opercularis (+54 +18 +38)	premotor cortex (BA 6), dorsal frontal cortex (BA 8)
4	Semantic_l_rolop	187	left rolandic operculum (-58 +4 +2)	superior temporal gyrus (BA 22)
5	Semantic_l_medsfg_2	110	left medial superior frontal gyrus (0 +60 +16)	dorsolateral prefrontal cortex (BA 9)
6	Semantic_r_midorbit	104	right middle orbital gyrus (+44 +54 -4)	anterior prefrontal cortex (BA 10), dorsolateral prefrontal cortex (BA 46)
7	Semantic_r_medsfg	78	right medial superior frontal gyrus (+2 +36 +34)	dorsal frontal cortex (BA 8), premotor cortex (BA 6)
8	Semantic_l_ang	77	left angular gyrus (-52 -60 +26)	angular gyrus (BA 39)
9	Semantic_l_parstriang	72	left inferior frontal gyrus/pars triangularis (-40 +34 +14)	dorsolateral prefrontal cortex (BA 48), dorsolateral prefrontal cortex (BA 9)
10	Semantic_r_medsfg	71	right medial superior frontal gyrus (+8 +58 0)	anterior prefrontal cortex (BA 10)

The table 5.2.2 lists the 10 clusters of the ICC analysis for semantic fluency and shows the cluster size, the location, the MNI coordinates of the peak voxel, and the BA numbers of the regions that are covered by the cluster.

b) Phonemic fluency

The ICCp map for phonemic fluency showed smaller and also fewer clusters in comparison to the ICCp map for semantic fluency. There were five clusters in total, three on the language dominant left side of the brain, two on the right hemisphere. These two right-sided clusters were also the most small-sized clusters. Again, one of the right-sided clusters had its peak voxel located in the medial part of superior frontal gyrus but extended into both hemispheres (Figure 5.2.2 and Table 5.2.3).

Figure 5.2.2 Illustration of the 5 ICC clusters for phonemic fluency:

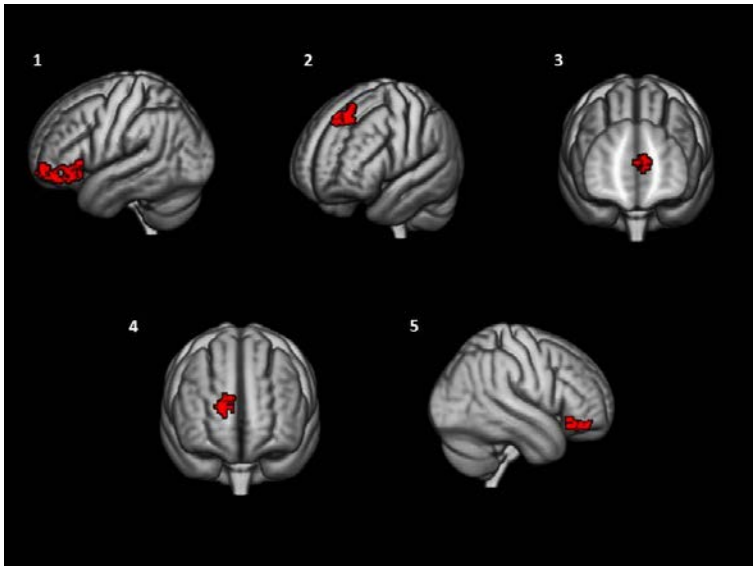

The figure 5.2.2 shows the 5 ICC cluster for phonemic fluency, arranged from the most extensive ICC cluster to the smallest: 1. Phonemic_l_mfg, 2. Phonemic_l_sfg; 3. Phonemic_l_medsfg; 4. Phonemic_r_sfg; 5. Phonemic_r_parsorb. (High threshold peak voxels: $p < 0.01$ uncorr.; cluster threshold: Cluster $p < 0.001$ FDR corr.). For the cluster sizes, coordinates of the peak voxels and the locations of the clusters please see table 5.2.3.

Table 5.2.3 The 5 clusters of the ICC analysis for phonemic fluency:

	ICC Cluster Name	Cluster Size	Location of the Peak Voxel and MNI Coordinates	Regions
1	Phonemic_ l_mfg	281	left middle frontal gyrus (-42 +56 0)	interior prefrontal cortex (BA 10), inferior prefrontal cortex (BA 47)
2	Phonemic_l_sfg	146	left superior frontal gyrus (-20 +34 +54)	premotor cortex (BA 6),
3	Phonemic_l_medsfg	93	left medial superior frontal gyrus (-4 +48 +20)	dorsolateral prefrontal cortex (BA 9)
4	Phonemic_r_sfg	90	right superior frontal gyrus (+18 +58 +22)	dorsolateral prefrontal cortex (BA 9)
5	Phonemic_r_parsorbit	77	right inferior frontal gyrus/pars orbitalis (+48 +38 -16)	inferior prefrontal gyrus (BA 47)

The table 5.2.3 lists the 5 Clusters of the ICC analysis for phonemic fluency and shows the cluster size, the location, the MNI coordinates of the peak voxel, and the BA numbers of the regions that are covered by the cluster.

III Results for the connectivity analyses

In this section we refer to the ROIs/nodes using the following naming scheme:
The ROIs constructed from the clusters of the ICC maps connote 1) the respective verbal fluency test and 2) the macro-anatomical location of the peak coordinate of the cluster. Thus, the name "Semantic_l_mfg" refers to a ROI/node in the left middle frontal region that is involved in semantic fluency processing.

The ROIs of the Shirer parcellation are named to connote 1) the functional ICN to which the node belongs and 2) the brain region in which it is mainly located. Thus, the name "dorsal DMN/l_ang" refers to a node of the dorsal default mode network, which is located in the left angular gyrus.

IV Results of the connectivity analysis for semantic fluency: The general connection profiles of the ten semantic fluency source ROIs

The connectivity analysis over all ten semantic fluency source ROIs revealed that these regions were interacting most strongly with regions of the left ECN, the dorsal (but not the ventral) DMN, the right ECN and the language network (Figure 5.2.3: Table 5.2.4).

Figure 5.2.3 The semantic fluency connection profile:

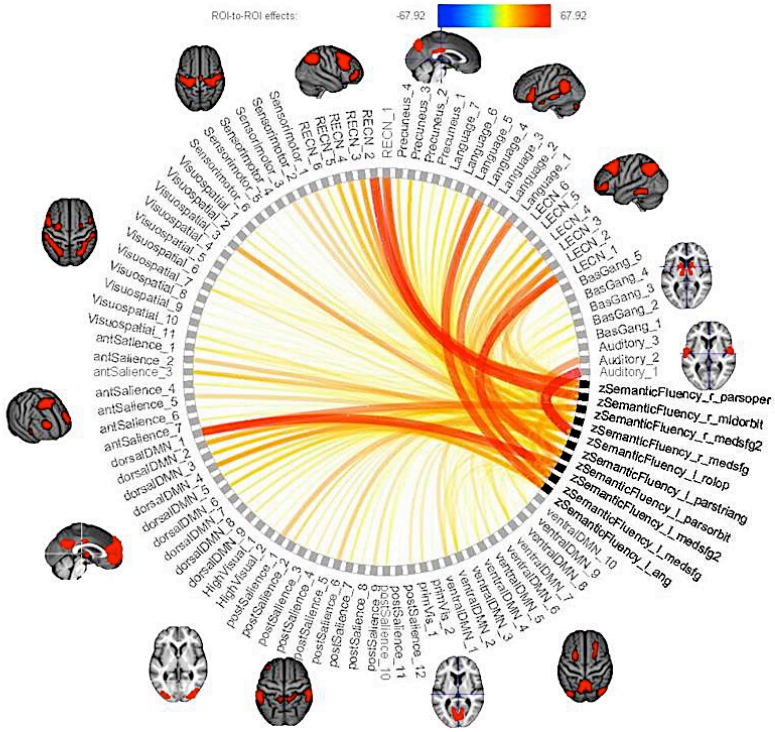

The figure 5.2.3 shows the 10 semantic fluency source ROI's and their positive connections with the networks and ROIs of the Shirer parcellation (Shirer et al., 2012).The intensity of the color symbolizes the strength/significance of the respective connection ((Analysis Level = ROI-to-ROI connections p-FDR 0.05 (seed-level); Seed ROI (NBS; by size): 0.05 p-FDR; one-sided positive).

Table 5.2.4 Semantic fluency: General connection profile of the 10 semantic source ROIs – the most important target ROI

Network Affiliation	Analysis Unit	Statistic	p-uncorr	p-FDR	p-FWE		Anterior-posterior connection
	SF_left_parsorbit	**F(38)(144) = 117.90**	**< 0.001**	**< 0.001**			
		Intensity = 1184.47	**< 0.001**	**< 0.001**	**< 0.001**		
		Size = 89	**< 0.001**	**< 0.001**	**< 0.001**		
	Language_1/l_ifg	T(181) = 52.27	< 0.001	< 0.001			
	LECN_2/l_porbit	T(181) = 49.44	< 0.001	< 0.001			
	LECN_1/l_mfg	T(181) = 33.02	< 0.001	< 0.001			
	LECN_3/l_ipl	T(181) = 32.46	< 0.001	< 0.001		Long Distance	Parietal Cortex
	Language_5/r_ifg	T(181) = 28.76	< 0.001	< 0.001		Long Distance	
	LECN_4/l_mtg	T(181) = 28.50	< 0.001	< 0.001		Long Distance	
	SF_left_medsfg	T(181) = 28.02	< 0.001	< 0.001			
ECN	Visuospatial_3/l_poper	T(181) = 27.69	< 0.001	< 0.001			
	SF_right_midorbit	T(181) = 27.19	< 0.001	< 0.001		Long Distance	
	RECN_2/r_porbit	T(181) = 26.90	< 0.001	< 0.001		Long Distance	
	Language_3/l_mtg	T(181) = 26.88	< 0.001	< 0.001		Long Distance	
	Language_4/l_ang	T(181) = 26.61	< 0.001	< 0.001		Long Distance	Parietal Cortex
	LECN_5/r_cerebcrus2	T(181) = 24.74	< 0.001	< 0.001		Long Distance	Cerebellum
	Precuneus_3/l_ang	T(181) = 23.87	< 0.001	< 0.001		Long Distance	Parietal Cortex

	SF_left_ang	T(181) = 23.42	< 0.001	< 0.001		Long Distance	Parietal Cortex
	SF_right_parsoper	**F(38)(144) = 91.53**	**< 0.001**	**< 0.001**			
		Intensity = 1065.98	**< 0.001**	**< 0.001**	**< 0.001**		
		Size = 82	**< 0.001**	**< 0.001**	**0.0003**		
	RECN_1/r_mfg	T(181) = 58.11	< 0.001	< 0.001			
	RECN_3/r_ipl	T(181) = 39.02	< 0.001	< 0.001		Long Distance	Parietal Cortex
	RECN_5/l_cerebcrus2	T(181) = 30.69	< 0.001	< 0.001		Long Distance	cerebellum
	RECN_2/r_porbit	T(181) = 29.50	< 0.001	< 0.001			
	LECN_3/l_ipl	T(181) = 29.20	< 0.001	< 0.001		Long Distance	Parietal Cortex
	SF_right_midorbit	T(181) = 26.92	< 0.001	< 0.001			
	Precuneus_4/r_ang	T(181) = 26.62	< 0.001	< 0.001		Long Distance	Parietal Cortex
ECN	LECN_1/l_mfg	T(181) = 25.67	< 0.001	< 0.001		Long Distance	
	LECN_4/l_mtg	T(181) = 25.48	< 0.001	< 0.001		Long Distance	
	Precuneus_3/l_ang	T(181) = 25.34	< 0.001	< 0.001		Long Distance	Parietal Cortex
	ventralDMN_9/r_mog	T(181) = 22.89	< 0.001	< 0.001		Long Distance	Visual Cortex
	SF_right_medsfg	T(181) = 22.62	< 0.001	< 0.001			
	SF_left_medsfg	T(181) = 22.28	< 0.001	< 0.001		Long Distance	
	ventralDMN_2/l_sfg	T(181) = 21.32	< 0.001	< 0.001		Long Distance	
	SF_left_parsorbit	T(181) = 20.89	< 0.001	< 0.001		Long Distance	
	SF_right_medsfg	**F(38)(144) = 56.71**	**< 0.001**	**< 0.001**			
		Intensity = 953.05	**< 0.001**	**< 0.001**	**< 0.001**		
		Size = 75	**< 0.001**	**< 0.001**	**0.0006**		
	RECN_4/r_medsfg	T(181) = 35.16	< 0.001	< 0.001			
	antSalience_3/bilateral_acc	T(181) = 32.42	< 0.001	< 0.001		Long Distance	
	LECN_1/l_mfg	T(181) = 32.07	< 0.001	< 0.001		Long Distance	
	SF_left_medsfg	T(181) = 29.67	< 0.001	< 0.001		Long Distance	
	RECN_1/r_mfg	T(181) = 28.83	< 0.001	< 0.001			
	dorsalDMN_1/bilateral_medsg	T(181) = 26.27	< 0.001	< 0.001			
	LECN_3/l_ipl	T(181) = 24.01	< 0.001	< 0.001		Long Distance	Parietal Cortex
ECN	SF_left_parsorbit	T(181) = 23.37	< 0.001	< 0.001		Long Distance	
	SF_left_medsfg_2	T(181) = 22.91	< 0.001	< 0.001		Long Distance	
	SF_right_parsoper	T(181) = 22.62	< 0.001	< 0.001			
	ventralDMN_7/r_sfg	T(181) = 20.42	< 0.001	< 0.001			
	dorsalDMN_3/r_sfg	T(181) = 19.76	< 0.001	< 0.001			
	SF_left_ang	T(181) = 19.61	< 0.001	< 0.001		Long Distance	Parietal Cortex
	RECN_2/r_porbit	T(181) = 19.17	< 0.001	< 0.001			
	dorsalDMN_2/l_ang	T(181) = 18.68	< 0.001	< 0.001		Long Distance	Parietal Cortex
	SF_right_midorbit	**F(38)(144) = 89.71**	**< 0.001**	**< 0.001**			
		Intensity = 821.39	**< 0.001**	**< 0.001**	**< 0.001**		
		Size = 75	**< 0.001**	**< 0.001**	**0.0006**		
	RECN_2/r_porbit	T(181) = 64.41	< 0.001	< 0.001			
	RECN_1/r_mfg	T(181) = 33.01	< 0.001	< 0.001			
	RECN_3/r_ipl	T(181) = 30.44	< 0.001	< 0.001		Long Distance	Parietal Cortex
	LECN_2/l_porbit	T(181) = 28.47	< 0.001	< 0.001		Long Distance	
	SF_left_parsorbit	T(181) = 27.19	< 0.001	< 0.001		Long Distance	
	SF_right_parsoper	T(181) = 26.92	< 0.001	< 0.001			
	RECN_5/l_cerebcrus2	T(181) = 25.64	< 0.001	< 0.001		Long Distance	Cerebellum
ECN	Precuneus_4/r_ang	T(181) = 20.85	< 0.001	< 0.001		Long Distance	Parietal Cortex
	LECN_3/l_ipl	T(181) = 18.29	< 0.001	< 0.001		Long Distance	Parietal Cortex

	Precuneus_3/l_ang	T(181) = 17.61	< 0.001	< 0.001		Long Distance	Parietal Cortex
	SF_right_medsfg	T(181) = 16.66	< 0.001	< 0.001			
	RECN_4/r_medsfg	T(181) = 15.66	< 0.001	< 0.001			
	ventralDMN_7/r_sfg	T(181) = 14.98	< 0.001	< 0.001			
	dorsalDMN_6/r_ang	T(181) = 14.51	< 0.001	< 0.001		Long Distance	Parietal Cortex
	Visuospatial_7/r_poper	T(181) = 14.39	< 0.001	< 0.001			
	SF_left_parstriang	**F(38)(144) = 72.94**	**< 0.001**	**< 0.001**			
		Intensity = 849.98	**< 0.001**	**< 0.001**	**< 0.001**		
		Size = 74	**< 0.001**	**< 0.001**	**0.0007**		
	Visuospatial_3/l_poper	T(181) = 38.60	< 0.001	< 0.001			
	postSalience_1/l_mfg	T(181) = 34.79	< 0.001	< 0.001			
	postSalience_2/l_smg	T(181) = 25.15	< 0.001	< 0.001		Long Distance	Parietal Cortex
	LECN_2/l_porbit	T(181) = 23.55	< 0.001	< 0.001			
	Visuospatial_7/r_poper	T(181) = 23.36	< 0.001	< 0.001		Long Distance	
	Visuospatial_2/l_spl	T(181) = 20.98	< 0.001	< 0.001		Long Distance	Parietal Cortex
	Visuospatial_1/l_sfg	T(181) = 20.88	< 0.001	< 0.001			
Visuo-	ventralDMN_2/l_sfg	T(181) = 19.41	< 0.001	< 0.001			
spatial	Precuneus_3/l_ang	T(181) = 17.64	< 0.001	< 0.001		Long Distance	Parietal Cortex
	BasGang_3/l_ptriang	T(181) = 17.21	< 0.001	< 0.001			
	Visuospatial_10/r_cereb8	T(181) = 17.16	< 0.001	< 0.001		Long Distance	Cerebellum
	antSalience_1/l_mfg	T(181) = 17.12	< 0.001	< 0.001			
	antSalience_3/bilateral_acc	T(181) = 17.03	< 0.001	< 0.001		Long Distance	
	Visuospatial_4/l_itg	T(181) = 15.97	< 0.001	< 0.001		Long Distance	Parietal Cortex
	RECN_1/r_mfg	T(181) = 15.66	< 0.001	< 0.001		Long Distance	
	SF_left_medsfg	**F(38)(144) = 90.45**	**< 0.001**	**< 0.001**			
		Intensity = 985.23	**< 0.001**	**< 0.001**	**< 0.001**		
		Size = 65	**< 0.001**	**0.0001**	**0.0016**		
	LECN_1/l_mfg	T(181) = 59.89	< 0.001	< 0.001			
	dorsalDMN_1/bilateral_medsfg	T(181) = 31.20	< 0.001	< 0.001			
	LECN_3/l_ipl	T(181) = 30.69	< 0.001	< 0.001		Long Distance	Parietal Cortex
	SF_right_medsfg (ECN)	T(181) = 29.67	< 0.001	< 0.001			
	dorsalDMN_2/l_ang	T(181) = 29.39	< 0.001	< 0.001		Long Distance	Parietal Cortex
	SF_left_medsfg_2 (DMN)	T(181) = 28.95	< 0.001	< 0.001			
	LECN_4/l_mtg	T(181) = 28.51	< 0.001	< 0.001		Long Distance	
DMN &	dorsalDMN_3/r_sfg	T(181) = 28.11	< 0.001	< 0.001		Long Distance	
ECN	SF_left_parsorbit (ECN)	T(181) = 28.02	< 0.001	< 0.001			
	SF_left_ang (DMN&Language)	T(181) = 27.97	< 0.001	< 0.001		Long Distance	Parietal Cortex
	dorsalDMN_4/bilateral_pcc	T(181) = 26.48	< 0.001	< 0.001		Long Distance	Parietal Cortex
	LECN_5/r_cerebcrus2	T(181) = 25.53	< 0.001	< 0.001		Long Distance	Cerebellum
	RECN_1/r_mfg	T(181) = 24.27	< 0.001	< 0.001		Long Distance	
	Language_1/l_ifg	T(181) = 23.09	< 0.001	< 0.001			Parietal Cortex
	SF_right_medsfg_2 (DMN)	T(181) = 22.69	< 0.001	< 0.001			
	SF_left_rolop	**F(38)(144) = 108.42**	**< 0.001**	**< 0.001**			
		Intensity = 920.61	**< 0.001**	**< 0.001**	**< 0.001**		
		Size = 65	**< 0.001**	**0.0001**	**0.0016**		
	Auditory_1/l_stg	T(181) = 67.92	< 0.001	< 0.001			
	Auditory_2/r_stg	T(181) = 46.61	< 0.001	< 0.001			
	antSalience_2/l_ins	T(181) = 33.48	< 0.001	< 0.001			
	postSalience_6/r_smg	T(181) = 31.17	< 0.001	< 0.001		Long Distance	Parietal Cortex

	Sensorimotor_1/l_precent	T(181) = 30.09	< 0.001	< 0.001			
	Sensorimotor_2/r_precent	T(181) = 29.90	< 0.001	< 0.001		Long Distance	
	Sensorimotor_3/r_sma	T(181) = 29.85	< 0.001	< 0.001		Long Distance	
post	antSalience_5/r_ins	T(181) = 29.24	< 0.001	< 0.001		Long Distance	
Salience	postSalience_9/l_ins	T(181) = 24.11	< 0.001	< 0.001			
	antSalience_3/bilateral_acc	T(181) = 22.62	< 0.001	< 0.001		Long Distance	
	postSalience_12/r_ins	T(181) = 21.71	< 0.001	< 0.001		Long Distance	
	postSalience_5/r_spl	T(181) = 21.30	< 0.001	< 0.001		Long Distance	Parietal Cortex
	primVis_1/bilateral_calc	T(181) = 21.12	< 0.001	< 0.001			Visual Cortex
	postSalience_4/r_mcc	T(181) = 21.05	< 0.001	< 0.001		Long Distance	
	postSalience_3/l_precun	T(181) = 19.58	< 0.001	< 0.001		Long Distance	Parietal Cortex
	SF_left_ang	**F(38)(144) = 82.83**	**< 0.001**	**< 0.001**			
		Intensity = 831.96	**< 0.001**	**< 0.001**	**< 0.001**		
		Size = 57	**0.0001**	**0.0001**	**0.0034**		
	Language_4/l_ang	T(181) = 58.61	< 0.001	< 0.001			
	dorsalDMN_2/l_ang	T(181) = 34.33	< 0.001	< 0.001			
	LECN_1/l_mfg	T(181) = 30.36	< 0.001	< 0.001		Long Distance	Frontal Cortex
	dorsalDMN_4/bilateral_pcc	T(181) = 29.78	< 0.001	< 0.001			
	LECN_3/l_ipl	T(181) = 28.86	< 0.001	< 0.001			
	SF_left_medsfg (DMN&ECN)	T(181) = 27.97	< 0.001	< 0.001		Long Distance	Frontal Cortex
	dorsalDMN_6/r_ang	T(181) = 25.96	< 0.001	< 0.001		Long Distance	
DMN &	Language_3/l_mtg	T(181) = 24.52	< 0.001	< 0.001		Long Distance	
LANG	dorsalDMN_1/bilateral_medsfg	T(181) = 24.32	< 0.001	< 0.001		Long Distance	Frontal Cortex
	SF_left_medsfg_2 (DMN)	T(181) = 23.80	< 0.001	< 0.001		Long Distance	Frontal Cortex
	SF_left_parsorbit (ECN)	T(181) = 23.42	< 0.001	< 0.001		Long Distance	Frontal Cortex
	Language_7/l_cerebcrus2	T(181) = 22.19	< 0.001	< 0.001		Long Distance	Cerebellum
	Language_1/l_ifg	T(181) = 21.83	< 0.001	< 0.001		Long Distance	
	Language_2/l_antmtg	T(181) = 20.29	< 0.001	< 0.001		Long Distance	
	dorsalDMN_5/r_mcc	T(181) = 19.97	< 0.001	< 0.001		Long Distance	
	SF_left_medsfg_2	**F(38)(144) = 76.48**	**< 0.001**	**< 0.001**			
		Intensity = 716.78	**< 0.001**	**< 0.001**	**< 0.001**		
		Size = 50	**0.0002**	**0.0002**	**0.0056**		
	dorsalDMN_1/bilateral_medsfg	T(181) = 60.46	< 0.001	< 0.001			
	SF_right_medsfg_2	T(181) = 35.76	< 0.001	< 0.001		Long Distance	
	dorsalDMN_4/bilateral_pcc	T(181) = 32.90	< 0.001	< 0.001		Long Distance	Parietal Cortex
	SF_left_medsfg	T(181) = 28.95	< 0.001	< 0.001			
	dorsalDMN_2/l_ang	T(181) = 25.88	< 0.001	< 0.001		Long Distance	Parietal Cortex
	LECN_1/l_mfg	T(181) = 25.25	< 0.001	< 0.001			
	dorsalDMN_3/r_sfg	T(181) = 24.48	< 0.001	< 0.001		Long Distance	
DMN	SF_left_ang	T(181) = 23.80	< 0.001	< 0.001		Long Distance	Parietal Cortex
	SF_right_medsfg	T(181) = 22.91	< 0.001	< 0.001		Long Distance	
	dorsalDMN_5/r_mcc	T(181) = 22.20	< 0.001	< 0.001		Long Distance	
	ventralDMN_1/l_precun	T(181) = 20.86	< 0.001	< 0.001		Long Distance	Parietal Cortex
	Language_4/l_ang	T(181) = 19.46	< 0.001	< 0.001		Long Distance	Parietal Cortex
	dorsalDMN_6/r_ang	T(181) = 17.86	< 0.001	< 0.001		Long Distance	Parietal Cortex
	ventralDMN_5/r_precun	T(181) = 17.83	< 0.001	< 0.001		Long Distance	Parietal Cortex
	ventralDMN_7/r_sfg	T(181) = 16.79	< 0.001	< 0.001		Long Distance	
	SF_right_medsfg_2	**F(38)(144) = 51.06**	**< 0.001**	**< 0.001**	**< 0.001**		
		Intensity = 677.29	**< 0.001**	**< 0.001**	**< 0.001**		

		Size = 50	**0.0002**	**0.0002**	**0.0056**		
	dorsalDMN_1/bilateral_medsfg	T(181) = 48.68	< 0.001	< 0.001			
	SF_left_medsfg_2	T(181) = 35.76	< 0.001	< 0.001		Long Distance	
	dorsalDMN_4/bilateral_pcc	T(181) = 33.15	< 0.001	< 0.001		Long Distance	Parietal Cortex
	ventralDMN_1/l_precun	T(181) = 26.30	< 0.001	< 0.001		Long Distance	Parietal Cortex
	ventralDMN_5/r_precun	T(181) = 23.02	< 0.001	< 0.001		Long Distance	Parietal Cortex
	SF_left_medsfg	T(181) = 22.69	< 0.001	< 0.001		Long Distance	
DMN	dorsalDMN_2/l_ang	T(181) = 22.40	< 0.001	< 0.001		Long Distance	Parietal Cortex
	LECN_1/l_mfg	T(181) = 22.11	< 0.001	< 0.001		Long Distance	
	dorsalDMN_8/l_hippo	T(181) = 20.77	< 0.001	< 0.001		Long Distance	
	dorsalDMN_9/r_hippo	T(181) = 20.69	< 0.001	< 0.001		Long Distance	
	dorsalDMN_5/r_mcc	T(181) = 20.62	< 0.001	< 0.001		Long Distance	
	dorsalDMN_3/r_sfg	T(181) = 20.32	< 0.001	< 0.001			
	ventralDMN_7/r_sfg	T(181) = 19.55	< 0.001	< 0.001			
	dorsalDMN_7/l_thal	T(181) = 19.51	< 0.001	< 0.001		Long Distance	
	dorsalDMN_6/r_ang	T(181) = 18.98	< 0.001	< 0.001		Long Distance	Parietal Cortex

The table 5.2.4 shows the connection profile of the combined 10 semantic source ROIs – the most important target ROIs: The table shows the 10 semantic fluency source ROIs, the 15 most important target ROIs of each semantic fluency source ROI, the intensity of the connections, respectively the T value, the FDR corrected p values, and the functional network affiliation (Analysis Level = ROI-to-ROI connections p-FDR 0.05 (seed-level); Seed ROI (NBS; by size): 0.05 p-FDR; one-sided positive).

Eight of the ten semantic fluency source ROIs were located in frontal regions and showed similar connection profiles, i.e. they were either connected to neighboring frontal regions in the same hemisphere or to their homologous region in the other hemisphere, or over long-distance connections to regions in the posterior half of the brain, most prominently to parietal regions but also the middle temporal gyrus, the posterior cingulate gyrus, the precuneus and the cerebellum.

But it was possible to disentangle the individual connection profiles of the frontally located source ROIs even further: The Semantic_l_parsorbit, Semantic_l_parsoper, Semantic_r_medsfg, and Semantic_r_midorbit source ROIs were primarily connected to the left and the right ECN and thus emphasized the executive character of the semantic fluency task. A mixed connection profile characterized the Semantic_l_medsfg source ROI, since its 15 strongest links were to target ROIs of the ECN and the dorsal DMN in equal shares. The Semantic_l_medsfg_2 and the Semantic_r_medsfg_2 source ROIs were mainly connected with target regions belonging to the dorsal DMN and therefore might qualify as dorsal DMN sub-networks proper. In comparison to the other frontally located ICCp clusters, the Semantic_l_parstriang source ROI showed a very different connection profile because six of its 15 strongest links were to target ROIs of the visuospatial network, and two to the posterior salience network and the anterior salience network respectively. Another noteworthy feature is the fact that none of the other semantic ICCp clusters did belong to its 15 strongest connected target ROIs. With exception of another ICCp cluster, the Semantic_l_rolop ROI,

all other semantic source ROIs were also strongly inter-connected with at least one or more of the other seven semantic ICCp clusters.

Additionally, the two non-frontal source ROIs, the Semantic_l_ang and the Semantic_l_rolop ROIs likewise displayed connection profiles different from the frontal ones. The Semantic_l_ang source ROI was the only semantic fluency ICCp cluster located in the posterior part of the brain. Mainly, it was connected to nearby posterior regions in the bilateral parietal lobe or in the middle part of the cingulum, but also with the medial part of the superior frontal gyrus and the left pars orbitalis over long-distance connections. Its connection profile characterized the Semantic_l_ang source ROI as interacting mostly with DMN and language regions.

Although the cluster peak coordinates of the Semantic_l_rolop ROI lied in the left rolandic operculum, the major part of this ROI as well as the cluster centroid were located in the anterior part of the left superior temporal gyrus. Its connection profile displayed connections to the homologous region of the right superior temporal gyrus, to the left and the right insulae, to the left and the right precentral gyri, the bilateral anterior cingulate cortex, and the SMA. According to the ICNs identified by Shirer et al. (2012) these regions belonged to auditory, salience and sensorimotor networks. Likewise the Semantic_l_parstriang ROI, this cluster also showed no connections to any of the other semantic ICCp clusters.

V Results of the connectivity analysis for phonemic fluency: The general connection profiles of the ten phonemic fluency ICCp clusters

The functional connection profile over all five phonemic source ROIs showed that the phonemic source ROIs primarily connected to target ROIs of the left and right ECN, of the dorsal DMN, the language network.

In contrast to the semantic fluency ROIs, all phonemic fluency ROIs were frontally located and they mainly connected to nearby frontal regions in the same hemisphere as well as in the homologous regions of the other hemisphere and over long-distance connections to distant posterior regions of the brain, primarily to regions in the parietal lobe, the middle temporal gyrus, the middle cingulate and to the posterior cerebellum (Figure 5.2.4 and Table 5.2.5).

Figure 5.2.4 The phonemic fluency connection profile

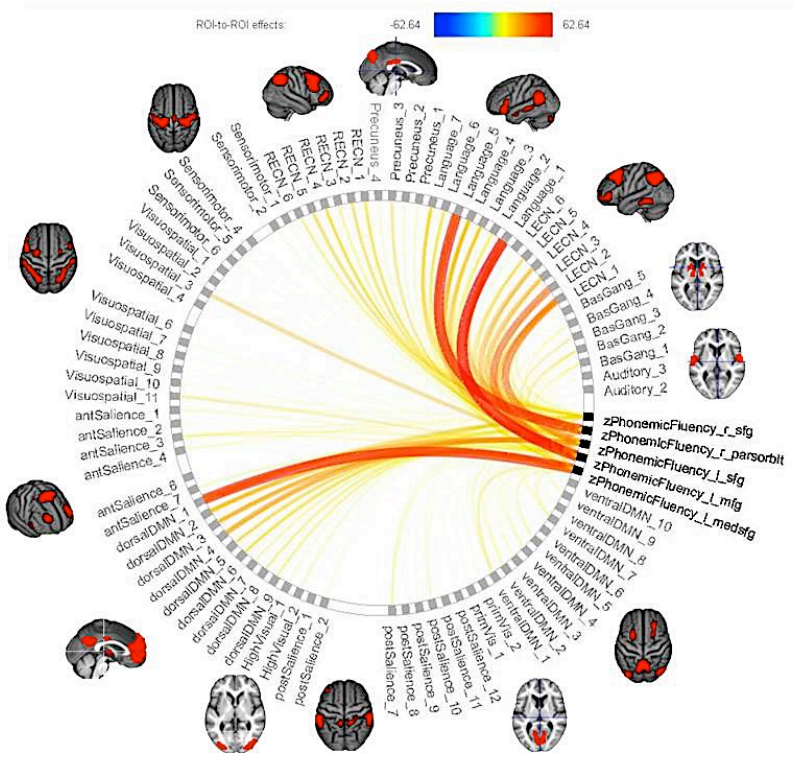

The figure 5.2.4 shows the 5 phonemic fluency source ROI's and their positive connections with the networks and ROIs of the Shirer parcellation (Shirer et al., 2012). The intensity of the color symbolizes the strength/significance of the respective connection (Analysis Level = ROI-to-ROI connections p-FDR 0.05 (seed-level); Seed ROI (NBS; by size): 0.05 p-FDR; one-sided positive).

Table 5.2.5 Phonemic fluency: General connection profile of the 5 phonemic source ROIs – the most important target ROIs

Network Affiliation	Analysis Unit	Statistic	p-uncorr	p-FDR	p-FWE		Anterior-posterior connection
	PF_left_mfg	**F(38)(144) = 103.32**	**< 0.001**	**< 0.001**			
		Intensity = 955.90	**< 0.001**	**< 0.001**	**< 0.001**		
		Size = 73	**< 0.001**	**< 0.001**	**0.0005**		
	Language_1/l_ifg	T(181) = 62.64	< 0.001	< 0.001			
	LECN_2/l_porbit	T(181) = 44.27	< 0.001	< 0.001			
	PF_right_parsorbit	T(181) = 34.26	< 0.001	< 0.001		Long Distance	
	LECN_4/l_mtg	T(181) = 29.39	< 0.001	< 0.001		Long Distance	
	LECN_3/l_ipl	T(181) = 29.11	< 0.001	< 0.001		Long Distance	Parietal Cortex
	Language_5/r_ifg	T(181) = 29.07	< 0.001	< 0.001		Long Distance	
	LECN_1/l_mfg	T(181) = 28.95	< 0.001	< 0.001			
ECN	Language_4/l_ang	T(181) = 27.29	< 0.001	< 0.001		Long Distance	Parietal Cortex
	Visuospatial_3/l_poper	T(181) = 25.94	< 0.001	< 0.001			
	Language_3/l_mtg	T(181) = 25.54	< 0.001	< 0.001		Long Distance	
	PF_left_sfg	T(181) = 22.23	< 0.001	< 0.001			
	LECN_5/r_cerebcrus2	T(181) = 21.95	< 0.001	< 0.001		Long Distance	Cerebellum
	Precuneus_3/l_ang	T(181) = 21.16	< 0.001	< 0.001		Long Distance	Parietal Cortex
	BasGang_2/l_cau	T(181) = 19.92	< 0.001	< 0.001		Long Distance	
	RECN_2/r_porbit	T(181) = 19.88	< 0.001	< 0.001		Long Distance	

	PF_right_parsorbit	**F(38)(144) = 95.33**	**< 0.001**	**< 0.001**			
		Intensity = 788.95	**< 0.001**	**< 0.001**	**< 0.001**		
		Size = 71	**< 0.001**	**< 0.001**	**0.0006**		
	Language_5/r_ifg	T(181) = 58.24	< 0.001	< 0.001			
	PF_left_mfg	T(181) = 34.26	< 0.001	< 0.001		Long Distance	
	Language_1/l_ifg	T(181) = 30.72	< 0.001	< 0.001		Long Distance	
	Language_7/l_cerebcrus2	T(181) = 23.09	< 0.001	< 0.001		Long Distance	Cerebellum
	RECN_5/l_cerebcrus2	T(181) = 22.08	< 0.001	< 0.001		Long Distance	Cerebellum
	Language_4/l_ang	T(181) = 20.08	< 0.001	< 0.001		Long Distance	Parietal Cortex
ECN	RECN_4/r_medsfg	T(181) = 19.96	< 0.001	< 0.001		Long Distance	
	LECN_2/l_porbit	T(181) = 19.86	< 0.001	< 0.001			
	RECN_1/r_mfg	T(181) = 19.73	< 0.001	< 0.001		Long Distance	
	LECN_4/l_mtg	T(181) = 19.09	< 0.001	< 0.001			
	LECN_1/l_mfg	T(181) = 18.97	< 0.001	< 0.001		Long Distance	
	dorsalDMN_6/r_ang	T(181) = 18.82	< 0.001	< 0.001		Long Distance	Parietal Cortex
	Language_6/r_mtg	T(181) = 18.41	< 0.001	< 0.001		Long Distance	
	LECN_3/l_ipl	T(181) = 18.29	< 0.001	< 0.001		Long Distance	Parietal Cortex
	RECN_2/r_porbit	T(181) = 18.11	< 0.001	< 0.001			
	PF_left_medsfg	**F(38)(144) = 66.99**	**< 0.001**	**< 0.001**			
		Intensity = 674.61	**< 0.001**	**< 0.001**	**0**		
		Size = 52	**0.0001**	**0.0001**	**0.0035**		
	dorsalDMN_1/bilateral_medsfg	T(181) = 56.48	< 0.001	< 0.001			
	dorsalDMN_4/bilateral_pcc	T(181) = 31.05	< 0.001	< 0.001		Long Distance	Parietal Cortex
	PF_left_sfg	T(181) = 27.43	< 0.001	< 0.001			
	LECN_1/l_mfg	T(181) = 26.13	< 0.001	< 0.001			
	dorsalDMN_2/l_ang	T(181) = 24.49	< 0.001	< 0.001		Long Distance	Parietal Cortex
	dorsalDMN_5/r_mcc	T(181) = 23.03	< 0.001	< 0.001		Long Distance	
	dorsalDMN_3/r_sfg	T(181) = 23.02	< 0.001	< 0.001		Long Distance	
dorsal	PF_right_sfg	T(181) = 21.19	< 0.001	< 0.001		Long Distance	
DMN	Language_4/l_ang	T(181) = 20.36	< 0.001	< 0.001		Long Distance	Parietal Cortex
	ventralDMN_1/l_precun	T(181) = 18.33	< 0.001	< 0.001		Long Distance	Parietal Cortex
	dorsalDMN_6/r_ang	T(181) = 17.69	< 0.001	< 0.001		Long Distance	Parietal Cortex
	Language_1/l_ifg	T(181) = 17.31	< 0.001	< 0.001		Long Distance	
	dorsalDMN_7/l_thal	T(181) = 16.55	< 0.001	< 0.001		Long Distance	
	Language_3/l_mtg	T(181) = 16.51	< 0.001	< 0.001		Long Distance	
	ventralDMN_7/r_sfg	T(181) = 15.76	< 0.001	< 0.001		Long Distance	
	PF_left_sfg	**F(38)(144) = 67.00**	**< 0.001**	**< 0.001**			
		Intensity = 709.65	**< 0.001**	**< 0.001**	**< 0.001**		
		Size = 52	**0.0001**	**0.0001**	**0.0035**		
	LECN_1/l_mfg	T(181) = 42.15	< 0.001	< 0.001			
	dorsalDMN_1/bilateral_medsfg	T(181) = 33.47	< 0.001	< 0.001			
	dorsalDMN_3/r_sfg	T(181) = 31.02	< 0.001	< 0.001		Long Distance	
	dorsalDMN_4/bilateral_pcc	T(181) = 27.57	< 0.001	< 0.001		Long Distance	Parietal Cortex
	PF_left_medsfg	T(181) = 27.43	< 0.001	< 0.001			
	dorsalDMN_2/l_ang	T(181) = 27.04	< 0.001	< 0.001		Long Distance	Parietal Cortex
dorsal	Language_1/l_ifg	T(181) = 22.34	< 0.001	< 0.001			
DMN	PF_left_mfg	T(181) = 22.23	< 0.001	< 0.001			
	Language_4/l_ang	T(181) = 21.43	< 0.001	< 0.001		Long Distance	Parietal Cortex
	LECN_4/l_mtg	T(181) = 20.37	< 0.001	< 0.001		Long Distance	

	Language_3/l_mtg	T(181) = 19.85	< 0.001	< 0.001		Long Distance	
	LECN_3/l_ipl	T(181) = 19.78	< 0.001	< 0.001		Long Distance	Parietal Cortex
	PF_right_sfg	T(181) = 19.61	< 0.001	< 0.001		Long Distance	
	dorsalDMN_6/r_ang	T(181) = 18.95	< 0.001	< 0.001		Long Distance	Parietal Cortex
	LECN_5/r_cerebcrus2	T(181) = 18.18	< 0.001	< 0.001			Cerebellum
	PF_right_sfg	**F(38)(144) = 29.98**	**< 0.001**	**< 0.001**			
		Intensity = 531.99	**< 0.001**	**< 0.001**	**< 0.001**		
		Size = 51	**0.0001**	**0.0001**	**0.0036**		
	dorsalDMN_1/bilateral_medsfg	T(181) = 24.81	< 0.001	< 0.001			
	PF_left_medsfg (DMN)	T(181) = 21.19	< 0.001	< 0.001			
	Language_4/l_ang	T(181) = 19.67	< 0.001	< 0.001		Long Distance	Parietal Cortex
	PF_left_sfg (DMN)	T(181) = 19.61	< 0.001	< 0.001		Long Distance	
	dorsalDMN_5/r_mcc	T(181) = 18.45	< 0.001	< 0.001		Long Distance	
	Language_7/l_cerebcrus2	T(181) = 17.91	< 0.001	< 0.001		Long Distance	Cerebellum
	dorsalDMN_3/r_sfg	T(181) = 17.62	< 0.001	< 0.001			
LANG	Language_6/r_mtg	T(181) = 17.59	< 0.001	< 0.001		Long Distance	
& DMN	Language_5/r_ifg	T(181) = 16.98	< 0.001	< 0.001			
	LECN_1/l_mfg	T(181) = 16.32	< 0.001	< 0.001		Long Distance	
	Language_1/l_ifg	T(181) = 15.67	< 0.001	< 0.001		Long Distance	
	RECN_4/r_medsfg	T(181) = 14.98	< 0.001	< 0.001			
	PF_right_parsorbit (ECN)	T(181) = 14.56	< 0.001	< 0.001			
	dorsalDMN_4/bilateral_pcc	T(181) = 14.49	< 0.001	< 0.001		Long Distance	Parietal Cortex
	Language_3/l_mtg	T(181) = 14.31	< 0.001	< 0.001		Long Distance	

The table 5.2.5 shows the connection profile of the 5 phonemic source ROIs – the most important target ROIs: The table shows the 5 phonemic fluency source ROIs, the 15 most important target ROIs of each phonemic fluency source ROI, the intensity of the connections, respectively the T value, the FDR corrected p values, and the functional network affiliation (Analysis Level = ROI-to-ROI connections p-FDR 0.05 (seed-level); Seed ROI (NBS; by size): 0.05 p-FDR; one-sided positive).

As before, the connection profiles of the individual ROIs allowed to further characterize them: The Phonemic_l_sfg and the Phonemic_l_medsfg ROIs were mainly connected to regions belonging to the dorsal DMN and thus might qualify as dorsal DMN sub-networks, while the Phonemic_l_mfg and the Phonemic_r_parsorbit mostly connected to regions belonging the left, and the right LECN. The Phonemic_r_sfg ROI showed a mixed connection profile, targeting dorsal DMN regions as well as regions belonging to the language network.

VI The core regions involved in both forms of verbal fluency and differences between semantic and phonemic fluency

The connection profiles showed the ten semantic source ROIs together targeting 57 different ROIs of the Shirer parcellation while the five phonemic source ROIs connected to 26 different Shirer ROIs. The semantic and phonemic source ROIs had 24 target ROIs in common, ROIs belonging to the right and left ECN, the language network, the dorsal DMN and two ROIs of the ventral DMN as well as one ROI of the visuospatial network (Table 5.2.6). Mainly two semantic source ROIs were accountable for

the large number and variety of the semantic target ROIs: The Semantic_l_rolop source ROI was exhibiting 12 unique connections to target ROIs of the auditory network, the post salience network, and the sensorimotor network, the Semantic_l_parstriang source ROI was exhibiting 6 unique connections to the visuospatial and the post salience networks.

Especially when considering the functional variety of the 57 ROIs targeted by the ten semantic source ROIs the functional specificity of these target ROIs for verbal fluency might be called into question. We are well aware that each of these verbal fluency ICCp clusters alone is probably multifunctional, i.e. subserving more than just one specific cognitive function in different configurations with other brain regions. It was exactly this expected multi-functionality of the individual ICCp clusters that prompted us to analyze not the connection profile of the individual source ROIs separately, but solely the connection profile of the combined ten semantic source ROIs, of the combined five phonemic source ROIs respectively. While each individual ICCp cluster is probably multifunctional, the particular combination of ICCp clusters is considerably more specific for verbal fluency and therefore should allow sound conclusions about the networks involved in the performance of verbal fluency.

Table 5.2.6 Comparison of the semantic and phonemic fluency target ROIs: Overlap and Differences

Semantic	Phonemic	Common ROIs
Auditory_1/l_stg (Semantic_l_rolop)	BasGang_2/l_caud	**LECN_1/l_mfg**
Auditory_2/r_stg (Semantic_l_rolop)	**LECN_1/l_mfg**	**LECN_2/l_porbit**
BasGang_3/l_ptriang	**LECN_2/l_porbit**	**LECN_3/l_ipl**
LECN_1/l_mfg	**LECN_3/l_ipl**	**LECN_4/l_mtg**
LECN_2/l_porbit	**LECN_4/l_mtg**	**LECN_5/r_cerebcrus2**
LECN_3/l_ipl	**LECN_5/r_cerebcrus2**	**Language_1/l_ifg**
LECN_4/l_mtg	**Language_1/l_ifg**	**Language_3/l_mtg**
LECN_5/r_cerebcrus2	**Language_3/l_mtg**	**Language_4/l_ang**
Language_1/l_ifg	**Language_4/l_ang**	**Language_5/r_ifg**
Language_2/l_antmtg	**Language_5/r_ifg**	**Language_7/l_cerebcrus2**
Language_3/l_mtg	Language_6/r_mtg	**RECN_1/r_mfg**
Language_4/l_ang	**Language_7/l_cerebcrus2**	**RECN_2/r_porbit**
Language_5/r_ifg	**RECN_1/r_mfg**	**RECN_4/r_medsfg**
Language_7/l_cerebcrus2	**RECN_2/r_porbit**	**RECN_5/l_cerebcrus2**
Precuneus_3/l_ang	**RECN_4/r_medsfg**	**dorsalDMN_1/bilateral_medsfg**
Precuneus_4/r_ang	**RECN_5/l_cerebcrus2**	**dorsalDMN_2/l_ang**
RECN_1/r_mfg	**dorsalDMN_1/bilateral_medsfg**	**dorsalDMN_3/r_sfg**
RECN_2/r_porbit	**dorsalDMN_2/l_ang**	**dorsalDMN_4/bilateral_pcc**
RECN_3/r_ipl	**dorsalDMN_3/r_sfg**	**dorsalDMN_5/r_mcc**
RECN_4/r_medsfg	**dorsalDMN_4/bilateral_pcc**	**dorsalDMN_6/r_ang**
RECN_5/l_cerebcrus2	**dorsalDMN_5/r_mcc**	**dorsalDMN_7/l_thal**
Sensorimotor_1/l_precent (Semantic_l_rolop)	**dorsalDMN_6/r_ang**	**Visuospatial_3/l_poper**
Sensorimotor_2/r_precent (Semantic_l_rolop)	**dorsalDMN_7/l_thal**	**ventralDMN_1/l_precun**
Sensorimotor_3/r_sma (Semantic_l_rolop)	**Visuospatial_3/l_poper**	**ventralDMN_7//r_sfg**
Visuospatial_1/l_sfg (Semantic_l_parstriang)	**ventralDMN_1/l_precun**	
Visuospatial_2/l_spl (Semantic_l_parstriang)	**ventralDMN_7/r_sfg**	
Visuospatial_3/l_poper		
Visuospatial_4/l_itg (Semantic_l_parstriang)		
Visuospatial_7/r_poper		
Visuospatial_10/r_cereb8 (Semantic_l_parstriang)		
antSalience_1/l_mfg		
antSalience_2/l_ins		
antSalience_3/bilateral_acc		
antSalience_5/r_ins		
dorsalDMN_1/bilateral_medsfg		
dorsalDMN_2/l_ang		
dorsalDMN_3/r_sfg		

dorsalDMN_4/bilateral_pcc **dorsalDMN_5/r_mcc** **dorsalDMN_6/r_ang** **dorsalDMN_7/l_thal** dorsalDMN_8/l_hippo dorsalDMN_9/r_hippo *primVis_1/bilateral_calc (Semantic_l_rolop)* *postSalience_1/l_mfg (Semantic_l_parstriang)* *postSalience_2/l_smg (Semantic_l_parstriang)* *postSalience_3/l_precun (Semantic_l_rolop)* *postSalience_4/r_mcc (Semantic_l_rolop)* *postSalience_5/r_spl (Semantic_l_rolop)* *postSalience_6/r_smg (Semantic_l_rolop)* *postSalience_9/l_ins (Semantic_l_rolop)* *postSalience_12/r_ins (Semantic_l_rolop)* **ventralDMN_1/l_precun** ventralDMN_2/l_sfg ventralDMN_5/r_precun **ventralDMN_7/r_sfg** ventralDMN_9/r_mog		

The core regions involved in both forms of verbal fluency and differences between semantic and phonemic fluency: The table 5.2.6 lists the 57 target regions involved in the semantic fluency and the 26 target regions supporting the processing of phonemic fluency. The 26 common target regions are marked by bold letters and separately listed in the third column. 13 of the common target ROIs are located in the left nine on the right side of the brain.

5.2.4 Discussion

This study was designed to examine the intrinsic functional baseline configuration in a large sample of older subjects and to explore whether specific features of this configuration are associated with verbal fluency performance. Particularly, we were interested to study whether we can identify traces of typical adaption and compensation strategies even during a task-free baseline condition as they have been often reported for the aging brain using task-inducted fMRI studies.
Different to previous task-free fMRI studies we used an entirely data driven approach to investigate the functional relationship of brain regions associated with performance in verbal fluency. In the first step by using the ICCp index (Martuzzi et al., 2011) we determined the brain regions whose degree of connectedness were correlated positively with performance in semantic and phonemic fluency. Although both ICCp maps also displayed right-sided clusters, the ICCp maps for semantic as well as for phonemic fluency showed a left dominance with the cluster pattern for phonemic fluency being more strongly left lateralized than the semantic fluency pattern. The cluster regions for semantic and phonemic fluency were fairly identical with two exceptions: 1. The ICCp map for semantic fluency additionally showed an involvement of the left superior temporal gyrus and the left angular gyrus. 2. The clusters of the semantic fluency ICCp map covered an almost three times larger area of the brain than the phonemic fluency clusters (1765 vs. 624 voxels).

In a second step, we wanted to understand the connection profiles of these regions highlighted by the ICCp analysis for the purpose of elucidating their relation with other major ICNs and to get an understanding which brain regions have to be engaged for a successful performance of verbal fluency despite age-related structural decline. The results of the connectivity analyses showed that verbal fluency in the aging brain was supported by a coordinated cooperation of different networks, but mainly by the left and the right executive control networks, the language network and the dorsal DMN. Apart from other nearby frontal regions, especially preserved functional long-distance connections, mainly to the parietal regions, i.e. angular gyri, but also to the middle temporal gyrus, the middle and posterior cingulate cortices, precuneus and to the posterior part of the cerebellum, seemed to be essential for the performance of semantic and phonemic fluency. In the following sections we will interpret the findings of the ICCp analyses at first and then combine them with the results of the subsequent connectivity analyses.

a. New insights from the brain regions involved in the processing of verbal fluency

Overall, in respect of the brain regions recruited for the processing of verbal fluency tasks, our data driven approach could confirm findings of previous studies (Marsolais et al., 2014; Meinzer et al.,

2009; Meinzer et al., 2012a; Nagels et al., 2012; Persson et al., 2004) but also brought new insights, especially in respect to the parietal and temporal regions involved in semantic fluency.

An ICC analysis is the method of choice to determine brain regions whose degree of connectedness with other regions is associated with characteristics of interest like cognitive performance or pre-/post-treatment changes. The most prominent characteristic of the ICCp cluster maps for semantic as well as for phonemic fluency was their specific anterior-posterior and left-right distribution, since we observed a distinct left prevalence of the cluster patterns and an emphasis on mainly frontal regions encompassing bilateral medial frontal regions, superior, middle, and inferior gyri. Additionally, the semantic ICCp cluster map showed two additional clusters, one in the left superior temporal gyrus and one in the left inferior parietal lobe. Thus the spatially more extensive ICCp cluster map for sematic fluency reflected the findings of Robinson et al. (2012) in patients with left frontal, right frontal or posterior brain lesions. The authors showed that the performance in semantic fluency was always impaired regardless of the lesion's location. In contrast, a deficit in phonemic fluency was highly sensitive for a lesion in the left inferior frontal gyrus.

The connection profile revealed the Semantic_l_ang source ROI as interacting with regions of two other networks in equal shares, the dorsal DMN and the language network. The left angular region seems to be a functionally very heterogeneous region subserving the DMN as well as language. Seghier et al. (2010) demonstrated that the left angular gyrus can be functionally segregated at least in three partitions, a mid-region that overlaps partially with the DMN, a ventrolateral region that activates especially during a semantic matching task, and a dorsomesial region that is activated by quite a number of different tasks. In a more recent paper, Seghier described the left angular gyrus as "a cross-modal hub where converging multisensory information is combined and integrated to comprehend and give sense to events, manipulate mental representations, solve familiar problems, and reorient attention to relevant information" (Seghier, 2013).

The relevance of the temporal lobe for successful performance in semantic fluency was already stressed by two previous meta-analyses (Henry & Crawford, 2004; Henry et al., 2004) arguing that both versions of verbal fluency heavily rely on executive functions but that semantic fluency is more dependent on an intact semantic memory than phonemic fluency. Although we found an ICCp cluster in the temporal lobe, its location might not corroborate the relevance of an intact semantic store for semantic fluency. The ICCp cluster was located in the anterior part of the superior temporal cortex. Furthermore, its connection profile displayed connections to core regions of the anterior and posterior salience networks, i.e. to the left and the right insulae and the anterior cingulate cortex but also to the homologous region of the superior temporal gyrus, and to the bilateral precentral gyri, and the SMA, i.e. three regions belonging to the sensorimotor network. Based on its connection profile, the temporal

ICCp cluster can be more adequately characterized as auditory-somatosensory transition zone (Pascual et al., 2013).

b. Frequently practiced cognitive functions and everyday tasks have a stronger imprint on the intrinsically active baseline configuration of the brain

Taking into account the different extent of the two ICCp cluster maps and the potential biological relevance of ICNs might explain why the phonemic fluency task is experienced as more difficult than the semantic fluency task. ICNs can be strikingly similar to task-induced activity patterns (Cordes et al., 2000; Damoiseaux et al., 2006; De Luca et al., 2006). Therefore, they are sometimes interpreted as an imprint or a trace caused by means of a Hebbian-like mechanism when the same configuration of brain regions for a common function is recruited again and again (Wig et al., 2011). Accordingly, intrinsic connectivity configurations as for example the dorsal attention network, the language network, or the executive control network, can be understood as the brain's proactive and dynamic prediction about future demands (Fox & Raichle, 2007; Deco et al., 2011) in order to be able to act almost immediately and energetically highly efficient as soon as it is required by the situation.

The semantic fluency task requires retrieval of semantic knowledge that is stored in the memory hierarchically by categories. These categories are organized in natural subcategories that allow a simple heuristic of sampling subdomains, e.g. from animals in a zoo to animals in the forest, with minimal risk of repeating an already used word (Azuma, 2004). Categorization of new information and retrieval of already categorized knowledge to assess new information is an everyday activity that we perform constantly, almost unknowingly. Based on that, one would expect to find an imprint of that intensive practice in the intrinsic activity pattern of the brain, especially for the retrieval of categorized information. In contrast, the purely lexical retrieval of words that begin all with the same first letter is not an everyday task, and natural subcategories for letters as a guiding principle for the retrieval are non-existent. Therefore, the performing of the phonemic fluency task requires non-habitual, non-heuristic and cognitive more demanding search and organization strategies (Azuma, 2004). Hence, when performing a phonemic fluency task, the brain cannot rely on already proactively warmed-up network configurations but has to engage in the much more demanding process of reconfiguring and coordinating the relevant brain regions ad hoc.

In that context, it is interesting to note that potential age-effects do not anymore seem to be so significant as soon as the task at hand requires a network configuration that is not or only partially mirrored in the in the baseline configuration. At least this would explain why older participants often perform at the same level than young adults in the phonemic fluency task (Meinzer et al., 2009; Meinzer et al., 2012a; Strauss et al., 2006). Consequently, one might speculate that the ability to

reconfigure the networks of the brain for an unfamiliar and rather artificial task involving language could be fairly well preserved into old age.

c. The involvement of the right hemispheric frontal regions in verbal fluency is already apparent in the functional baseline configuration of the old brain

The second interesting finding of the ICCp analysis was the localization and hemispheric distribution of the ICCp clusters on both maps. The ICCp cluster maps highlighted primarily frontal regions as relevant for a successful performance of verbal fluency tasks. Although the patterns of both verbal fluency tasks showed a clearly left-sided prevalence, there were also right-sided frontal clusters on both ICCp cluster maps. The fact that older adults activate additional right-sided frontal homologous when performing a verbal fluency task in the scanner whereas younger adults only exhibit left-sided activation is a common finding of the majority of studies using task-induced fMRI paradigm (e.g. Birn et al., 2010; Destrieux et al., 2012, Fu et al., 2006; Marsolais et al., 2014; Meinzer et al., 2009, Meinzer et al., 2012a; Meinzer et al., 2012b; Nagels et al., 2012; Persson et al., 2004, Persson et al., 2007). With a few exceptions (e.g. Meinzer et al., 2012a) these additional right-hemispheric activation patterns were interpreted as more or less successful compensation mechanisms of the older adults' brains and often related to the HAROLD model (Cabeza et al., 2002). The HAROLD model is probably the most invoked compensation mechanism in order to explain the differences in the activation patterns of young and older adults. HAROLD is the acronym for "age-related reduction of hemispheric asymmetry in the aging brain" and describes the observation that the aging brain not only seems to make up for age-related alterations by an increased activation of the functionally relevant brain regions but also by activating additional brain regions in the frontal cortex. Especially tasks that induce usually a strongly lateralized frontal activation pattern in young subjects appear to additionally activate the frontal homologs in the functionally not dominant hemisphere in the older adults' brains.

Nevertheless, the ICCp results showed an involvement of the right frontal and prefrontal regions as relevant for a successful performance in verbal fluency as early as in the functional baseline configuration. The finding was further corroborated by the subsequent connectivity analyses. One possible interpretation of this finding is that in our study population the compensatory involvement of the right-sided homolog is so indispensable that an imprint of that steady involvement already shows up in the intrinsic connectivity pattern. However, per definition, a compensatory mechanism should be an additional resource that can be flexibly applied whenever greater effort is needed. An alleged compensatory mechanism that already seems to be solidly incorporated in the functional baseline configuration might have lost its capacity to flexibly counteract higher efforts and therefore might not anymore qualify as a true compensation mechanism. Based on these considerations, we suggest that our finding of right-sided clusters being essential for successful verbal fluency performance as early as

in the intrinsically active functional baseline might rather be interpreted as age-related functional dedifferentiation than successful compensation.

The subsequent connectivity analyses with the verbal fluency ICC clusters as source ROIs revealed three main findings.

d. Common functional core regions support semantic and phonemic fluency

Firstly, the connectivity analyses for the semantic and phonemic fluency source ROIs could demonstrate that verbal fluency is not a distinct cognitive function, which imprints its own ICN in the intrinsically active brain, but is supported by a coordinated interplay of three different ICNs. Mainly the left and to a lesser extent the right ECN, the dorsal DMN and the language network as the minor partner seem to constitute the functional base to process verbal fluency.

The involvement of the executive-control network and the language network was to be expected. On the one hand verbal fluency stands for one of the most basic components of language, the ability to produce fluent speech. On the other hand, successful performance requires executive abilities like the initiation of organized search strategies, semantic retrieval, the monitoring of already used words and inhibition of false answers as well as the switching between different subcategories or clusters. Therefore, in addition to the typical verbal abilities, verbal fluency assesses all the classical executive core functions of monitoring/inhibition, switching/shifting and updating (Miyake et al., 2000).

At first glance, the positive correlations of the semantic and phonemic source ROIs with the core regions of the dorsal DMN and therefore the dorsal DMN's role in verbal fluency might be less intuitively comprehensible. Positive correlations of ICNs or of single regions primarily signify that these regions act in a synchronized manner, i.e. they act simultaneously at the same time point. Based on a positive correlation alone it is impossible to deduce, which forms of action, i.e. activation or deactivation is simultaneously undertaken, because both are theoretically possible. Thus, on the one hand a positive intrinsic connectivity correlation can mean that two different networks habitually do exactly the same and activate both simultaneously for the purpose to interact actively together. That is probably the explanation of the positive correlations between the phonemic and semantic source ROIs and their ECN and language network target regions. On the other hand a positive intrinsic connectivity correlation can as well imply that one of the involved networks usually deactivates in a synchronized manner as soon as the other starts to activate for the purpose of a specific goal-directed behavior. That might be a plausible explanation for the observed positive correlations between the dorsal DMN and the ECN and the language network. In order to appreciate the meaning of this finding, it is necessary to look more closely on the complex mechanism of the DMN.

Until a few years ago, the DMN was mostly seen as a non-divisible entity, but now the evidence is mounting that the DMN consists of different sub-networks with quite different, and depending on the task at hand, dynamically adapting activation and deactivation profiles (De Pasquale et al., 2012; Grigg & Grady, 2010; Leech et al., 2012, Spreng et al., 2010b). Regarding semantic and phonemic fluency, Shapira-Lichter and colleagues (2013) showed that the default mode regions exhibited task-specific deactivation patterns. While some DMN regions always deactivated in relation to their baseline activity during fluency tasks, especially the left inferior parietal gyrus, the anterior medial prefrontal cortex, the left hippocampus, and the precuneus showed distinct activity patterns for each of the two versions of verbal fluency.

To date, the full complexity of the DMN and its sub-components is far from understood. Regarding the dorsal and the ventral sub-networks, first evidence for age-related changes is available. Thus older brains show a weaker connectivity within the ventral DMN sub-system in comparison to younger, while the connectivity within the dorsal sub-network increases significantly during the lifespan (Campell et al., 2013). This age-related dedifferentiation of the two DMN sub-systems may manifest itself in the disruption and subsequent slowing-down of the temporally fine-tuned interplay between activation and deactivation of these two subsystems with detrimental effects for performance. Persson et al. (2007) as well as Meinzer and colleagues (2012b) have demonstrated that older participants showed not only a diminished pattern of DMN deactivation but could also associate this observation with a poorer performance of the older adults.

e. Preserved functional frontal-parietal long-range connections are essential for verbal fluency

The second finding of the connectivity analysis revealed that the frontal fluency source ROIs form primarily long-distance connections to parietal regions, the posterior cingulate, precuneus and to the posterior part of the cerebellum. However, the relevance of such long-distance connections for efficient cognitive functioning and the fact that these connections might be especially prone to age-related decline have been already demonstrated by previous studies (Andrews-Hanna et al., 2007; Meunier et al., 2009; Tomasi & Volkow, 2012; Zhang et al., 2014). In this context it is far more interesting that the ICCp analyses only emphasized the degree of connectedness of the frontal regions as associated with successful performance in verbal fluency but not the connectedness of these posterior regions as well. This could indicate that a certain degree of connectedness of the frontal regions has to be maintained in order to perform verbal fluency tasks and that the ability to maintain that necessary degree of connectedness might also be the limiting factor in the aging brain. Most certainly this finding seems to suggest a difference in the amount or character of connectedness between the anterior and posterior part of the brain.

f. The involvement of the attentional and salience networks in semantic fluency might indicate an age-related functional degradation or an additional compensation mechanism

Two of the ten semantic source ROIs showed an unambiguous affiliation with the DMN, the Semantic_l_medsfg_2 and the Semantic_r_medsfg_2 source ROIs, and two additional source ROIs were at least characterized by a mixed connection profile likewise involving the DMN: The Semantic_l_ang source ROI displayed connections with the ROIs of the dorsal DMN and the language network while the Semantic_l_medsfg was primarily connected to target ROIs of the DMN and ECN. In this context it is striking that the ICCp cluster map for semantic fluency also highlighted two semantic ICCp clusters, i.e. Semantic_l_rolop and Semantic_l_parstriang, which both mainly targeted ROIs belonging to the visuospatial network (also called dorsal attention network in the literature), the two salience sub-networks and the sensorimotor network. All four networks usually exhibit strong anti-correlations with the DMN in the intrinsically active baseline configuration of the brain.

Without task-induced fMRI data we can only speculate about the relevance of this finding. There are three possible explanations. First, the connection profiles of the Semantic_l_rolop and the Semantic_l_parstriang source ROIs stressing attention, salience and sensorimotor networks as the most important targets could be artifacts caused by the specific characteristics of the Shirer parcellation (Shirer et al. 2012). Shirer and colleagues (2012) used an ICA to parcellate the brain into 90 nodes belonging to 14 functional networks. It is in the nature of every brain parcellation generated by an ICA that it is not capable to cover the brain entirely; there are always some regions, which are not accounted for. An ICC is a voxel-wise fine-grained analysis method completely covering the entire brain. Therefore, it could be that the voxels or regions exhibiting connections with the Semantic_l_rolop and the Semantic_l_parstriang clusters on the voxel-level were not accurately covered by the Shirer parcellation. ICCp clusters when individually analyzed can be potentially multifunctional. When the brain regions or voxels, which originally triggered the association with verbal fluency on the ICC level were only partially or not at all covered by the target ROIs of the Shirer parcellation, the connection profiles of Semantic_l_rolop and the Semantic_l_parstriang ROIs might have stressed the target ROIs, which were functionally the next most specific for these clusters but were not anymore related to semantic fluency. However, if this were the case, one would still expect that the Semantic_l_rolop and the Semantic_l_parstriang should exhibit strong connections to the other semantic source ROIs but they did not. Second, the presence of the Semantic_l_rolop and the Semantic_l_parstriang clusters on the ICCp cluster map could indicate functional dedifferentiation of the network structure caused by decreasing positive and negative correlation strengths with age (Betzel et al., 2014; Meunier et al., 2009). As a consequence, originally anti-correlated networks will successively merge into each other. Again, if this were the case, one would also expect the Semantic_l_rolop and the Semantic_l_parstriang displaying connections to the other semantic source

ROIs. Third, apart from the involvement of right sided frontal regions that we interpreted in the section c as an indicator of an age-related compensation mechanism already present as early as in the intrinsically active baseline-configuration of the aging brain, the presence of the Semantic_l_rolop and the Semantic_l_parstriang ICCp clusters could be interpreted as an additional indicator of another age-related compensation strategy. The dorsal attention network or visuospatial attention network is considered to be engaged in selective attention, while the salience network or cingulo-opercular network is associated with tonic alertness, a general mechanism, which is important for task maintenance and shielding the current cognitive process from external unwanted inputs (Sadaghiani & D'Esposito, 2014). While the ECN, DMN and language network are highly specific for verbal fluency, the aging brain might increasingly become dependent on the support of these additional attentional resources in order to sustain successful performance of verbal fluency.

Limitations

Our study has some limitations. First, one limitation might be the fact that we focused on just one connectivity index designed to measure one specific aspect of connectivity, i.e. global connectivity, while there are other aspects of connectivity and also other connectivity indexes capable to capture these other aspects. But one of our main interests was to understand better the relevance of previous findings that the efficiency of long-distance connections and therefore the capacity for global information processing decreases with increasing age. Additionally, as already explained in the methods section, we did not want to define a priori ROIs or a threshold because both procedures are arbitrary to some extent and have – especially when investigating the aging brain - the potential to heavily influence the results. Therefore, the ICCp analysis that works without the need to define ROIs or a threshold fitted our needs best. Second, the data came from a longitudinal project and that fact implies some restrictions on the available data as soon as the data are used outside the longitudinal context. Thus, it was not possible to compare our findings with task-induced fMRI data from our study population or with the data of a young population that has undergone the same tests and MRI exams in order to differentiate the networks involved in verbal fluency clearly from age-effects. We also have to acknowledge that the LHAB study population is in some way not necessarily representative for that age cohort. Since the participants are generally characterized by a high educational and socio-economic status, by good health and by a still very active life style. However, the LHAB project has its focus on the cognitive and neurophysiological mechanisms of healthy aging and in that context our study sample seems to be highly representative as the over-average high mental and health composite scores of the SF-12 demonstrate.

Conclusion

We speculated that by looking at the functional base configuration of the aging brain, from which it is altogether starting when performing a goal-directed task like verbal fluency, we would get complementary insights that were missed by the previous studies, which all mostly analyzed task-induced fMRI data.

If we recap our findings, we see a mixed picture: The results of the ICC analysis showed two important findings. On the one side, the preserved capability of the aging brain to adequately reconfigure its networks for a new, untrained task and perform behaviorally in the same range like young adults was demonstrated. On the other side, the involvement of the right-sided frontal regions might not be interpreted as a successful compensatory strategy but one might very cautiously suggest that we see a first indicator of age-related dedifferentiation of the involved network configurations. The subsequent connectivity analyses also revealed two interesting results: Firstly, it replicated the finding of other studies on the aging brain and showed again the relevance of preserved functional long-range connections from the frontal regions to the lateral and medial parietal lobe and to the cerebellum. Secondly, it demonstrated the involvement of the dorsal DMN whose highly synchronized deactivation is a necessary prerequisite for the successful interaction of the ECN and the language network.

Acknowledgements

The current analysis incorporates data from the Longitudinal Healthy Aging Brain (LHAB) database project, which is carried out as one of the core projects at the International Normal Aging and Plasticity Imaging Center / INAPIC and the University Research Priority Program “Dynamics of Healthy Aging” of the University of Zurich. The following members of the core INAPIC team were involved in the design, set-up, maintenance and support of the LHAB database: Anne Eschen, Lutz Jäncke, Mike Martin, Susan Mérillat, Christina Röcke, and Jacqueline Zöllig.

5.3 Third Study

Successful functional compensation or age-related decline - What can we learn by looking at the intrinsically active baseline of the healthy aging brain?

5.3.1 Introduction

Age inevitably seems to be accompanied by cognitive and behavioral changes, as well as structural degeneration such as progressive gray matter atrophy or loss of white matter integrity as evidenced by structural neuroimaging methods (Fjell et al., 2009; Good et al., 2001; Jäncke et al., 2015; Raz et al., 1997; Salat et al., 2004; Sowell et al., 2003). However, functional neuroimaging methods like PET and fMRI have been able to provide a slightly different point of view: older brains often show activation patterns that distinctly differ from those observed in young brains, even though young and old still perform at the same level. The activation patterns in older adult brains are not only spatially increased in comparison to young adults, but additional brain regions are recruited. Especially for functions that show strong lateralized activation in young subjects, older brains seem to rely on the additional participation of homologous areas in the contralateral hemisphere. One possible interpretation for these findings is that the aging brain might be able to preserve its behavioral and cognitive performance by functionally adapting and/or compensating in different ways for age-related structural degeneration. However, another explanation is equally plausible: Age-related differences in activation patterns might indicate a functional dedifferentiation of the regions and networks supporting the investigated function. This interpretation is supported by a number of studies that have found evidence that the same activation patterns, which were interpreted by other studies as compensation strategies, are likewise observed in combination with age-related cognitive and behavioral degradation (Meinzer et al., 2012; Persson et al., 2007).

In order to decide whether the observed age-specific differences in activation patterns represent compensation mechanisms or the first signs of functional disorder, it could help to take into account the intrinsic network architecture, which at least partly influences the functional network architecture supporting cognition and goal-driven behavior as observed in the scanner (Sadaghiani et al., 2014). Of course, functional compensation is a modus operandi of the brain that can only be observed when the brain is actively engaged in goal-directed behavior. Therefore, investigating the characteristics of the intrinsically active baseline configuration in order to understand the aging brain's potential for compensation may at first seem counter-intuitive. However, the brain's task-evoked network architecture and the intrinsic network architecture have been shown to be highly related. Cole and

colleagues (2014) demonstrated that the intrinsic baseline architecture of the brain is the dominant configuration during all brain states (i.e. intrinsic vs. evoked) and shapes the general task-evoked architecture of the brain. Needless to say, task-specific changes in the functional connectivity architecture are also present but these seem to be rather small in comparison to the dominant intrinsic network architecture (Cole et al., 2014). Likewise, the brain's intrinsic activity is not just the starting-point from which the brain generates the actual goal-driven behavior, but it still continues while the brain performs the behavior and influences its outcome (Hesselmann et al., 2008a, Hesselmann et al., 2008b, Sadaghiani et al., 2010). While one might reasonably question the actual impact that the intrinsically active baseline configuration has on the activation patterns observed during goal-directed behavior in the scanner, this does not imply that there is no relation between the task-positive and the task-negative states of the brain at all. The evidence from the literature suggests that it is reasonable to assume that the condition of the intrinsically active functional baseline configuration might have at least some impact on the brain's potential to compensate for age-related constraints. Therefore, in this study, we analyzed the intrinsically active functional baseline configuration of a large sample of adults during the transition from old age to very old age. Our aim was to investigate which regions of the aging brain might possess the qualities necessary to compensate for the structural and functional decline of others as well as which brain regions might exhibit the indicators of functional degradation already inherent in intrinsic network organization.

A number of models have been formulated in the attempt to provide an overarching explanation for the age-related differences in brain activity observed in task-induced fMRI studies: Nevertheless, we decided to relate our findings to only two of these compensation models. Unlike the other models, the HAROLD (Cabeza et al., 2002) and PASA (Davis et al., 2008) compensation models make relatively precise assumptions about which regions may be involved in the alleged compensatory mechanisms. HAROLD is the acronym for "age-related reduction of hemispheric asymmetry in the aging brain" (Cabeza et al., 2002) and is based on the observation that tasks that induce a strongly lateralized activation pattern in young subjects appear to activate additional homologous regions in the functionally non-dominant hemisphere of older adults' brains in such a way that the functional asymmetry seems to be reduced or suspended. This reduction in asymmetry is mainly observed in the frontal regions. PASA is the acronym for "posterior-anterior shift in aging" and relies on the observation that older brains show an age-related reduction in temporo-occipital activity, combined with higher metabolic activity in the frontal regions. The PASA and the HAROLD models, and the anterior-posterior and left-right compensation patterns proposed by these models, shall be the guiding principles based on which we will examine the degree to which the aging brain's intrinsically active functional baseline configuration might preserve basic resources for functional compensation.

In order to guarantee an unbiased perspective, we decided to pursue a purely data driven approach without the need for a priori assumptions. We used graph theoretical analysis (GTA) because it allows us to describe the functional architecture of the brain in its entirety as well as to investigate the relationships between every individual brain region. Previous studies using task-free fMRI data have repeatedly demonstrated that the intrinsic connectivity networks (ICNs) of the aging brain are characterized by a decrease in intra-network correlations and an increase in inter-network correlations (Betzel et al., 2014; Geerligs et al., 2014; Meunier et al., 2009). Based on previous findings, we analyzed a positively and negatively weighted graph-network in order to account for the age-typical alterations in the correlation range of the connections. The intrinsically active baseline configuration is not stationary but is, at every time point, characterized by a dynamic trade-off between stability and flexibility, driven by a highly dynamic and fine-tuned interplay of different networks and brain regions (Jones et al., 2012, Hutchison et al., 2013). To describe such a network one must account for both characteristics. Therefore, we used the GTA measures of "nodal strength," "nodal diversity coefficient", and "nodal centrality," which is a combination score of nodal strength and nodal diversity (Rubinov & Sporns, 2011) to investigate the capacity of the aging brain's baseline configuration for compensation. While nodal strength is able to capture a node's number of connections and their stability, nodal diversity accounts for the flexibility, i.e. the number of inter-modular connections that a node sustains during a given period of time. Only nodes that combine both characteristics to a high degree, i.e. high positive nodal diversity and high positive nodal strength, qualify as highly influential nodes, which might have the capacity to counteract the functional degradation of other nodes.

To the best of our knowledge, this study is the first to use the combination of these GTA measures to investigate the intrinsically active functional baseline configuration of an aging study sample.

5.3.2 Methods

I Participants

The MRI and behavioral data come from the first data acquisition time-point of the Longitudinal Healthy Aging Brain (LHAB) database. The LHAB is a longitudinal database project, which started at the International Normal Aging and Plasticity Imaging Center (INAPIC) of the University of Zurich in 2011 and is currently run at the University Priority Project "Dynamics of Healthy Aging". The LHAB project aims to investigate the complex relationships between cognition and structural and functional correlates of the aging brain (Zöllig et al., 2011).

In order to qualify for the participation in the LHAB project, the candidates had to be 65 years or older, right-handed, native Swiss-German or native German speakers and healthy. To assess physical and mental health, the 12-Item Short-Form Health Survey (SF-12) was administered. The self-reported mean physical health composite score in the LHAB sample was 50.8 (SD = 7.2), which is well above the US norm mean of 43.9 (age group between 65 and 74 years). The self-reported mean mental health composite score was 55.0 (SD = 6.0), which is slightly above the US norm mean of 51.6 points (age group between 65 and 74 years).

Besides the standard safety criteria relevant for MRI assessments the participants had to fulfill the following inclusion criteria: no history or current diagnosis of psychiatric or neurologic diseases, e.g. Parkinson's disease, Alzheimer's dementia, multiple sclerosis, migraine, a MMSE score > 26, and no medical conditions such as diabetes, tinnitus, and diseases of the hematopoietic system. All participants gave written informed consent to the participation of the longitudinal project under the approval of the local ethics committee and in accordance with the Helsinki declaration.

221 persons participated in the first wave of the LHAB project; the data of 186 participants (mean age = 70.4; SD = 4.8; 89 men and 97 women; for the age distribution please see Figure 5.3.1) were used in this project as they fulfilled the study-specific inclusion criteria such as completeness of the MRI data and motion parameters < 2mm.

Figure 5.3.1 Age distribution

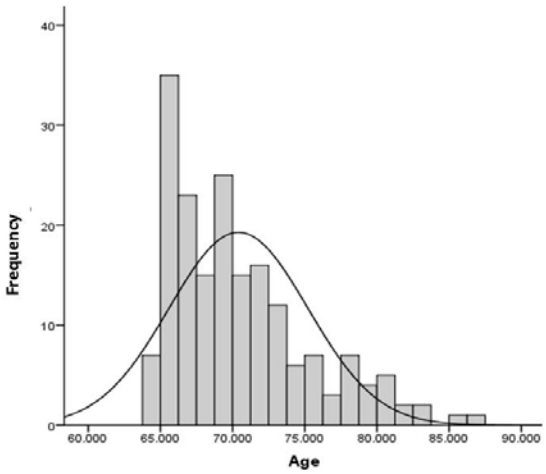

The figure 5.3.1 shows the age distribution for the 186 participants whose data were used in this study.

II Neuropsychological data

At every data collection time-point, the participants of the LHAB-project have to take an intensive cognitive assessment. The LHAB test-battery consists of 33 different neuropsychological tests that cover reasoning (3), verbal intelligence (3), verbal fluency (2), executive functions (3), processing speed (3), attention (3), working memory (3), memory (3), spatial orientation (3), spatial reasoning (4), and motoric and fine motoric coordination (3).

The aim of the study was to investigate the intrinsically active functional brain architecture in order to understand better to which degree it might be still able to compensate for already present structural and functional age-related decline affecting cognition. For that reason, we decided to focus on three cognitive domains, which we hypothesized to be particularly vulnerable to age-related functional dedifferentiation of the intrinsic network architecture: 1) Inductive reasoning as one of the cognitive domains mainly relying on fluid intelligence, which is known to decline with increasing age (Craik & Bialystok, 2006; Kaufman & Horn, 1996), 2) processing speed, which is hypothesized to be the underlying cause of all cognitive changes in old age (Salthouse, 1996), and 3) memory. The selection of this last domain was primarily guided by the findings of an un-published VBM study of the same 186 participants, which had revealed the hippocampi and the limbic system as well as the temporal cortices as most affected by age-related atrophy in this study sample (Table 5.3.1).

Table 5.3.1 Summary of the tests used

Cognitive Domain	Test	Source	Description	Mean	SD
Inductive reasoning	LPS Subtest 3	Leistungsprüfsystem (LPS)	Detecting ir-/regularities in geometrical figures	23.27	4.69
	LPS Subtest 4	Leistungsprüfsystem (LPS)	Detecting ir-/regularities in numbers and letters	26.29	4.48
	Number Series	Educational Testing Service Kit (ETS)	Detecting ir/regularities in numbers	5.52	3.21
Perceptual speed	Identical Pictures	Educational Testing Service Kit (ETS)	Matching the corresponding picture to a template	48.34	10.21
	LPS Subtest 14	Leistungsprüfsystem (LPS)	Comparing and detecting differences	58.82	4.75
	Digit Symbol	Wechsler Intelligenztest für Erwachsene (WIE)	Matching the corresponding symbol to a number	20.64	12.85
Memory	VLMT (sumscore)	Verbaler Lern- und Merkfähigkeitstest (VLMT)	Memorizing wordlists and reproducing them	56.67	9.60
	DCS (sumscore)	Diagnosticum für Cerebralschädigung (DCS)	Memorizing figures and reproducing them	31.49	12.52

We transformed the scores of the eight sub-tests selected for this study into z-scores and then computed composites for each cognitive domain to be used in the following analyses.

III MRI-data acquisition

All MRI-data were acquired on the same Philips 3T Ingenia Medical Scanner with a Philips 15 channel head-coil at the University Hospital Zurich.

The following images were acquired: 1. A T1 weighted TFE- SENSE sequence with TR = 8.2ms, TE = 3.7ms, Flip Angle = 90 (FOV = 240 × 160 × 240mm^3, matrix size = 256 × 256, isotropic voxel size = 0.94 × 0.94 × 1mm) 160 slices per volume. 2. A T2 weighted TSE- SENSE sequence with TR = 3000ms; TE = 80ms Flip Angle = 90 (FOV 512 x 28 x 512mm^3; matrix size = 488 x 309, anisotropic voxel size 0.45/ 5/ 0.45mm) 28 slices per volume. 3. A task-free blood oxygenation level-dependent signals (BOLD) single shot whole brain EPI with a TR = 2000ms, TE = 21ms, Flip Angle = 76; 43 transverse slices (FOV = 220 × 150 × 220mm^3, matrix size = 64 × 64, ascending acquisition without gap, anisotropic voxel size = 1.72/ 1.72/ 3.50mm, aligned to the AC-PC line), acquisition time 7.39 min, 225 volumes.

For this part of the data acquisition, the participants were instructed to relax but also to lay as motionless as possible, to keep the eyes open while fixating a cross that was displayed on a screen outside the scanner and was visible for the participant by means of a mirror system attached to the receiver coil. Immediately after the task-free scan, each participant was asked if he/she had fallen asleep. All participants confirmed that they were fully awake during the exam.

IV Pre-processing of the MRI data

All pre-processing steps were performed with the SPM8 software (http://www.fil.ion.ucl.ac.uk/spm) and the VBM8 toolbox for SPM8 (http://dbm.neuro.uni-jena.de/vbm) implemented in Matlab (MATLAB R2011B, The Math Works Inc.).

Before the actual pre-processing two additional preparatory steps were executed: First, the first six volumes of the EPI data were discarded allowing for T1 saturation effects, leaving 219 volumes for the analysis, then a first alignment of the EPI-data was performed: Only the «mean-image» and the «motion-parameter-file» of this step were used in the further pre-processing steps. Second, the generation of a study population specific gray matter template to be used in the DARTEL procedure implemented in SPM8 (Ashburner, 2007), since the DATREL procedure allows for a high dimensional and non-linear registration of the anatomical and functional images and their subsequent normalization.

The actual pre-processing consisted of the following steps: 1. The T2-weighted images were coregistered to the T1-weighted images as a reference. 2. The mean EPI-images from the first preparatory step were coregistered to the T2-weighted images. 3. The final realignment of the functional images was done in two steps. During the first run the functional images were aligned to the first image. In this first run, the mean EPI-images, which had been coregistered to the T2-weighted image in step 2, were defined as the reference or first images. In the second run, all functional images were then aligned to the new mean EPI-images produced during the first run of the actual alignment. 4. The fMRI time-series were slice time corrected for the ascending acquisition. 5. The T1 images were anew segmented into gray matter, white matter and CSF tissue maps using the segmentation procedure implemented in VBM8. 6. The DARTEL procedure was run using the GM study group template generated in the second preparatory step. 7. The functional and structural images were normalized into the MNI space, resampled to a 2x2x2mm voxel size, and only minimally smoothed using an isotropic Gaussian kernel (FWHM 1mm) in order minimize possible spurious correlations for the following GTAs.

V Graph theoretical analyses

GTA is a mathematical branch and ideally suited to describe complex large network structures like the human brain. Some abstractions are needed to apply GTA to the brain. Structurally, i.e. macro-anatomically, functionally determined brain regions, or even single voxels are defined as nodes/vertices and structural connections like the white matter fiber tracts or statistical dependencies like the correlation of the BOLD signal between different regions/nodes of the brain are defined as edges/links. These two elements, nodes and edges, are the all information needed to compute a correlation matrix, in which the nodes are represented in the first column and the first row of the matrix and the edges between them are entered in the respective fields of the matrix. Based on the correlation matrix different graph theory measures can be computed each describing another aspect or characteristic of a node in respect to the whole brain and/or in respect to every other single node of the network.

Vi Denoising of the task-free fMRI data, partition of the brain, and generation of subject-specific correlation matrixes

For the generation of subject specific adjacency matrixes the Conn Toolbox (version15a; http://www.nitrc.org/projects/conn) for SPM (Whitfield-Gabrieli & Nieto-Castanon, 2012) was used.

Vii Denoising and band-pass filtering of the data

Next, although we had already discarded all fMRI data-sets of participants displaying motion artifacts of 2mm translation or higher, we additionally performed an outlier detection and scrubbing procedure using the toolbox ART as implemented in the pre-processing pipeline of Conn (scan-to-scan global signal z value threshold = 9; scan-to-scan composite motion threshold = 2mm). Instead of actually removing the time-points identified as outliers, ART works by effectively removing these using dummy-coded regressors during the denoising step. This approach has the advantage that the continuity of the time-series is still preserved, which is an important assumption for the subsequent band-pass filtering.

The spontaneous, coherent, and low frequent fluctuations of the BOLD-signal are used for intrinsic connectivity analyses. As non-neural low frequent (< 0.1 Hz) signals such as heart rate or respiration are able to modulate the BOLD-signal, they may likewise influence the intrinsic connectivity maps. Hence, a further important step is to correct for these physiological confounding signals. The Conn Toolbox accomplishes this by means of the CompCor method (Behzadi et al., 2007). In the first part of the denoising step implemented in the Conn toolbox the BOLD time-series for each participant were extracted and the motion parameters as well as the confounding signals calculated by the ART outlier detection procedure and the CompCor method were regressed out. The denoising procedure was finalized by band-pass-filtering (0.008 – 0.09 Hz), despiking, and detrending of the individual BOLD time-series.

Viii Partition of the brain and defining functional meaningful nodes

The best method to partition the brain into functional meaningful nodes for GTA is a highly debated question. The three most commonly used approaches to define a node are a) to define every single voxel of the brain as a node b) to use macro-anatomical or cyto-architectonical defined regions as node or c) to use clusters/components extracted by statistical methods like independent component analyses or cluster analyses methods. Currently, none of these three approaches might qualify as the gold standard because all come with some weaknesses (Stanley et al., 2013).

However, an ideal node for a functional GTA should be in itself as intra-nodal homogeneous and inter-nodal heterogeneous as possible (Fornito et al. 2013). Based on these specifications, we wanted to optimize the functional homogeneity and therefore decided to use the third approach by which the brain is functionally partitioned using purely data-driven statistical methods like clustering analysis or independent component analysis (ICA) on the BOLD-time-series of the fMRI data. We are well aware of the fact that this approach also has its weaknesses. Thus, the researcher applying these statistical

methods has to make some preliminary decisions like the number of clusters or components to extract, which can influence the results heavily. Furthermore, the results of these partition methods do not only vary from study sample to study sample, but even within the same study sample because the algorithms of both statistical methods come with some heuristics. Therefore, the outcome may vary from run to run.

In order to be able to compare the results with previous studies, we decided to use the already existing and commonly used partition of Shirer and colleagues (Shirer et al. 2012). This partition was computed by means of a low-dimensional independent component analysis (ICA) on task free fMRI data of a sample of 15 healthy young adults. It consists of 90 nodes, representing 14 well established functional ICNs: Auditory = auditory network (4 nodes); BasGang = basal ganglia network (5 nodes); LECN = left executive control network (6 nodes); Language = language network (7 nodes); Precuneus = precuneus network (4 nodes); RECN = right executive control network (6 nodes); Sensorimotor = sensorimotor network (6 nodes); Visuospatial = visuospatial or dorsal attention network (11 nodes); antSalience = anterior salience or cingulo-opercular network (7 nodes); dorsal DMN = dorsal part of the default mode network (9 nodes); highVisual = higher visual network (2 nodes); postSalience = posterior salience network (12 nodes), ventralDMN = ventral part of the default mode network (10 nodes).

Viv Whole brain graph theoretical analysis

For all following GTAs we used the Brain Connectivity Toolbox (BCT) of Rubinov and Sporns (Rubinov & Sporns (2010) or https://sites.google.com/site/bctnet/).

a) Thresholding the networks

Although the definition of a threshold, which the connections have to surpass in order to separate the strongest and supposedly most important edges from weak edges is a standard procedure for GTA we decided to analyze weighted and un-thresholded networks. The reasons for this decision are as follows: 1. A finding, on which most of the studies investigating age-related changes in the brain agree, is that the ICNs are characterized by dedifferentiation processes with advancing age. The positive within-network correlations decrease while intra-network correlations seem to increase or show a trend to decrease toward zero in the case of anti-correlated networks. As a result, the functional networks are not anymore clearly differentiated but merge into each other (Betzel et al., 2014; Geerligs et al., 2014; Meunier et al., 2009). Based on these observations, the degree of still preserved positively and negatively correlated networks seems to be especially informative for the understanding of the aging brain, and we could risk losing this important information when analyzing binarized networks or only positive weighted networks. 2. As mentioned above, under the assumption that only very strong connections reliably convey information about the functional organization of the brain,

researchers using GTA usually prefer high thresholds resulting in sparse networks. By doing this, they might lose important information. Santarnecchi et al., (2014) could show that a two-level connectivity structure, which combines the information of very strong but also of moderately weak connections was better suited to explain inter-individual differences in IQ in a sample of young to middle aged adults (mean age = 34 years). They demonstrated that strong connections carried the information about the general functional organization of intelligence in the human brain, and weaker connections explained the inter-individual variability in intelligence. However, the finding of Santarnecchi and colleagues (2014) in combination with the aforementioned age-related decrease of within-network correlations makes it difficult to define a cut-off value, that reliably differentiates between weak but still information carrying edges and weak edges representing just noise.

b) GTA measures apt to characterize the most central nodes of positively and negatively weighted networks but also to detect indicators of node or network disorder

Highly influential nodes of the brain are characterized by their tendency to be connected to other likewise highly connected regions in the brain, by the strength of these connections, and by the regional connection diversity (Rubinov & Sporns, 2011). To determine the most central and influential nodes but to be also able to detect potential age-related disorganization of the intrinsic network architecture of our study sample we used the following GTA measures:

- **Nodal strength:** Nodal strength is the sum of all weighted positive and negative connections of a node (Rubinov & Sporns, 2011). Two strength values can be computed for every node; one combining the number and the weights of all positive connections and another combining the number and weights of all negative connections of the node.

- **Nodal diversity coefficient:** Brain networks can be divided into smaller sub-networks or modules. Nodes constituting a module are more strongly connected to each other than to all other nodes of the brain. The nodal diversity coefficient quantifies a node's number of connections with the different modules of the brain. Nodes with a high diversity coefficient display a relatively even distribution of connections with all modules of the brain (Fornito et al. 2012; Rubinov & Sporns, 2011). Again, two diversity coefficients can be computed for every node, one value representing all positive inter-modular connections and another representing all negative inter-modular connections. The concept of the positive diversity coefficient is intuitively comprehensible. A node sustaining many positive connections to the modules of the brain is a transitional node, a node apt to integrate the information across these different modules (Fornito et al., 2012). A high negative diversity coefficient characterizes a node that shows a large number of anti-correlated connections with the modules of the brain. Such a differentiated connection profile is characteristic of a functionally highly specific node.

Therefore, the combination of both diversity coefficients can be quite informative, because a node characterized by a high positive diversity coefficient as well as a high negative diversity coefficient does not hold the same capacity for information integration as a node displaying a high positive diversity coefficient in combination with a low positive diversity coefficient. Only the last might possess the qualities of a very central and influential hub depending on the strength of the positive connections.

- **Nodal centrality:** Rubinov and Sporns (2011) define nodes characterized by high positive strength and high positive diversity coefficients in combination with low negative strength and low negative diversity coefficients as central and very influential nodes. Such highly central nodes are very dynamically and efficiently interacting with many sub-groups and or modules and coordinating the information flow between them.

In order to assess the non-randomness of our findings and to prove their neurobiological relevance for the aging brain, we computed for each participant two different versions of random networks based the subject's individual correlation matrix. To ensure the non-randomness of the investigated strength distribution we generated random networks, which did preserve neither the strength nor the degree distribution of the original subjects' matrixes. To ensure the non-randomness of the diversity distribution we applied criteria that were more rigorous and generated random networks using the null-model algorithm from the BCT toolbox with 30 bin swaps, which preserves the original weight, the original degree as well the original strength distribution (Rubinov & Sporns, 2011). In a second step, we then assessed the non-randomness of the empirical distributions of our sample by using the non-parametric two samples Kolmogorov-Smirnov test combined with the Monte Carlo method to generate 10'000 samples.

Vv The aging brain's intrinsic functional architecture on a macro-scale level: Composing regional composites

The HAROLD and the PASA compensation models make clear assumptions about how the regions of the aging brain interact with each other in order to compensate for functional decline of the gray matter. As we aimed to relate our findings of the GTAs to these compensation models, we pooled the single nodes to form different regional composites representing macro-scale regions like the anterior part vs. the posterior part of the brain, which are hypothesized by these models to be able to compensate for the functional degradation of their respective counterpart.

For that reason, we combined the graph measures of positive/negative strength and positive/negative diversity of all cortical nodes located in frontal part of the brain (i.e. frontal cortex to precentral gyrus)

into an anterior composite and all cortical nodes located in the posterior part of the brain (i.e. postcentral gyrus to the occipital cortex) into a posterior composite in order to further investigate these composites' functional configuration in relation to each other. The temporal lobes, the cerebellum and all subcortical regions were omitted for this anterior-posterior comparison. Likewise, we pooled all left-sided cortical, subcortical, and cerebellar nodes into a large left-hemispheric composite and also all right-sided nodes in to a right-hemispheric composite thereby omitting just the nodes covering the midline of the brain, which could not be clearly assigned to one of the hemispheres. As the HAROLD pattern was mostly observed for the frontal cortex, we additionally build a left and a right frontal cortex composite consisting of the nodes located in the prefrontal cortex and the insulae.

Next, we computed for each of the regional composites described above the means in positive and negative strength, and in positive and negative diversity. By using t-tests with a bootstrapping procedure (1000 samples) or Kolmogorov-Smirnov two-samples in combination with the Monte Carlo method (10'000 samples), whenever the composites' values were not normally distributed, we then tested for significant differences between the macro-scale composites' strength and diversity characteristics. We repeated the same computations for the two random network versions generated for each participant in order to assure that the left-right or anterior-posterior specific brain characteristics found in the study sample could not also be observed in the random equivalents.

5.3.3 Results

In this section we refer to the ROIs/nodes using the following naming scheme: The ROIs of the Shirer partition are named to connote 1) the functional ICN to which the node belongs and 2) the brain region in which it is mainly located. Thus, the name "dorsal DMN/l_ang" refers to a node of the dorsal default mode network, which is located in the left angular gyrus.

I The neurobiological relevance of the GTA results

We compared the GTA values in nodal strength and nodal diversity of our 186 empirical networks against the values computed for the 186 equivalent random networks using the non-parametric two samples Kolmogorov-Smirnov test. The results are listed in the table below (Table 5.3.2):

Table 5.3.2 The neurobiological relevance of the GTA results: Nodes exhibiting random characteristics

	Positive Strength	Negative Strength	Positive Diversity	Negative Diversity
Significant different from the equivalent random nodes ($p < 0.05$)	85 nodes	78 nodes	86 nodes	84 nodes
Characteristics not significant different from the equivalent random nodes	LECN_2/l_porbit Language_1/l_ifg Visuopspatial_5/r_precent antSalience_4/r_mfg postSalience_1/l_mfg	BasGang_5/brainstem LECN_1/l_mfg Visuospatial_2/l_spl Visuospatial_4/l_ifg Visuospatial_6/r_spl Visuospatial_7/r_poper Visuospatial_8/r_itg Visuospatial_9/l_cerebellum8 antSalience_1/l_mfg dorsalDMN_5/r_mcc ventralDMN_8/l_parahipp ventralDMN_10/r_cerebellum8	BasGang_3/l_parstriang BasGang_5/brainstem Sensorimotor_6/r_thal Visuospatial_3/l_poper	BasGang_1/r_caud BasGang_5/brainstem LECN_6/l_thal, Precuneus_2/bilateral_precun Sensorimotor_6/r_thal ventralDMN_6/bilateral_precun

When subsuming all nodes exhibiting random characteristics in one or more of the four GTA measures used for this study, two features stood out. 1) Almost all nodes of the visuospatial network, i.e. eight of eleven nodes, showed random qualities in at least one of the investigated GTA measures. 2) The node BasGang_05/brainstem showed random characteristics in all investigated GTA measures except for positive nodal strength.

We did not exclude the nodes showing random characteristics from the further analyses and interpretations since the fact that some single nodes do not differ in their GTA characteristics from random nodes might have diagnostic relevance for the questions at hand. In the results and discussion section, in all figures and tables we will always clearly mark these nodes showing random characteristics to make sure that the readers are aware of these nodes' particular characteristics at any time.

II The results for the GTAs on node level

Up to now, there exists no commonly accepted standard procedure to define a cut-off value for a certain GTA measure in order to determine the really high loading and therefore significant nodes and to isolate these from the less important nodes. A cut-off often used is the mean or the values being one or two standard deviations above the mean. As the nodal GTA measures of our analyses showed no normal distribution, we decided to concentrate on the topmost third of the nodes, i.e. the 30 nodes with the highest values for the respective GTA measure.

a) Positive nodal Strength

Figure 5.3.2 Illustration of the positive strength distribution

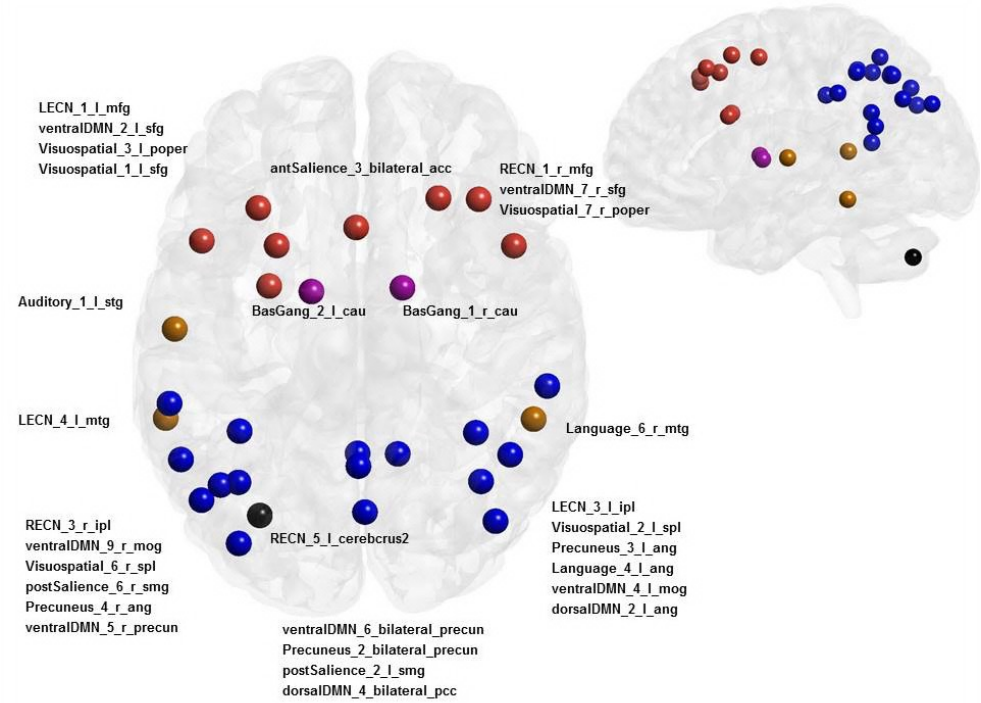

The figure 5.3.2 shows the 30 nodes belonging to the topmost third exhibiting the highest values of positive strength. (Color code for the nodes: Red = anterior part of the cortex; blue = posterior part of the cortex; orange = temporal lobes, purple = subcortical regions, i.e. basal ganglia and thalamus; yellow = limbic system; black = cerebellum; nodes with random characteristics are also pointed out by asterisks in the legends).

When analyzing the distribution of the nodal strength over the topmost 30, one feature stood out: 1. The prominence of the posterior regions in the highest third, more than the half of the nodes, i.e. 16 of the 30 nodes, were located in posterior regions, mainly in the lateral and medial parietal regions. In contrast, only eight nodes were located in the frontal part of the brain. In comparison, the temporal lobes, the subcortical regions and the cerebellum seemed to be under-represented, because just three, respectively two and one node from these regions qualified for the topmost third.

b) Negative nodal strength

Figure 5.3.3 Illustration of the negative strength distribution

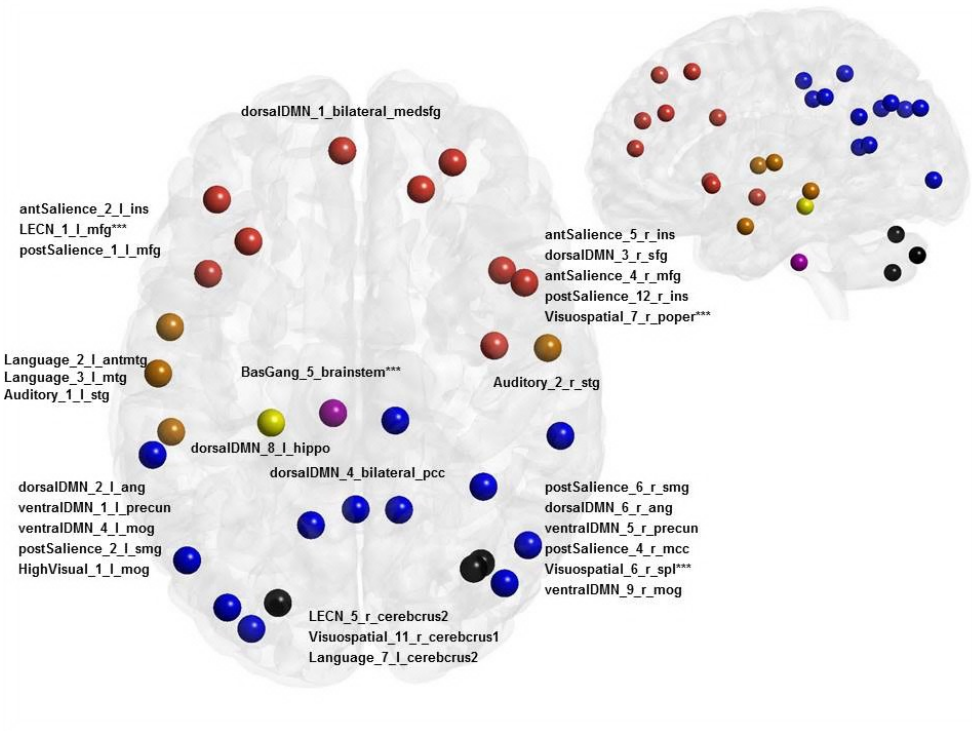

The figure 5.3.3 shows the 30 nodes belonging to the topmost third exhibiting the highest values of negative strength. (Color code for the nodes: Red = anterior part of the cortex; blue = posterior part of the cortex; orange = temporal lobes, purple = subcortical regions, i.e. basal ganglia and thalamus; yellow = limbic system; black = cerebellum; nodes with random characteristics are also pointed out by asterisks in the legends).

The distribution of the 30 nodes displaying the highest values of negative nodal strength was fairly well balanced across the brain: 12 nodes were located in the posterior part of the brain, nine nodes in the anterior part of the brain, four in the temporal regions, three in the cerebellum and one in the subcortical areas. No obvious lateralization effect could be observed as 17 nodes were located in the left hemisphere and 13 nodes in the right hemisphere.

c) Positive nodal diversity

Figure 5.3.4 Illustration of the positive diversity distribution

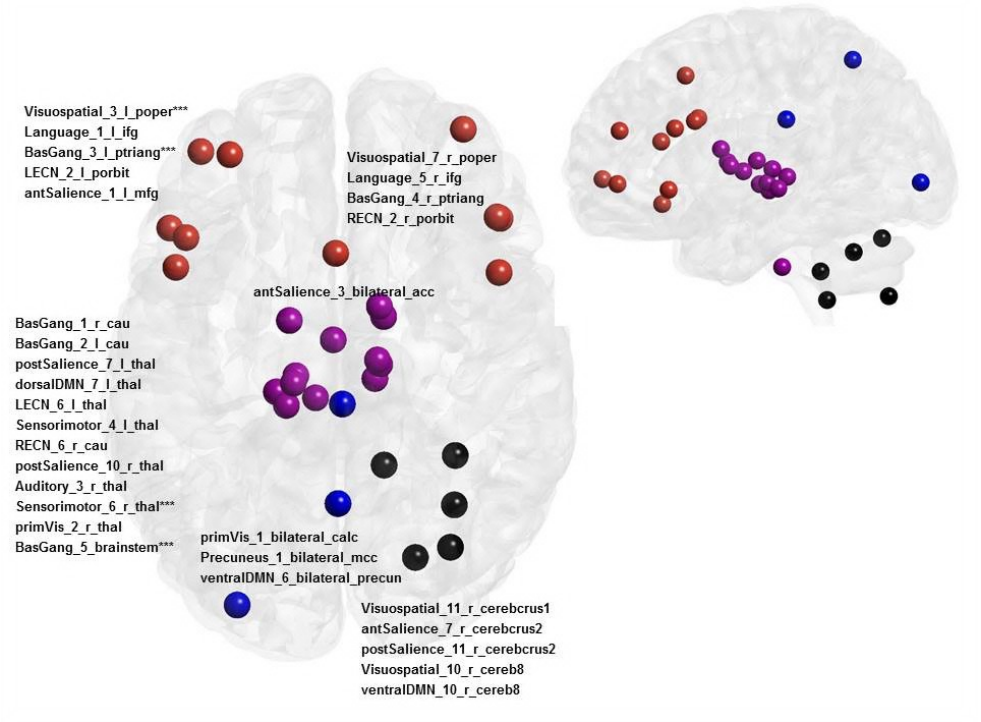

The figure 5.3.4 shows the 30 nodes belonging to the topmost 30 of nodes exhibiting a high positive diversity coefficient. (Color code for the nodes: Red = anterior part of the cortex; blue = posterior part of the cortex; orange = temporal lobes, purple = subcortical regions, i.e. basal ganglia and thalamus.

A very different pattern emerged for the distribution of positive nodal diversity. Two features stood out: 1. Subcortical nodes dominated the topmost third of nodes in terms of high values in nodal diversity, i.e. 12 of the 30 topmost nodes were located in sub-cortical regions, ten nodes in the anterior part of the brain and five nodes in the cerebellum. 2. As before for the positive strength distribution, we found an anterior-posterior pattern: While ten nodes located in the anterior part of the brain belonged to the topmost third of nodes displaying high values for positive diversity only three nodes of the posterior part of the brain displayed similar high values.

d) Negative nodal diversity

Figure 5.3.5 Illustration of the negative diversity distribution

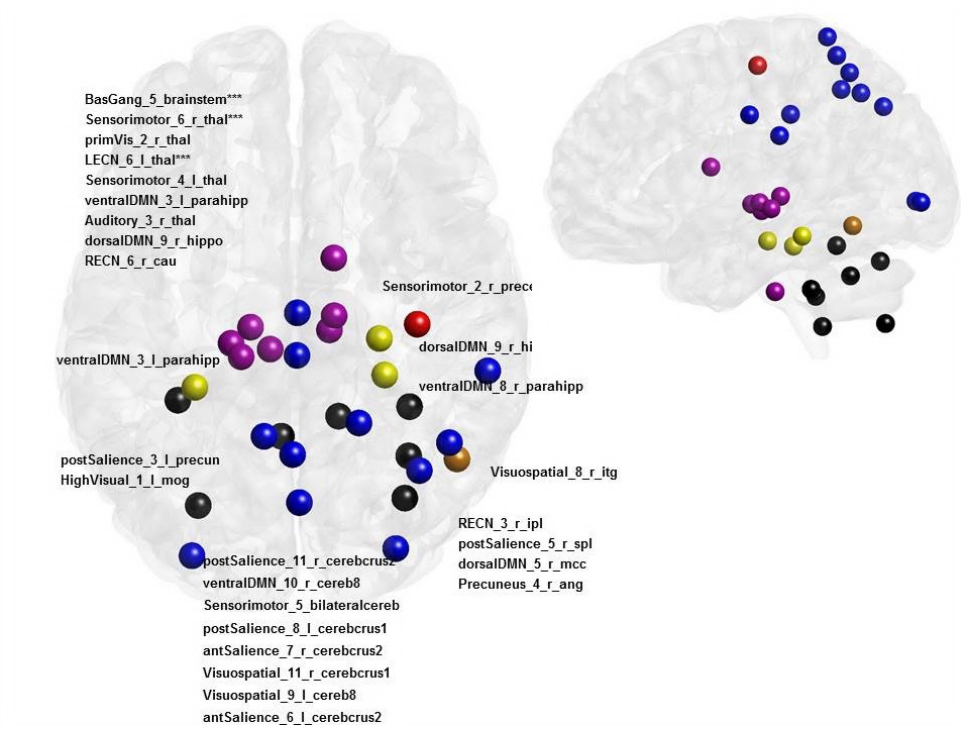

The figure 5.3.5 shows the 30 nodes belonging to the topmost 30 of nodes exhibiting a high negative diversity coefficient. (Color code for the nodes: Red = anterior part of the cortex; blue = posterior part of the cortex; orange = temporal lobes, purple = subcortical regions, i.e. basal ganglia and thalamus; yellow = limbic system; black = cerebellum; nodes with random characteristics are also pointed out by asterisks in the legends).

Quite the opposite distribution was found for the negative diversity coefficient. A third of the 30 nodes exhibiting high values for negative diversity were located in subcortical regions, another third was located in the posterior part of the brain and 8 nodes were located in the cerebellum. The anterior part of the brain was clearly under-represented because only one node in the right precentral gyrus showed a value high enough to qualify it for the topmost 30 nodes in negative diversity.

e) Nodal centrality

Only three nodes, one located in the anterior cingulate cortex and two located in the left and the right caudate nucleus qualified as very influential and central nodes because they were the only ones characterized by high values in positive strength and positive diversity and low values in negative strength and negative diversity. Because we hypothesized that very central nodes might have the potential for compensation, we correlated the nodes' positive strength and diversity coefficients with the cognitive performance of the participants but found no significant association (please see figure 5.3.6).

Figure 5.3.6 Illustration of the three most central nodes

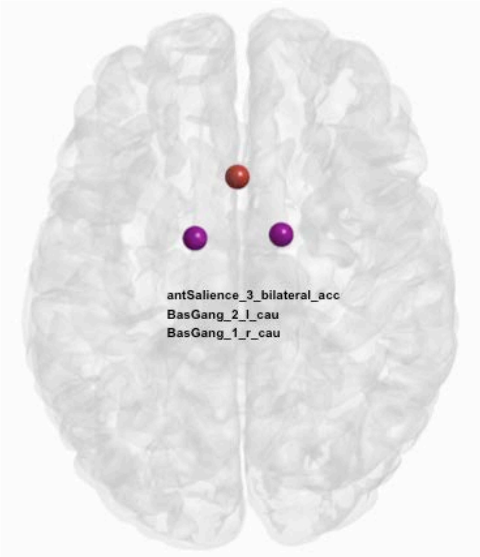

The figure 5.3.6 shows the three nodes qualifying as highly central nodes because they belong to the topmost third of nodes scoring high in nodal strength as well as in nodal diversity. (Color code for the nodes: Red = anterior part of the cortex; blue = posterior part of the cortex; orange = temporal lobes, purple = subcortical regions, i.e. basal ganglia and thalamus; yellow = limbic system; black = cerebellum; nodes with random characteristics are also pointed out by asterisks in the legends).

III GTA results for the regional composites

All t-tests and Kolmogorov-Smirnov two sample tests described below were also computed for the two random network versions. We did not observe any significant differences in nodal strength or diversity for the anterior-posterior or left-right configurations of the equivalent random networks. In contrast all statistical tests constantly showed highly insignificant results.

A. Anterior-posterior configuration

a) Positive strength

We generally observed lower means in positive strength for the anterior composite than for the posterior composite. The subsequent t-test showed that the posterior composite (M = 15.39; SD = 2.85) was characterized by significantly higher means in positive strength (t (370) = - 4.71; p < .001) than the anterior composite (M = 13.99; SD = 2.86). Next, we computed the anterior-posterior difference (= anterior mean value – posterior mean value) for all 186 participants and correlated these values with the participants' age. Age and the anterior-posterior difference showed a significant correlation (Spearman r = - .151; p = .039) – the anterior-posterior difference in positive strength increased with higher age of the participants. As we were interested in the cognitive relevance of this anterior-posterior imbalance in positive strength we computed next the anterior-posterior ratio (= anterior mean value / posterior mean value) and then correlated this ratio with the participants' scores in reasoning, processing speed and memory. We found significant correlations for processing speed (Spearman r = .155; p = .036) and memory (Spearman r = .185; p = .013). Successful performance in these three cognitive domains was significantly associated with a well-balanced ratio of the anterior composite and the posterior composite in positive strength or to put it another way, the higher the anterior composite's values in positive strength in relation to the values of the posterior composite the higher the participants' performance in memory and processing speed.

In this context, we wanted to know which of the posterior nodes might be especially important for the aging brains preserved cognitive performance. Consequently, we correlated the values in positive strength of the 16 posterior nodes from the topmost third with the participants' scores in reasoning, processing speed and memory and found that positive strength values of five posterior nodes showed significant associations (Table 5.3.3). However, none of the correlations was sufficiently strong enough to survive the Bonferroni correction for multiple comparisons.

Table 5.3.3 Association of positive strength and cognition on nodal level

Node	Reasoning	Memory	Processing Speed
Precuneus_2/bilat_precuneus	Spearman r = -.147; p = 0.048	Spearman r = -.190; p = .012	-
Precuneus_3/l_ang	Spearman r = -.167; p = .024	-	-
postSalience_6/r_smg	-	Spearman r = -.162; p = .032	-
ventralDMN_5/r_precun	Spearman r = -.202; p = .006)	Spearman r = -.0159; p = .035	-
ventralDMN_9/r_mog	-	Spearman r = -.165; p = .029	-

b) Negative strength

Again, we observed that the negative strength mean values of the anterior composite were generally lower that the negative strength means for the posterior composite. The subsequently computed t-tests showed that the posterior composite (M = 4.53; SD = 1.35) was characterized by significantly higher values in negative strength (t (370) = 2.00; p = 0.45) than the anterior composite (M = 4.22; SD = 1.35). However, as we subsequently computed associations of the anterior-posterior difference and anterior-posterior ratio in negative strength with age these were not anymore significant.

c) Positive diversity

In contrast to the observations for nodal strength where we found that the posterior regions generally showed higher values than the frontal regions, we now observed the inverse pattern because the frontal regions constantly exhibited higher means in positive diversity than the regions constituting the posterior composite. The t-test showed that the means in positive diversity of the anterior composite (M = 0.737; SD = 0.060) indeed were significantly (t (370) = 9.341; p < .001) higher than the means in positive strength of the posterior composite (M = 0.674; SD = 0.070). However, all following analyses testing the association of this anterior-posterior imbalance in positive diversity with age or cognitive performance showed no significant results.

d) Negative diversity

While found a clear anterior-posterior pattern for positive diversity on the level of the macro-scale composites, we could not observe a similar pattern or a pattern at all for the anterior-posterior configuration of negative diversity. Likewise, we found no association of the anterior-posterior distribution of negative diversity with age or cognitive performance in our study sample.

B. Left-right configuration

a) Positive Strength: Generally, we observed higher means in positive strength for the left hemispheric composite and likewise for the left frontal composite in comparison to their right-sided counterparts. The means of the left-right hemispheric composites and the means of the left-right frontal composites were not normally distributed and therefore we used the Kolmogorov-Smirnov two samples test to assess the significance of the observed left-sided predominance in positive strength. Only the result for the hemispheric composites was significant: The left hemispheric composite was characterized by significantly higher values in positive strength ($p = .035$) than the right hemispheric composite. Further analyses with the aim to associate the observed imbalance between the left and the right hemispheric composite with the age or the cognitive performance of the participants were all without a significant result.

b) Negative strength: We observed a tendency for the right hemispheric composite and a clear pattern for the right frontal composite to exhibit higher values in negative strength than their left-sided counterparts did. As we statistically assessed this observed left-right imbalance and its potential relevance for age and cognition, we found that the ratio of the left hemispheric composite to the right hemispheric composite showed a significant correlation with reasoning (Pearson $r = -.152$; $p = .044$), or in other words higher negative strength of the right hemisphere was associated with better performance in reasoning. However, the correlation was not adequately strong enough to survive the Bonferroni correction for multiple comparisons.

c) Positive diversity: The left hemispheric composite and the left frontal composite generally exhibited higher values in positive diversity than their right-sided composites. We examined the significance of these imbalances with t-tests: The left frontal composite exhibited significantly ($t(370) = 5.78$; $p = .001$) higher mean values for positive diversity ($M = 0.762$; $SD = 0.058$) than its right-sided counterpart ($M = 0.723$; $SD = 0.071$), the t-test for the hemispheric composite was not significant. Again, we computed further analyses to assess the association of age and cognition with the observed imbalance of the left-right configuration in the aging brain. We found no significant association with cognitive performance, but two significant associations with age. The left frontal composite (Pearson $r = .147$; $p = .045$) and the right frontal composite (Pearson $r = .145$; $p = .045$) showed significantly higher values for positive diversity with increasing age. However, neither correlation was sufficiently high enough to survive the Bonferroni correction for multiple comparisons.

d) Negative diversity: The right hemispheric composite and right frontal composite generally exhibited higher values in negative diversity in comparison to their left-sided equivalents. The

subsequent t-tests showed that this imbalance was significant (t (370) = -3.09; p = .002) for the hemispheric composites, the right hemispheric composite (M = 0.646; SD = 0.100) displayed higher values in negative diversity than its left-sided counterpart (M = 0.606; SD = 0.106). Based on this finding, we further examined the association of the left-right ratio of the hemispheric composites with age and cognition and found a significant correlation between the left-right ratio of the hemispheric composites and age (Spearman r = .148; p = .044): The hemispheric imbalance seems to balance out with increasing age. Again, there is a caveat because the correlation was not sufficiently high enough to survive the Bonferroni correction for multiple comparisons.

5.3.4 Discussion

A large number of task-induced fMRI studies have demonstrated that healthy young and old participants show characteristic differences in the observed hemodynamic patterns while performing the same task in the scanner. The interpretation of these differences is controversial and ranges from them being successful compensation strategies to indicators of functional dedifferentiation. The intrinsically active network structure is shaping the network architecture of all goal-driven behavior and therefore may at least partly influence the brain's capacity to compensate age-related structural and functional alterations. With these considerations in mind, our study aimed to investigate the intrinsic network architecture of a large sample of older adults using GTA measures. We wanted to evaluate which regions might retain qualities necessary for successful compensation strategies and which brain areas might already show the characteristics of disorder or disintegration as early as is seen in the intrinsically active functional baseline configuration.

As it has been repeatedly demonstrated that the aging brain is affected by decreased positive and negative connections resulting in a successive dedifferentiation of the networks and sub-networks, we investigated the aging brain's intrinsic functional architecture using GTA measures that are especially apt to describe un-thresholded and positively and negatively weighted networks. Because we wanted to interpret our findings in the context of two well-established compensation models, HARLOD and PASA, we performed our analyses on two resolution levels: the more fine-grained level of single nodes as defined by the ICA partition by Shirer and colleagues (2012) and the level of macro-scale composites representing the large-scale architecture of the brain, such as the anterior-posterior configuration or the left vs. right hemispheric organization.

On the nodal level, we found a clear difference in the anterior-posterior distribution of the nodes in the upper third in terms of positive nodal strength. More than the half (16 of 30 nodes) of the nodes characterized by the highest values of positive strength were located in the posterior part of the brain

and only eight nodes of those were found in the frontal part. A similar pattern was observed for the distribution of the topmost third of nodes exhibiting the highest values of negative strength. More than one third (12 of 30) of those nodes were located in the posterior part of the brain, while only nine nodes qualifying as top nodes in negative strength were found in the frontal cortex. To sum up the findings for nodal strength, the nodes in the posterior part of the brain generally displayed higher values of positive and in negative strength than the nodes in the anterior part of the brain, while nodes located in the subcortical regions, the temporal lobes and the cerebellum were always clearly under-represented in the topmost third.

The inverse distribution pattern was observed for the highest third of nodes in positive diversity. More than a third (12 of 30) of these were located in subcortical areas, especially in the thalami and the basal ganglia, followed by ten nodes located in the frontal cortex, and only three nodes in the posterior part of the brain. The distribution for the highest third in terms of negative diversity showed a prominent under-representation of nodes located in the anterior part of the brain (one node in the right precentral gyrus) and in the temporal lobes (one node in the right inferior frontal gyrus). The majority of nodes exhibiting high values of negative diversity were located in the subcortical regions (10 of 30), the parietal cortex (10 of 30) and the cerebellum (eight nodes). To sum up the findings for diversity, the subcortical nodes, while certainly under-represented in the topmost third in terms of nodal strength, were among the nodes displaying the highest values of both positive and negative diversity. This finding makes intuitive sense based on the dense interconnectivity between the subcortical regions and all other regions of the brain that is well known from anatomical studies. The combination of high positive and high negative diversity values allows these nodes to function as proper relay stations capable of integrating information in a functionally differentiated manner.

Although the nodes of the posterior part of the brain constantly displayed some of the highest values for positive and negative strength, none of them could qualify as central and therefore highly influential node. Out of 90 nodes, only three nodes exhibited the characteristics of central nodes; these were a node in the anterior cingulate cortex and two nodes in the right and left caudate nucleus.

On the level of macro-scale composites, we found clear anterior-posterior differences for three investigated GTA measures. While the posterior part of the brain generally showed higher values of positive and negative strength, the anterior part of the brain was characterized by higher positive diversity. This anterior-posterior difference was significant for both positive and negative strength as well as for positive diversity. Most importantly, we could show that this anterior-posterior imbalance in positive strength is more pronounced in older participants and has an impact on cognition: a disturbed balance between the anterior and posterior parts of the brain, i.e. very high positive strength

values in the posterior composite in relation to the positive strength values in the anterior composite, was significantly associated with poorer performance in processing speed and memory.

Likewise, we found characteristic differences in strength and diversity between the left and the right hemispheres, and more specifically between the left and the right frontal cortices. The left hemisphere generally showed higher values in positive strength and positive diversity, while the right hemisphere exhibited higher values for negative strength and negative diversity. This left-right imbalance in strength and diversity seems to be behaviorally relevant, as a higher negative strength of the right hemisphere was associated with better performance in reasoning. However, the differences in negative diversity seem to have a tendency to level out with increasing age, as we found a positive association between the left-right ratio in negative diversity and age.

In the following sections, we will discuss the findings from the macro-scale composites in terms of the PASA and HAROLD models.

a) Evidence of PASA in the intrinsically active functional baseline-configuration of the aging brain

The PASA model proposes an age-related posterior-anterior dichotomy insofar as the frontal regions are hypothesized to compensate for already manifest functional degradation of the posterior brain regions. Indeed, we found anterior-posterior differences that were already inherent in the intrinsically active network architecture of our study sample.

The nodal strength distribution showing a clear predominance of the posterior regions and a relative under-representation of the frontal regions replicated the findings of Cole et al. (2010), who analyzed a young sample using a voxel-wise analysis approach. Therefore, the asymmetric anterior-posterior distribution observed in our study population might still represent the normal baseline configuration of the brain.

Nevertheless, we also found clear evidence of age-effects on the positive strength distribution. Some of the younger participants showed only minimal anterior-posterior differences in the strength distribution or higher strength values in the anterior composite than in the posterior composite. In contrast, the posterior regions' predominance in terms of positive nodal strength was most pronounced in the oldest of the participants and the extent of this anterior-posterior difference was significantly associated with increased age.

On the one hand, strongly connected nodes form highly synchronized and robust connections and might thus guarantee the stability of the respective network. One the other hand, high stability might

not always be so beneficial, especially if functional stability becomes functional rigidity. Such a shift from stability to rigidity might be particularly detrimental in hub-like positions where dynamic switching between different networks and configurations is a prerequisite. Very strongly connected nodes could suffer from a retrenched ability to reconfigure their network affiliations in a timely and flexible manner. These considerations imply that there could exist something like an optimal trade-off between stability and flexibility, particularly for nodes that dynamically interact with more than one network. In fact, we may have found evidence for this hypothesized balance between stability and flexibility, which is disturbed by increasing anterior-posterior imbalance related to age that in turn seems to have a negative impact on cognition: not higher but lower positive strength values for the posterior part of the brain were significantly associated with successful performance in processing-speed and memory, and not higher but lower positive strength values for the precuneus were significantly correlated with higher scores in reasoning and memory. Therefore, an intrinsic functional network architecture characterized by a more balanced anterior-posterior strength distribution seems to be beneficial for cognitive performance.

Based on this, one might very carefully speculate that the posterior brain regions of our study sample might be showing the first evidence of an age-related hyper-connectivity or functional rigidity, which in turn might impact their capacity to interact with the anterior regions in a timely manner. If we analyzed the behavior of such hyper-connected nodes using a task-induced fMRI paradigm, we would obtain a PASA-specific activation pattern. We would observe weak and/or dynamically delayed BOLD-signal changes in the hyper-synchronized nodes located mainly in the posterior regions of the brain. In contrast, we would observe timely and distinct BOLD activity in the frontal regions, which have a lower degree of rigidity and therefore might be still capable of flexibly activating or deactivating depending on their respective network affiliation.

Quite the inverse pattern was observed for the positive diversity distribution: the anterior regions showed significantly higher values of positive diversity than the posterior regions. One might interpret the anterior regions' predominance in positive diversity as evidence that the anterior brain areas indeed have a higher potential for information integration, which might be an advantageous quality whenever compensation strategies are needed to preserve high-level cognitive functioning. Therefore, when combining the results for the nodal strength and diversity distributions, our findings for the intrinsic anterior-posterior baseline configuration of the aging brain seem to confirm one of the main assumptions of the PASA model: despite manifest structural decline the frontal regions of the aging brain might still have the capacity to counteract the age-related functional degradation of the posterior part of the brain.

Nevertheless, there might be a caveat regarding the intrinsic network architecture's seemingly beneficial anterior-posterior differences: as mentioned previously, the anterior regions of the aging brain are also characterized by generally lower strength values in comparison to the posterior regions and this strength imbalance is more pronounced in older participants. Likewise, we observed a significant positive association between the positive diversity values of the frontal regions and age. In combination, the two age trends might be become detrimental over time since high positive diversity is only beneficial as long as the strength values of nodes displaying such high diversity are sufficiently high to form stable connections. As soon as there exists a distinct imbalance between positive diversity and positive strength, the affected nodes might no longer be capable of information integration since they are beginning to show the characteristics of functional disintegration and disorder.

b) Evidence of HAROLD in the intrinsically active functional baseline-configuration of the aging brain

The HAROLD compensation model is based on the observation that older adults seem to rely on the additional support of homologous brain regions in the non-dominant hemisphere for cognitive functions that induce a strongly lateralized activation pattern in young subjects. By recruiting these additional homologous regions, older adults are thought to be capable of compensating for the functional degradation of the regions originally supporting these functions in young adults.

The HAROLD specific reduction in hemispheric asymmetry has been observed for strongly left- and right-sided cognitive functions (Cabeza, 2002). By interpreting additional BOLD activation in the homologous regions of the functionally non-dominant hemisphere as a compensation mechanism, the HAROLD model seems to make the indirect assumption that both hemispheres have the same capacity for compensation.

In contrast to the assumptions of the HAROLD model, we found different GTA characteristics for the left and the right hemispheric composites as well as for the left and right frontal composites. The left hemispheric composite and the left frontal composite generally exhibited higher values of positive strength and higher values of positive diversity than their right-sided counterparts. As the combination of high strength and high positive diversity is the hallmark of very central nodes, one could very cautiously speculate that the left frontal cortex and the left hemisphere might possess a higher potential for compensation than their right-sided analogs. In contrast, the right-sided composites exhibited the opposite characteristics showing higher negative strength and higher negative diversity than their left sided counterparts. The right-sided composites also seemed to exhibit a more

functionally differentiated connection-profile and might therefore be less qualified whenever compensation mechanisms are needed to counteract the functional degradation of other brain regions.

Limitations

The LHAB database was especially designed to fulfill the specific requirements of a longitudinal analysis approach. To ensure the possibility of studying the individual age trajectories of a very large study group of older adults over several years, primarily older adults belonging to the younger side of the age spectrum were recruited. As a result, participants covering a relatively small age range from 65 to 70 are overrepresented in the LHAB sample. As a result, the age distribution of our 186 study subjects might be not ideal for the cross-sectional approach used for the present study. Because the participants belonging to the younger end of the age spectrum are overrepresented the effects of age on cognition and intrinsic network architecture observed in our study group were to a large extent so small that they frequently did not survive the subsequent corrections for multiple comparisons.
However, while the biased age-distribution is a specific characteristic of the LHAB database as a longitudinal project, correlations between connectivity and cognition tend to be rather small to moderate in general. Given that the true relationship between connectivity and cognition is r = .25 or less, Shaw et al., (2015) showed that one needs a sample of at least 96 subjects to detect such a small effect even under the most lenient statistical requirements, i.e. one-tailed $\alpha = 0.05$ and no further corrections for multiple comparisons needed. Although the LHAB study population counts 230 participants and is by no means an under-powered sample, it is still not large enough to allow the reliable detection of small effects in data-driven and explorative projects as the present study when the formulation of a priori hypotheses was not possible because there exist no comparable previous studies on which to base such hypotheses.

Until now, the major contribution to our understanding of the aging brain either comes from studies comparing young with old or from studies investigating pathological aging and using the healthy aging older adults as control group. In consequence, we know relatively well, what distinguishes young from old brains and pathological from healthy aging but that does not mean that we really understand the structural and functional transformations that characterize the healthy aging brain. For that reason, despite not having the ideal age distribution for a cross-sectional approach we feel sure that our study is still justified because it is able to elucidate the specifics of the intrinsic network architecture of the age group in the transition from old age to very old age that is still understudied. While we concede that within the scope of our study the relevance of these age-group specific network configurations for cognition must remain just descriptive as none of the associations did survive the Bonferroni correction for multiple comparisons, we still believe the findings could be useful for future hypothesis formulation by researchers working with very large samples.

Conclusion

Task-induced activation patterns in older adults are often distinct from these found in younger adults performing the same task in the scanner. The meaning of these differences is highly controversial. When interpreting these fMRI activation patterns we propose that one might gain additional insight by being aware of the age-specific characteristics of the underlying functional baseline configuration. The intrinsic network architecture defines the starting point from which the brain generates different cognitive and behavioral functions and might thus shape the workings of the brain during active goal-directed behavior (Cole et al., 2014). We therefore used the GTA measures of nodal strength and nodal diversity along with a combination of these measures to investigate whether and which parts of the intrinsically active functional baseline configuration show the qualities and resources necessary to compensate for age-related functional degradation when brain is engaged in active goal-directed behavior.

On the nodal level, we observed that the subcortical regions exhibited indicators for age-related functional disintegration and dedifferentiation as early as seen in the intrinsically active baseline configuration of the brain. On the macro-scale level of the regional composites, we looked for configuration patterns of the intrinsic network architecture of the aging brain that might elucidate the meaning of age-typical activation differences observed between old and young adults. The PASA pattern appeared to be already present in the functionally active baseline configuration. We observed a clear age-related anterior-posterior dichotomy for strength: nodes in the posterior part of the brain generally showed a tendency toward hyper-synchronization compared to nodes in the anterior regions, which were characterized by a higher potential for information integration and might thereby possess the necessary qualities for compensation mechanisms. In contrast, the observed characteristics of the intrinsic network architecture supported the HAROLD compensation model only to a certain degree. While the HARLOD model seems to assume that the homologous regions of the functionally non-dominant hemisphere are similarly capable of compensating for the age-related functional degradation of their counterparts, we found a qualitative asymmetry between the left and the right frontal cortices as well as between the left and the right hemispheres. In comparison to their right-sided counterparts, the left hemisphere and the left frontal cortex seemed to possess a higher capacity for compensation as they showed a higher degree of the functional qualities needed for information integration.

Acknowledgements

The current analysis incorporates data from the Longitudinal Healthy Aging Brain (LHAB) database project, which is carried out as one of the core projects at the International Normal Aging and Plasticity Imaging Center / INAPIC and the University Research Priority Program “Dynamics of

Healthy Aging” of the University of Zurich. The following members of the core INAPIC team were involved in the design, set-up, maintenance and support of the LHAB database: Anne Eschen, Lutz Jäncke, Mike Martin, Susan Mérillat, Christina Röcke, and Jacqueline Zöllig.

6 General Discussion

The general discussion is organized in three subparts. Firstly, the most important findings of the three studies presented in the previous section of this doctoral thesis are reviewed in relation to the aims and research questions that originally motivated the studies. Then, some more methodical aspects of these findings are discussed in respect of the longitudinal design of the LHAB database project although all three studies presented here had a cross-sectional design. The discussion closes with recommendations for further steps.

6.1 Discussion of the most important findings from the three studies

6.1.1 **Research question 1:** The potential of the ICC analysis to detect age-related changes in the intrinsic network architecture of the brain.

The results of study 1 (*Small changes, but huge impact? The right anterior insula's loss of connection strength during the transition of old to very old age*) suggest that an ICC analysis might indeed have the potential to detect even subtle age-related functional degradation of older adults' intrinsic network architecture.

Age-related alterations of the DMN's functioning, especially a failure of the DMN to deactivate during cognitive demanding tasks in a timely manner, have been repeatedly demonstrated by a number of previous studies investigating the aging brain (Gordon et al., 2014, Grady et al., 2006, Grady et al., 2010, Meinzer et al., 2012, Persson et al., 2007). However, a new and also a very important finding of study 1 was that the right anterior insula could have a causal influence on this age-related dysfunctional deactivation of the DMN because the ICC results revealed that this region was predominantly affected by an age-related loss of connectedness. The right anterior insula is considered one of the most influential output hubs of the brain (Sridaharan et al., 2008) because it causally initiates the switching from the brain's internal modus operandi to the external modus operandi vital for all successful goal-directed behavior (Goulden et al., 2014; Menon & Uddin, 2010; Sridaharan et al., 2008). The internal modus operandi of the brain is characterized by high activity of the DMN. Although the DMN's role in the brain is still not fully understood, the so called "default mode" of the brain can be described as a highly dynamic and exploratory state of the brain characterized by a high variance of synchrony over time (Hellyer et al. 2014). In order to successfully perform goal-directed behavior the brain has to switch from the rather unconstrained default mode state into a functionally focused state, which is characterized by increased global synchrony and by coordinated activity of the

control and attention networks of the brain (Hellyer et al., 2014). The right anterior insula initiates this switching from one brain state into the other by signaling the DMN to deactivate and the ECN to activate. Study 1 showed for the LHAB study sample that the dynamic interplay of these three networks might be impaired by a higher degree of functional dedifferentiation of the DMN and the cingulo-opercular network in the older LHAB subjects.

A second interesting finding of study 1 was that the ICCp analysis on voxel-level mainly highlighted frontal regions as affected by age-related decline of connectedness in the LHAB study sample. This finding was remarkable insofar as the subsequent connectivity analyses revealed that frontal long-distance connections into target regions of the posterior part of the brain were also affected by this decrease in connection strength. To understand the paradox that the ICC analysis stressed the frontal source regions but not their respective target ROIs located in the posterior parts of the brain, one has to look closer at the ICCp index. The value of the ICCp index is determined by the existence of a connection and by the strength of this connection. When only frontal source ROIs show a decrease in the ICCp index but not their posterior target regions then this unilateral phenomenon can only be explained by a decrease in connection strength of the frontal regions while the posterior regions do not show such a degradation. Therefore, we speculated in study 1 that the results of the ICCp analyses could indicate that the anterior frontal regions of the brain show a different trajectory for connection strength, respectively a faster decrease in connection strength than the posterior parts of the brain with increasing age. This speculation was later supported by the results of study 3 where we found clear evidence that the frontal regions indeed seem to be affected by a more progressive loss of connection strength than posterior regions and that the strength imbalance between anterior and posterior brain regions seemed to increase with the age of the participants.

6.1.2 **Research question 2:** Are the ICC analysis and the ICCp index sensitive enough to detect the small to moderate associations that generally characterize relationships between intrinsic connectivity/intrinsic network architecture and cognitive performance and behavior?

The results of study 2 (*Older but still fluent? Insights from the intrinsically active baseline configuration of the aging brain using a data driven graph-theoretical approach*) show that it is possible to elucidate the brain-behavior relationship with an ICC analysis. The study replicated not just the findings of previous task-induced fMRI studies investigating the processing of verbal fluency in older adults (Marsolais et al. 2014; Meinzer et al., 2009; Meinzer et al., 2012a; Nagels et al., 2012; Persson et al., 2004) but also brought new insights.

Our study demonstrated that verbal fluency is not a distinct cognitive function, which imprints its own ICN in the intrinsically active brain, but seems to be supported by a coordinated interplay of three

different ICNs. Mainly the left and to a lesser extent the right ECN, the dorsal DMN and the language network as the minor partner seem to constitute the functional base for verbal fluency.

Three details of the findings of study 2 are particularly noteworthy. Firstly, we found potential indicators for a preserved capability of the aging brain to reconfigure its networks for a new, untrained task in an adequate way and to perform behaviorally in the same range like young adults.

Second, most of the previous studies investigating the processing of verbal fluency in the aging brain reported the involvement of right-sided frontal regions, mostly the homologs of the left-sided frontal language regions that are reliably found to be engaged by language functions. This additional recruitment of the right-sided counterparts in older adults is usually interpreted as a compensation mechanism (Birn et al., 2010; Destrieux et al., 2012, Fu et al., 2006; Marsolais et al., 2014; Meinzer et al., 2009; Nagels et al., 2012; Persson et al., 2004, Persson et al., 2007). Nevertheless, the results of study 2 showed an involvement of the right frontal and prefrontal regions as relevant for a successful performance in verbal fluency as early as in the functional baseline configuration. One possible interpretation of this finding is that in our study population the compensatory involvement of the right-sided homologs is so indispensable that an imprint of that steady involvement already shows up in the intrinsic connectivity pattern. However, per definition, a compensatory mechanism should be an additional resource that can flexibly be applied whenever greater effort is needed. An alleged compensatory mechanism that already seems to be solidly incorporated in the functional baseline configuration might have lost its capacity to flexibly counteract higher efforts. Therefore, it might not anymore qualify as a true compensation mechanism but should be rather interpreted as age-related functional dedifferentiation than successful compensation. Of course, all these deliberations are just speculative at the moment and further analyses using a combination of task-free and task-induced fMRI data would be necessary to prove this point. However, the results of the third study conducted in the context of this doctoral thesis support these speculations by demonstrating that the network characteristics of the right frontal cortex are indeed less suitable to counteract age-related functional degradation but rather showing indicators of network dedifferentiation.

Third, apart from the age-related involvement of right-sided frontal regions clusters, study 2 indicated that the aging brain might become increasingly dependent on the support of additional attentional resources in order to sustain successful performance of verbal fluency. While the dynamic interaction of ECN, DMN and language network is specific for the performance of verbal fluency; the ICC analysis discovered that a successful performance of verbal fluency in the LHAB-subjects seemed to be associated with a recruitment of additional attentional resources, i.e. the dorsal attention network and the cingulo-opercular network. The dorsal attention network or visuospatial attention network is considered to be engaged in selective attention, while the salience network or cingulo-opercular

network is associated with tonic alertness, a general mechanism, which is important for task maintenance and shielding the current cognitive process from external unwanted inputs (Sadaghiani & D'Esposito, 2014).

6.1.3 Research question 3: What are the characteristics of the intrinsic network architecture of healthy older adults in the transition from old to very old age in general and do there exist brain regions that seem to possess some sort of intrinsic potential for compensation as indicated by their specific combination of GTA characteristics?

The most important finding of study 3 (*Successful functional compensation or age-related decline - What can we learn by looking at the intrinsically active baseline of the healthy aging brain?*) was the anterior-posterior asymmetric distribution of two GTA measures, one describing the connectedness of single nodes, i.e. nodal strength, and the other describing their capacity for integrated information processing, i.e. diversity coefficient. While brain regions located in the anterior part of the brain were characterized by higher capacity for information integration in relation to the regions of the posterior part of the brain, the latter scored higher in terms of nodal strength. Furthermore, the degree of this anterior-posterior asymmetry was positively associated with the age of the LHAB subjects. Already study 1 had provided first indications that there might exist different age-trajectories for posterior and anterior brain regions in terms of connectedness.

Another interesting finding in this context was, that the negative association between high nodal strength in posterior brain regions with successful performance in processing speed and memory tasks. This negative association could suggest that there exists something like an optimal anterior-posterior balance of connection strength. As soon as the connection strength of the posterior regions is too high in relation to the connection strength of the posterior regions, the latter become "hyper-connected" and might lose their capacity to flexibly switch between different network configurations.

The distribution of the diversity coefficient exhibited the inverse asymmetry: The anterior regions exhibited significantly higher values of positive diversity than the posterior regions. One might interpret the anterior regions' predominance in positive diversity as an indication that the anterior brain areas have indeed a higher potential for information integration, which might be an advantageous quality whenever compensation strategies are needed in order to preserve high-level cognitive functioning. Therefore, when combining the results for the nodal strength and diversity distributions, our findings for the intrinsic anterior-posterior baseline configuration of the aging brain seemed to confirm one of the main assumptions of the PASA compensation model of Davies and colleagues (2008). The specifics of the intrinsic network architecture as established for the LHAB study sample indicate, that the frontal regions of the aging brain might still have the capacity to

counteract the age-related functional degradation of the posterior part of the brain despite manifest structural decline.

However, we also observed a significant positive association between the positive diversity values of the frontal regions and age. In combination, the two age trends might become detrimental over time because high positive diversity is only beneficial as long as the strength values of nodes displaying such high diversity are sufficiently high enough to form stable connections. As soon as there is a distinct imbalance between positive diversity and positive strength, the affected nodes might be no longer capable of information integration since they are beginning to show the characteristics of functional disintegration and disorder.

While we found evidence, that the intrinsic network architecture of the LHAB study sample might indeed possess the functional resources to allow PASA-like compensation mechanisms during active goal-driven behavior, the assumptions of the other highly popular compensation model, the HAROLD model, were not supported. In contrast to the HAROLD model that presumes that both hemispheres of the brain possess the functional resources to compensate for the age-related degradation of the other, we found different GTA characteristics for the left and the right hemisphere and also for the left and right frontal cortex. The left hemisphere and the left frontal cortex generally exhibited higher values in positive strength and higher values in positive diversity than their right-sided counterparts. As the combination of high strength and high positive diversity is the hallmark of very central nodes, one could very cautiously speculate that the left frontal cortex as well as the left hemisphere might possess a higher potential for compensation than the right-sided analogs. In contrast, the right hemisphere and the right frontal cortex exhibited the opposite characteristics, because they showed higher negative strength and higher negative diversity than their left-sided counterparts. In relation to their left-sided counter-parts, the right-sided brain regions also seemed to exhibit a functionally more differentiated connection-profile and might therefore be less qualified whenever compensation mechanisms are needed to counteract the functional degradation of other brain regions.

6.2 From cross-sectional to longitudinal – what can we learn from the three studies presented here for future longitudinal analyses

All three studies presented in the context of this doctoral thesis had a preliminary and exploratory character in regard of the planned longitudinal analysis of the LHAB data. Therefore, it is now the time to ask, what can we learn from these three studies for the planned longitudinal analyses?

The ICC approach used in two of the three studies was chosen with the objective of evaluating its suitability for longitudinal analyses. At first sight, the ICC analysis proved itself as an expedient method as we were able to replicate previous findings regarding the specifics of brain regions recruited by the aging brain in a compensatory manner when performing fluency tasks. We were likewise able to elucidate further the frequently reported finding of studies investigating the aging brain. Regarding the repeatedly observed delayed deactivation or reduced deactivation of the DMN in older adults, we could show that the right anterior insula of the LHAB sample was affected by an age-related loss of connectedness that resulted in a disturbed dynamic between ECN and CON which might be one of the causes for the DMN dysfunction.

Nonetheless, the ICC approach cannot be recommended for the longitudinal analysis of the LHA data for the following reason. The ICC analysis works on the most fine-grained resolution, i.e. on the level of the single voxel. In contrast to structural MR images, which have a high spatial resolution that allows a trained expert to discern even such subtle anatomical structures like the different layers of the hippocampus, functional MR are acquired at a lower resolution to compensate for the lower signal to noise signal, and thus only the larger anatomic landmarks can be reliably detected. In order to identify the anatomical origins of the BOLD-signal changes captured by the fMRI time-series, the structural image is standardly co-registered to the functional images during the pre-processing procedure. Likewise, the parameters from the normalization of the structural image are applied to the functional images in order to allow statistical tests on group level. Both pre-processing steps inevitably cause a certain blurring of the data, which is much more serious in older brains, because they come in very different stages of brain atrophy and are therefore more prone to be blurred than younger adults' brains when normalized into the MNI space. This pre-processing induced blurring of fMRI data gives rise to spurious correlations between the voxels and also compromises the exact mapping of structure to function – both artifacts interfere with the validity and reliability of an ICC analysis. Because of the high variance in brain atrophy in the LHAB study sample it was a very time-consuming to find a procedure that ensured the optimal mapping of function and structure for the data used in the two ICC studies presented here. Even then, the result of it was not totally satisfactory because the ICC maps showed indicators of unsuccessful coregistration and blurring, i.e. definitively erroneous ICC cluster located around the ventricles which could easily be eliminated by a rigorous statistical threshold. However, as one can reasonably expect that the already existing variance in brain atrophy will increase further over the course of the LHAB database project, the risk also increases that the results of ICC analyses with data from later measurement time points will be contaminated by a rather higher proportion of artifacts and spurious correlations, and it could become impossible to differentiate between these artifacts and true effects of age.

Another issue that should be carefully considered when selecting an analysis method for the longitudinal analysis of the task-free fMRI data is the rather moderate to small association of behavioral data with intrinsic connectivity. Large data sets with 200 and more subjects (Biswal et al., 2010; Shaw et al., 2015) are needed to reliably detect such small effects. To be sure, the data of 230 subjects were acquired within the scope of the first data collection wave of the LHAB project, but the data of 186 participants could actually be used for the three studies presented here. Despite this still respectable sample size, we already encountered the same problems as other smaller studies investigating age-effects of intrinsic activity (Geerligs et al., 2015; Sadaghiani et al., 2015), which is that the brain-behavior relationship did not anymore survive the necessary correction for multiple comparisons. Regarding the LHAB database project, the problem of an inadequate sample size might get even more serious over time because of participant attrition which is one of the biggest challenges for all longitudinal studies.

6.3 Future directions

After reviewing the results and experiences from the three studies presented in the context of this thesis and drawing attention to some challenges for the longitudinal analysis of the LHAB data in the previous sections, it seems appropriate to discuss an alternative way of looking at the task-free fMRI data of the LHAB project.

Fact is, there exists a wealth of information about the functioning of the aging brain in the task-free fMRI data of the LHAB database project that could not be appropriately assessed for the want of suitable analysis methods until recently. The task-free fMRI analysis approaches used for the three studies presented here all analyzed the BOLD-signal time series in what can be called for the lack of a better term “traditional way”, i.e. based on correlations calculated over the total requisition time. This traditional approach makes therefore the implicit assumption that the synchronized intrinsic activity between distinct brain regions is constant throughout the duration of the data acquisition.

Although the assumption of stationarity provides an appropriate framework in which some aspects of the brain’s intrinsic activity can be reasonably explored and interpreted and the studies using these stationary approaches have produced valuable insights about the intrinsic functional brain organization, the assumption is not correct as has been repeatedly demonstrated by an increasing number of studies published over the last five years (Chang & Glover, 2010; Hutchison et al., 2013; Jones et al., 2012). These studies showed that the brain’s intrinsic network architecture as measured by task-free fMRI is dynamic and not static. The strength as well as the directionality of the connections between brain regions vary over short time scales from seconds to minutes, and even the DMN and the

DAN that are characterized by strong anticorrelations when their time courses are averaged over the entire length of the data acquisition show periods of synchronized activity when shorter time windows are analyzed (Chang & Glover, 2010). The most intriguing aspect of the dynamics of the intrinsic brain activity in the context of the specific challenges regarding the longitudinal analysis of the LHAB data though is that it might capture aspects that are completely missed by the stationary approach and thus provides crucial insights into the functional underpinnings regarding individual differences in aging, cognition and behavior. Jia, Hu and Deshpande (2014), for example, showed that metrics of dynamic functional connectivity, i.e. MTST = mean time before state transition and STST = standard deviation of the time before state transition, were able to explain in a sample of 40 subjects (22-35 years) more than twice of the variance in 75 behaviors across different domains spanning from alertness, cognition to emotion and personality than the standardly used metrics of static functional dynamics.

Since the first studies demonstrating the dynamic nature of the intrinsic connectivity, new and promising analysis approaches for the quantifying of the dynamics of intrinsic connectivity have been developed. By now, there exist quite a number of different approaches for dynamic analyses of the brain's intrinsic activity, some of these approaches characterize changes in temporal coupling over time while assuming fixed functional unities, other approaches model changes in spatial activity pattern over time and a third group that works by modeling the changes of GTA measures over time (Calhoun, Miller, Pearlson & Adali, 2014). However, in the context of this thesis, I will confine myself on presenting only the most commonly used approach, the sliding windows analysis approach, because of the sparsity of empirical studies that have used one of the other approaches. The aim of the following sections will be to illustrate how the sliding windows analysis works, which new insights can be obtained by applying dynamic analysis approaches and why these methods might be a good choice for a more in depth analysis of the LHAB fMRI data.

The sliding windows analysis works by defining a set of brain regions by an ICA or another statistical method to parcellate the brain in functionally meaningful units. Next, a time window of a fixed length is selected; windows of 30 – 60 s of fMRI data have been shown to produce robust results (Hutchison et al., 2013). The time window is shifted in time by a fixed number of time points, ranging from 1 repetition time (TR) to the entire length of the window and correlation matrices are computed for each individual time window. Next, clustering methods or modularity/community algorithms from GTA are applied in order to search for transient and reproducible patterns in these correlation matrices (Hutchison et al., 2013). The result of such a cluster analysis is a much smaller number of time-varying but reoccurring distinct connectivity patterns, so called brain states (Calhoun et al., 2014). For a deeper understanding of individual differences in cognition or the effect of age, or the difference

between health and disease, the researcher can compute the number of different states for each individual or the time an individual subjects spends in each state, i.e. “dwell time”.

Using a sliding windows approach in combination with a GTA, Jones and colleagues (2012) for example found for a very large sample of cognitive normal older adults (n = 892, age 70-90) that they still showed a highly complex dynamic network architecture, since the number of modules within a graph computed for a single time window of 33s could vary between two and five. However, configurations characterized by a small number of modules were predominant as the three module configuration was in 72.38% and the two module configuration was in 23.63% of the acquisition time present while the five module configuration could be found in only 0.01% of the time (Jones et al., 2012). Jones and colleagues’ finding for a small subgroup of Alzheimer’s patients and a gender, age and education matched control group was even more interesting regarding the LHAB database project. The patient group had a significantly shorter dwell time in a configuration that was characterized by strong contribution of the posterior DMN sub-network but a significantly higher dwell time in an anterior DMN configuration than the healthy controls (Jones et al., 2012). In the context of the LHAB, it would not just be interesting to replicate the findings of Jones et al., (2012) but also to compare the dynamics of the different DMN sub-networks and the cognitive development of the subgroup of LHAB participants who were identified as carriers of the APOE ε4 allele and are therefore at higher risk for Alzheimer’s dementia with the intrinsic dynamics and cognitive performance of the non-carriers in a longitudinal approach.

However, the sliding windows approach has also the potential to elucidate age-related development and functional brain maturation. Hutchison and Morton (2015), for example, found that the transition from childhood into adulthood was characterized not by the number of brain states, but by a change of the dwell time in selected states (Hutchison & Morton, 2015). Additionally, they could show that increasing age was associated with greater variability of connection strength across time at rest, but with higher levels of global synchronization during cognitive demanding tasks (Hutchison & Morton, 2015). In the context of the three studies presented here, we found evidence for increasing functional dedifferentiation in the LHAB sample with age. By performing a dynamic analysis, one could investigate whether this functional dedifferentiation is rather caused by an increase in functional variability resulting in a decrease of functional segregation of ICNs or is caused by a decrease in functional variability that impairs the flexible and timely reconfiguration of the networks essential for the switch between internal and external focus of attention. Furthermore, Qin and colleagues (2015) used the age-dependent differences in temporal variability of the intrinsic functional inter-network connections between the visual network, salience network, the DMN and the cerebellum network and of the within-network connections of the DMN and the cerebellum network to predict the brain maturity in a large sample of children and young adults (n =183, age = 7-30). In the context of the

LHAB project, a joint analysis combining the structural data as well as the functional data to predict individual brain age could be an interesting new approach to elucidate the complex structure-function relationship.

Dynamic analysis approaches are still very much in their infancy and there exist many critical issues and open questions like the uncertainty about the neural origins of the dynamics of intrinsic connectivity, or the appropriateness of some of the assumptions underlying the approaches used for the analysis of dynamic connectivity like the optimal windows size, filtering of the data, the use of the Pearson correlation to model the relationship between brain regions or the challenge to generate appropriate null distributions for significance testing (Hutchison et al., 2013). However, that should not prevent researchers of using these new methods as long as they are well aware of the limitations inherent of these techniques and very cautious when interpreting their findings.

7 References

Abrahamson, K., Clark, D., Perkins, A., & Greg, A. (2012). Does cognitive impairment influence quality of life among nursing home residents? *The Gerontologist, 52,* 632 - 640.

Andrews-Hanna, J.R., Snyder; A.Z., Vincent, J.L., Lustig, C., Head, D., Raichle, M.E., & Buckner, R. (2007). Disruption of large-scale brain systems in advanced aging. *Neuron, 56,* 924 – 935.

Andrews-Hanna, J.R., Smallwood, J., Spreng, R.N. (2014). The default network and self-generated thought: component processes, dynamic protocol, and clinic relevance. *Ann NY Acad Sci, 1316,* 29 - 52.

Aschenbrenner, S., Tucha, O., & Lange, K. W. (2000). RWT. Regensburger Wortflüssigkeits - Test. Göttingen: Hogrefe

Ashburner, J. (2007). A fast diffeomorphic image registration algorithm. *Neuroimage, 38,* 95 - 113.

Azuma, T. (2004). Working memory and perseveration in verbal fluency. *Neuropsychology, 18 (1),* 69 – 77.

Barulli, D., & Stern, Y., (2013). Efficiency, capacity, compensation, maintenance, plasticity: emerging concepts in cognitive reserve. *Trends Cogn Sci, 17 (10*), 502 - 509.

Behzadi, Y., Restom, K., Liau, J., & Liu, T.T. (2007). A component based noise correction method (CompCor) for BOLD and perfusion based fMRI. *Neuroimage, 37,* 90 - 101.

Berlingeri, M., Danelli L., Bottini, G., Sberna, M., & Paulesu, E. (2013). Reassessing the HARLOD model: Is the hemispheric asymmetry reduction in older adults a special case of compensatory-related utilisation of neural circuits? *Exp Brain Res, (224),* 393 - 410.

Betzel, R.F., Byrge, L., He, Y., Goni, J., Zuo, X., & Sporns, O. (2014). Changes in structural and functional connectivity among resting-state networks across the human lifespan. *Neuroimage, 102,* 345 - 357.

Birn, R.M., Kenworthy, L., Case, L., Caravella, R., Jones, T.B., Bandettini, P.A., & Martin, A. (2010). Neural systems supporting lexical search guided by letter and semantic category cues: A self-paced overt response fMRI study of verbal fluency. *Neuroimage, 49,* 1099 - 1107.

Birn, R.M., Molloy, E.K., Patriat, R., Parker, T., Meier, T.B., Kirk, G.R., Nair, V.A., et al. (2013). The effect of scan length on the reliability of resting-state fMRI connectivity estimates. *Neuroimage, 83,* 550 - 558.

Birn, R.M., Conejo, M.D., Molloy, E.K., Patriat, R., Meier, T.B., Kirk, G.R., Nair, V.A., et al. (2014). The influence of physiological noise correction on test-retest reliability of resting-state functional connectivity. *Brain Connect, 4 (7),* 511 - 522.

Biswal, B.B., Yektin, F.Z., Haughton, V.M., & Hyde, J.S. (1995). Functional connectivity in the motor cortex of the resting human brain using echo-planar MRI. *Magn Reson Med, 34,* 537 - 541.

Biswal, B.B., Mennes, M., Zuo, X.N., Gohel, S., Kelly, C., Smith, S.M., Beckmann, F.C., et al. (2010). Towards discovery science of human brain function. *Proc Natl Acad Sci U S A, 107 (10),* 4734 - 4739.

Bonelle, V., Ham, T.E., Leech, R., Kinnunen, K.M., Mehta, M.A., Greenwod, R.J., & Sharp, D. (2012). Salience network integrity predicts default mode network function after traumatic brain injury. *Proc Natl Acad Sci U S A, 109 (20*), 4690 - 4695.

Brier, M.R., Thomas, J.B., Snyder, A.Z., Wang, L, Fagan, A.M., Benziger, T., Morris, J.C., et al., (2014). Unrecognized preclinical Alzheimer disease confounds rs-fcMRI studies of normal aging. *Neurology, 83 (18),* 1613 - 1619.

Buckner, R.L., Sepulcre, J, Talukdar, T., Krienen, F.M., Liu, H., Hedden. T., Andrews-Hanna, J.R., et al. (2009). Cortical hubs revealed by intrinsic functional connectivity: mapping, assessment of stability, and relation to Alzheimer's disease. *J. Neurosci, 29 (6),* 1860 - 1873.

Bullmore, E., Barnes, Bassett, D.S., Fornito, A., Kitzbichler, M., Meunier, D., & Suckling, J. (2009). Generic aspects of complexity in brain imaging data and other biological systems. *Neuroimage, 47,* 1125 - 1134.

Bullmore, E. & Sporns, O. (2012). The economy of brain network organization. *Nat Rev Neurosci, 13,* 336 - 349.

Cabeza, R. (2002). Hemispheric asymmetry reduction in older adults: The HAROLD model. *Psychol Aging, 17 (1),* 85 - 100.

Cabeza, R., Daselaar, S.M., Dolcos, F., Prince, S.E., Budde, M., & Nyberg, L., (2002). Age-related differences in neural activity during memory encoding and retrieval: a positron emission tomography study. *The J Neurosci, 17,* 391 - 400.

Calhoun, V.D., Adali, T., Pearlson, G.D., & Pekar, J.J. (2001). A method for making group inferences from functional MRI data using independent component analysis. *Hum Brain Mapp, 14,* 140 - 151.

Calhoun, V.D. Miller, R., Pearlson, G., & Adali, T. (2014). The chronnectome: Time varying connectivity networks as the next frontier in fMRI data discovery, *Neuron, 84,* 262 - 274.

Campell, K.L., Grigg, O., Saverino, C., Churchill, N., & Grady C.L. (2013). Age differences in the functional connectivity of the default network subsystems. *Front Aging Neurosci, 5 (73).*

Cao, M., Wang, J.H., Dai, Z.J., Cao, X.Y., Jiang, L.L., Fan, F.M., Song, X.W., et al. (2014). Topological organization of the human brain functional connectome across lifespan. *Dev Cog Neurosci, 7,* 76 - 93.

Chai X.J., Nieto-Castanon A, Öngür D., & Whitfield-Gabrieli, S. (2012): Anticorrelations in resting-state networks without global signal regression. *Neuroimage, 59(2),* 1420 - 1428.

Chan, M.Y., Park, D.C., Savalia, N.K., Petersen, S.E., & Wig, G.S., (2014). Decreased segregation of brain systems across the healthy adult lifespan. *Proc Natl Acad Sci U S A, 111 (46*), E4997 - E5006.

Chang, C. & Glover, G.H. (2010). Time-frequency dynamics of resting-state brain connectivity measured with fMRI. *Neuroimage, 50,* 81 - 98.

Chao-Gan & Yu-Feng. (2010). DPARSF: A MATLAB toolbox for "pipeline" data analysis of resting-state fMRI. *Front Syst Neurosci, 4,* (article 13).

Chételat, G., La Joie, R., Villain, N., Perrotin, A., de La Sayette, V., Eustache, F., & Vandenberghe, R. (2013). Amyloid imaging in cognitively normal individual, at-risk populations and preclinical Alzheimer's disease. *Neuroimage Clinical, 2,* 356 - 365.

Clark, L.J., Gatz, M., Zheng, L., Chen, Y., McCleary, C., & Mack, W.J. (2009). Longitudinal verbal fluency in normal aging, preclinical, and prevalent Alzheimer's disease. *Am j Alzheimers Dis Other Demen, 24 (6),* 461 - 468.

Cohen, J.R., Gallen, C.L., Jacobs, E.G., Lee, T.G. & D'Esposito, M. (2014). Quantifying the reconfiguration of intrinsic networks during working memory. *PLOSone, 9 (9).* e106636.

Cole, D.M., Smith, S.M. & Beckmann, C. (2010). Advances and pitfalls in the analysis and interpretation of resting-state FMRI data. *Front Syst Neurosci, 4,* (article 8).

Cole, M.W., Pathak, S., & Schneider, W. (2010). Identifying the brain's most globally connected regions. *Neuroimage, 49,* 3132 - 3148.

Cole, M.W., Bassett, D.S., Power, J.D., Braver, T.S., & Petersen, S.E. (2014). Intrinsic and task-evoked network architectures of the human brain. *Neuron, 83,* 238 - 251.

Collin, G., Sporns, O., Mandl, R.C.W., & van den Heuvel, M.P. (2014). Structural and functional aspects relating to cost and benefit of rich club organization in the human cerebral cortex. *Cereb Cortex, 24,* 2258 - 2267.

Cordes, D., Haughton, V.M., Arfanakis, K., Wendt, G.J., Turski, P.A., Moritz, C.H., Quigley, M.A., et al., (2000). Mapping functionally related regions of brain with functional connectivity MRimaging. *AJNR Am J Neuroradiol, 21,* 1636 - 1644.

Craik, F.I.M., & Bialystock, E. (2006). Cognition through the Lifespan: mechanisms of change. *Trends Cogn Sci, 10 (3),* 131 - 138.

Damoiseaux, J.S., Rombouts, S.A., Barkhof, F., Scheltens, P., Stam, C.J., Smith, S.M., & Beckmann, C.F. (2006). Consistent resting-state networks across healthy subjects. *Proc Natl Acad Sci U S A, 103 (37),* 13,848 - 13,853.

Davis S.W., Dennis, N.A., Daselaar, S. M., Fleck, M.S., & Cabeza, R. (2008). Qué PASA? The posterior-anterior shift in aging. *Cereb Cortex, 18,* 1201 - 1209.

Deco, G., Jirsa, V.K., & McIntosh, A.R. (2011). Emerging concepts for the dynamical organization of resting-state activity in the brain. *Nat Rev Neurosci, 12 (1),* 43 - 56.

De Luca, M., Beckmann, C.F., De Stefano, N., Matthews, P.M., & Smith, S.M. (2006). FMRI resting-state networks define distinct modes of long-distance interactions in the human brain. *Neuroimage, 29,* 1359 - 1367.

De Pasquale, F., Della Penna, S., Snyder, A.Z., Marzetti, L., Pizzella, V., Romani, G.L., & Corbetta, M. (2012). A cortical core for dynamic integration of functional networks in the resting human brain. *Neuron, 74*, 753 - 764.

Destrieux, C., Hommet, C., Domenige, F., Boissy, J.-M. De Marco, G., Joanette, Y., Andersson, F., et al., (2012). Influence of age on the dynamics of fMRI activations during a semantic task. J. *Neuroradiol, 39, (3),* 158 - 166.

Draganski, B., Lutti, A., & Kherif, F. (2014). Impact of brain aging and neurodegeneration on cognition: evidence from MRI. *Curr Opin Neurol, 26(6),* 640 - 645

Dosenbach, N.U.F., Fair, D.A., Miezin, F.M., Cohen, A.L., Wenger, K.K., Dosenbach, R.A.T., Fox, M.D., et al., (2007). Distinct brain networks for adaptive and stable task control in humans. *Proc Natl Acad Sci U S A, 104 (26),* 11073 - 11078.

Doucet, G., Naveau, M., Petit, L., Zago, L., Crivello, F., Jobard, G., Delcroix, N., et al., (2012). Patterns of hemodynamic low-frequency oscillations in the brain at rest are modulated by the nature of free thought during rest. *Neuroimage, 59*, 3194 - 3200.

Ekstrom, R.B., French, J.W., Harman, H., & Derman, D. (1976). Kit of factor-referenced cognitive tests (Rev. ed.). Princeton, NJ: Educational Testing Service.

Ferreira, L.K., & Busatto, G.F., (2013). Resting-state functional connectivity in normal brain aging. *Neurosci Biobehav Rev, 37 (3),* 384-400.

Ferreira, L.K., Regina, A.C., Kovacevic, N., Martin, M.D., Santos, PP, Camelo, C.G., Kerr, D.S., et al., (2015), Aging effects on whole-brain functional connectivity in adults free of cognitive and psychiatric disorders. *Cereb Cortex, [Epub ahead of print]*.

Fjell, A.M., Westlye, L.T., Amlien, I., Espeseth, T., Reinvang, I., Raz, N., Agartz, et al., (2009). High consistency of regional cortical thinning in aging across multiple samples. *Cereb Cortex, 19,* 2001 - 2012.

Fjell, A.M., McEvoy, L., Holland, D., Dale, A.M., & Walhovd, K.B., for the Alzheimer's Disease Neuroimaging Initiative. (2013). Brain changes in older adults at very low risk for Alzheimer's disease. *The J Neurosci, 39 (19),* 8237 - 8242.

Fornito, A., Harrison, B.J., Zalesky, A., & Simmons, J.S. (2012). Competitive and cooperative dynamics of large scale functional networks supporting recollection. *Proc Natl Acad Sci USA, 109,* 9673 - 9678.

Fornito, A., Zalesky, A., & Breakspear, M. (2013). Graph analysis of the human connectome: Promise, progress, & pitfalls. *Neuroimage, 80,* 426 - 444.

Fox, M.D., Snyder, A.Z., Vincent, J.L., Corbetta, M., Van Essen, D.C., & Raichle, M.E. (2005). The human brain is intrinsically organized into dynamic, anticorrelated functional networks. *Proc Natl Acad Sci USA, 102,* 10046 - 10051.

Fox, M.D., & Raichle, M.E. (2007). Spontaneous fluctuations in brain activity observed with functional magnetic resonance imaging. *Nat Rev Neurosci, 8 (9),* 700 - 711.

Fox, M.D., Zhang, D., Snyder, A.Z., & Raichle, M.E. (2009). The global signal and observed anticorrelated resting-state brain networks. J. *Neurophysiol. 101,* 3270 - 3283.

Fox, P.T, Raichle, M.E., Mintun, M.A., & Dence, C. (1988). Nonoxydative glucose consumption during focal physiologic neural activity. *Science, 241,* 462 - 464.

Fu, C.H.Y., McIntosh, A.R., Kim, J., Chau, W., Bullmore, E.T., Williams, S.C.R., Honey, G.D., et al., (2006). Modulation of effective connectivity by cognitive demand in phonological verbal fluency. *Neuroimage, 30,* 266 - 271.

Geerligs, L., Renken, R.J., Saliasi, E., Maurits, N.M., & Lorist, M.M. (2014). A brain-wide study of age-related changes in functional connectivity. *Cereb Cortex, 25,* 1987 - 1999.

Glisky, E.L. (2007) Changes in cognitive function in human cognition. in Riddle, D.R., editor. Brain Aging: Models, Methods, & Mechanisms. Boca Raton (FL): CRC Press; 2007.

Grigg, O. & Grady C.L. (2010). Task-related effects on the temporal and spatial dynamics of resting-state functional connectivity in the default network. *PlosOne, 5* (10).

Good, C.D., Johnsrude, I.S., Ashburner, J., Henson, R.N., Friston, K.J., & Frackowiak, R.S. (2001). A voxel-based morphometric study of aging in 465 normal adult human brains. *Neuroimage, 14,* 861 - 863.

Gordon, B.A., Tse, C.Y, Gratton, G., & Fabiani, M. (2014). Spread of and deactivation in the brain: does age matter. *Front Aging Neurosci, 6 (288).* 1 - 14.

Gordon, E.M., Stollstroff, M., & Vaidya, C.J. (2012). Using spatial multiple regression to identify intrinsic connectivity networks involved in working memory performance. *Hum Brain Mapp, 33,* 1536 - 1552.

Gordon, E.M., Laumann, T.O., Adeyemo, B., Huckins, J.F., & Kelley, W. (2016). Generation and evaluation of a cortical area parcellation from resting-state correlations. *Cereb Cortex, 26 (1),* 288 - 303.

Goulden, N. Khusnulina, A., Davis, N.J., Bracewell, R.M., Bokde, A.L., McNulty, J.P. & Mulllins, P.G. (2014). The salience network is responsble for switching between default mode network and central executive network: Replication from DCM. *Neuroimage, 99,* 180 - 190.

Grady, C.L., Springer, M.V., Hongwanishkul, D., McIntosh, A.R., & Wincour, G. (2006). Age-related changes in brain activity across adult lifespan. *J Cogn Neurosci, 18 (2),* 227 - 241.

Grady, C.L. (2008). Cognitive Neuroscience in aging. *Ann N Y Acad Sci, 1124,* 127 - 144.

Grady, C.L., Protzner, A.B., Kovacevic, N., Strother, S.C., Afshin-Pou, B., Wojtowicz, et al. (2010). A multivariate analysis of age-related differences in default mode and task-positive networks across multiple cognitive domains. *Cereb Cortex, 20,* 1432 - 1447.

Greicius, M.D., Krasnow, B., Reiss, A.L., & Menon, V. (2003). Functional connectivity in the resting brain: A network analysis of the default mode hypothesis. *Proc Natl Acad Sci USA, 100,* 253 - 258.

Gusnard, D.A., Akbudak, E, Shulman, G.L., & Raichle, M.E. (2001). Medial prefrontal crtex and self-referential mental activity: Relation to a default mode of brain function. *Proc Natl Acad Sci U S A, 98, 7,* 4259 - 4264.

Hedden, T. and Gabrieli, J.D.E. (2004). Insights into the aging mind: A view from cognitive neuroscience. *Nat Rev Neurosci, 5,* 87 - 96.

Hellyer, P.J., Shanahan, M., Scott, R., Wise, R.J.S., Sharp, D.J., & Leech, R. (2014). The control of global brain dynamics: Opposing actions of fronto-parietal control and default mode networks on attention. *The J. Neurosci, 34 (2),* 451 - 461.

Helstaedter, C., Lendt, M., & Lux, S. (2001). Verbaler Lern- und Merkfähigkeistest (VLMT). Göttingen: Belz Test GmBH.

Henry, J.D. & Crawford, J.R. (2004). A meta-analytic review of verbal fluency performance in patients with traumatic brain injury. *Neuropsychologia, 18 (4),* 621 - 628.

Henry, J.D., Crawford, & J.R., Phillips, L.H. (2004). Verbal fluency performance in dementia of the Alzheimer's type: a meta-analysis. *Neuropsychologia, 42 (9),* 1212 - 1222.

Hesselmann, G., Kell, C. A., Eger, E., & Kleinschmidt, A. (2008a). Spontaneous local variations in ongoing neural activity bias perceptual decisions. *Proc Natl Acad Sci USA, 105*(31), 10984 - 10989.

Hesselmann, G., Kell, C. A., & Kleinschmidt, A. (2008b). Ongoing activity fluctuations in hMT+ bias the perception of coherent visual motion. *J Neurosci, 28*(53), 14481 - 14485.

Horn, W. (1983). Leistungsprüfungssystem (2end ed.). Göttingen: Hogrefe.

Huettel, S.A., Song, A.W. & McCarthy, G. (2014). Functional magnetic resonance imaging. Sunderland, Massachusetts: Sinauer Associates.

Hutchison, M.R., Womelsdorf, T., Allen, E.A., Bandettini, P.A., Calhoun, V.D., Corbetta, M., Della Penna S., et al. (2013). Dynamic functional connectivity: Promise, issues, & interpretations. *Neuroimage, 80,* 360 - 378.

Hutchison, M.R. & Morton, J.B. (2015). Tracking the brain's functional coupling dynamics over development. *J Neurosci, 35 (17),* 6849 - 6859.

Jäncke, L., Mérillat, S., Liem, F., & Hänggi, J. (2015). Brain size, sex, ad the aging brain. *Hum Brain Mapp, 36 (1),* 150 - 169.

Jagust, W. J., (2013). Vulnerable neural systems and the borderland of brain aging and neurodegeneration. *Neuron, 77,* 219 - 234.

Jagust, W.J. & Mormino, E.C. (2011). Lifespan brain activity, β-amyloid, and Alzheimer's disease. *Trends Cogn Sci, 15 (11),* 520 - 526.

Jia, H., Hu, X., & Deshpande, G. (2014). Behavioral relevance of the dynamics of the functional brain connectome. *Brain Connect, 4 (9),* 741 - 758.

Jilka, S.R., Scott, G., Ham, T., Pickering, A., Bonelle, V., Braga, R.M., Leech, R., et al., (2014). Damage to the salience network and interaction with the default mode network. *The J Neurosci, 34 (33),* 10798 - 10807.

Jones, D.T., Prashanti, V., Murphy, M.C., Gunter, J.L., Senjem, L.M., Machulda, M.M., Przybelski, S.A., et al., (2012). Non-stationarity in the "resting brain's" modular architecture. *PlosOne, 7(6):* e39731.

Kaufman, A.S., & Horn, J.L., (1996). Age changes on tests of fluid and crystalline ability for women and men on the Kaufman Adolescent and Adult Intelligence Test (KAIT) at ages 17-94 years. *Arch Clin Neuropsychol, 11 (2),* 97 - 212.

Keilholz, S.D. (2014). The neural basis of time-varying resting-state functional connectivity. *Brain Connect, 10 (4),* 769 - 779.

Kiviniemi, V., Starck, T., Remes, J., Long, X., Nikkinen, J., Haapea, M., Veijola, J., et al., (2011). Functional Segmentation of the brain cortex using high model order group ICA. *Hum Brain Mapp, 30,* 3865 - 3886.

Kolchinsky, A., van den Heuvel, M.P., Griffa, A., Hagmann, P., Rocha, L.M., Sporns, O., & Goñi, J. (2014). Multi-scale integration and predictability in resting state brain activity. *Front in Neuroinformatics, 8, 66,* 1 - 15.

Krauth, J. (1988). Distribution-free statistics. An application-oriented approach. Amsterdam, New York, Oxford: Elsevier.

Leech, R., Braga, R., & Sharp, D.L. (2012). Echos of the brain within the posterior cingulate cortex. *The J Neurosci, 32 (1*), 215 - 222.

Li, B., Wang, X., Yao, S., Hu, D., & Friston, K. (2012). Task-dependent modulation of effective connectivity within the default mode network. *Front in Psychology,* 3 (206), 1 - 11.

Liang, X, Zou, Q., He, Y, & Yang Y. (2015). Topologically reorganized connectivity architecture of default mode, executive-control and salience networks across working memory tasks, *Cereb Cortex, 26(4),* 1501 - 1511 doi: 10.1093/cercor/bhu316.

Lindauer, U., Dirnagl, U., Füchtemeier, M., Böttinger, C., Offenhauser, N., Leithner, C., & Roy, G. (2010). Pathophysiological interference with neurovascular coupling – when imaging based on hemoglobin might go blind. *Front Neuroenergetics, 2,* (25).

Lu, H., Zou, Q., Gu, H., Raichle, M.E., Stern, E.A., & Yang, Y. (2012). Rat brains also have a default mode network, *Proc Nat Acad Sci USA, 109,* 3979 - 3984.

Luis, E.O, Arrondo, G., Vidorreta, M., Matrinez, M., Loayza, F., Fernandez-Seara, M.A., & Pastor, M.A. (2015). Successful working memory processes and cerebellum in an elderly sample: A neuropsychological and fMRI study. *PLOSone, 10 (7).*

Marsolais, Y., Perlberg, V., Benali, H., & Joanette, Y. (2014). Age-related changes in functional network connectivity associated with high levels of verbal fluency performance. *Cortex, 58,* 123 - 138.

Martuzzi, R., Ramani, R., Qiu, M., Shen, X., Papademetris, X., & Constable, R.T. (2011). A whole-brain voxel based measure of intrinsic connectivity contrast reveals local changes in tissue connectivity with anesthetic without a priori assumptions on thresholds or regions of interest. *Neuroimage*, *58*, 1044 - 1050.

McAvoy, M., Mitra, A., Coalson, R.S., d'Avossa, Keidel, J.L., Petersen, S.E., & Raichle, M.E. (2015). Unmasking language lateralization in human brain intrinsic activity. *Cereb Cortex* [Epub ahead of print].

Meinzer, M., Flaisch, T., Wilser, L., Eulitz, C., Rockstroh, B., Conway, T., Gonzalez-Rothi, L., et al., (2009). Neural signatures of semantic fluency and phonemic fluency in young and old adults. *J Cogn Neurosci, 21 (10),* 2007 - 2018.

Meinzer, M., Flaisch, T., Seeds, L., Harnish, S., Antonenko, D., Witte, V., Lindenberg, R., et al., (2012a). Same modulation but different starting points: Performance modulates age differences in inferior frontal cortex activity during word retrieval. *PlosOne, 7 (3*), e33631.

Meinzer, M., Seeds, L., Flaisch, T., Harnish, S., Cohen, M.L., McGregor, K., Conway, T., et al., (2012b). Impact of changed positive and negative task-related brain activity on word-retrieval in aging. *Neurobiol Aging, 33 (4),* 656 - 669.

Menon, V. & Uddin L.Q. (2010). Saliency, switching, attention and, control: A network model of insula function. *Brain Struct Funct, 214,* 655 - 667

Meunier, D., Achard, S., Morcom, A., & Bullmore, E. (2009). Age-related changes in modular organization of human brain functional network. *Neuroimage, 44 (3),* 715 - 723.

Miyake, A., Friedman, N.P., Emerson, M.J., Witzki, A.H., Howerter, A., & Wager, T.D. (2000). The unity and diversity of executive functions and their contributions to complex "frontal lobe" tasks: a latent variable analysis. *Cogn Psychol, 41 (1),* 49 - 100.

Moran, L.V., Tagamets, M.A. Sampath, H., O'Donnell, A., Stein, E.A., Kochunov, P., & Hong, L.E. (2013). Disruption of anterior insula modulation of large-scale brain networks in schizophrenia. *Biol Psychiatry, 774*, 467 - 474.

Morcom, A.M. & Johnson, W. (2015). Neural reorganization and compensation in aging. *J Cogn Neurosci. 27 (7),*1275 - 1285.

Murphy, K., Birn, R.M., Handwerker, D.A., Jones, T.B., & Bandettini, P.A. (2009). The impact of global signal regression on resting state correlations: are there anticorrelated networks introduced. *Neuroimage, 44,* 893 - 905.

Murphy, K., Birn, R.M., & Bandettini, P.A. (2013). Resting-state fMRI confounds and cleanup. *Neuroimage, 80,* 349-359.

Nagels, A., Kircher, T., Dietsche, B., Backes, H., Marquetand, J., & Krug, A. (2012). Neural processing of overt word generation in healthy individuals: The effect of age and word knowledge. *Neuroimage, 61,* 832 - 840.

Nyberg, L., Lövdén, M., Riklund, K., Lindenberger, U. & Bäckman. (2012). Memory, aging, and brain maintenance. *Trends Cogn Sci, 16 (5),* 292 - 305.

Onoda, K., Ishihara, M., & Yamaguchi, S. (2012). Decreased functional connectivity by aging is associated with cognitive decline. *J Cogn Neurosci*, *24*, 2186 - 2198.

Park, D.C. & Reuter-Lorenz, P.A. (2009) The adaptive brain: Aging and neurocognitive scaffolding. *Annu Rev Psychol*, *60*, 173 -196.

Pascual, B., Masdeu, J.C., Hollenbeck, M., Makris, N., Insausti, R., Ding, S., & Dickerson, B.C. (2013). Large-scale brain networks of the left temporal pole: A functional connectivity MRI study. *Cereb Cortex,* Epub ahead of print.

Patriat, R., Molloy, E.K., Meier, T.B., Kirk, G.R., Nair, V.A., Meyerand, M.E., Prabhakaran, V., et al, (2013). The effect of resting condition on resting-state reliability and consistency: a comparison between resting with eyes open, closed, and fixated. *Neuroimage, 78,* 463 - 473.

Persson, J., Sylvester, C. C., Nelson, J.K. Welsh, K. M., Jonides, J., & Reuter-Lorenz P.A. (2004). Selection requirements during verb generation: differential recruitment in older and younger adults. *Neuroimage, 23,* 1382 - 1390.

Persson, J., Lustig, C., Nelson, J.K., & Reuter-Lorenz, P.A. (2007). Age differences in Deactivation: A link to cognitive control? *J Cogn Neurosci, 19 (6),* 1021 - 1032.

Persson, J., Pudas, S., Nilsson, L.G., & Nyberg, L. (2014). Longitudinal assessment of default-mode brain function in aging. *Neurobiol Aging, 35,* 2107 - 2117.

Pessoa, L. (2014). Understanding brain networks and brain organization. *Physics of Life Reviews, 11,* 400 - 435.

Petersen, S.E. & Sporns, O. (2015). Brain networks and cognitive architectures. *Neuron, 88,* 207 - 219.

Piccoli, T., Valente, G., Linden, D.E.J., Re, M., Esposito, F., Sack, A.T., & Di Salle, F.D. (2015). The default mode network and the working memory network are not anti-correlated during all phases of a working memory task. *PLOSone, 10 (4).*

Power, J.D., Cohen, A.L., Nelson, S.M., Wig, G.S., Bares, K.A., Church, J.A., Vogel, A.C., et al, (2011). Functional network organization of the human brain. *Neuron, 72,* 665 - 678.

Power, J.D., Schlaggar, B.L., & Petersen, S.E. (2014). Studying brain organization via spontaneous fMRI signal. *Neuron, 84,* 681 - 696.

Qin, J., Chen, S.G., Hu, D., Zeng, L.L., Fan, Y.M., Chen, X.P., & Shen, H. (2015). Predicting individual brain maturity using dynamic functional connectivity. *Front Hum Neurosci, 9,* (article 418).

Raichle, M.E. (2009). A paradigm shift in functional brain imaging. *J Neurosci, 29 (41),* 12729 - 12734.

Raichle, M.E. (2010). Two views of brain function. *Trends Cogn Sci, 14 (4),* 180-190.

Raichle, M.E. (2015a). The restless brain: how intrinsic activity organizes brain function. *Phil Trans R Soc B, 370,* 20140172.

Raichle, M.E. (2015b). The brain's default mode network. *Annu Rev Neurosci, 38,* 433 - 447.

Raichle, M.E., MacLeod, A.M., Snyder, A.Z., Powers, W.J., Gusnard, D.A., & Shulman, G.L. (2001) A default mode of brain function. *Proc Natl Acad Sci U S A, 98,* 676 - 682.

Raichle M.E. & Mintun, M.A. (2006). Brain work and brain imaging. *Annu Rev Neurosci, 29,* 449 - 76.

Raz, N., Gunning, F.M., Head, D., Dupuis, J.H., McQuain, J., Briggs, S.D., Loken, et al., (1997). Selective aging of the human cerebral cortex observed in vivo: Differential vulnerability of the prefrontal grey matter. *Cereb Cortex, 7,* 268 - 282.

Raz, N., Lindenberger, U., Rodrigue, K.M., Kennedy, K.M., Head, D., Williamson, A., Dahle, C., et al., (2005). Regional brain changes in aging healthy adults: General trends, individual differences and modifiers. *Cereb Cortex, 15,* 1676 - 1689.

Reuter-Lorenz, P.A., Jonides, & J., Smith, E. (2000). Age differences in the frontal lateralization of verbal and spatial working memory revealed by PET. *J Cogn Neurosci, 12 (1),* 174 - 187.

Reuter-Lorenz, P.A. & Cappell K.A., (2008). Neurocognitive Aging and the compensation hypothesis. *Current directions in psychological science, 17,* 177 - 182.

Reuter-Lorenz, P.A. & Park D.C. (2014). How does it STAC up? Revisiting the scaffolding theory of aging and cognition. *Neuropsychol Rev, 24,* 355 - 370.

Robinson, G., Shallice, T., Bozzali, M., & Cipolotti, L. (2012). The differing roles of the frontal cortex in fluency tests. *Brain, 135,* 2202 - 2214.

Rondinoni, C, Amaro, E., Cendres, F, dos Santos, A.C., & Salmon, C.E.G. (2013). Effect of scanner acoustic background noise on strict resting-state fMRI. *Braz J Med Biol Res. 46 (4),* 359 - 367.

Rubinov, M., & Sporns, O. (2010). Complex network measures of brain connectivity: uses and interpretations. *Neuroimage, 52,* 1059 - 1069.

Rubinov, M., & Sporns, O. (2011). Weight-conserving characterization of complex functional brain networks. *Neuroimage, 56,* 2068 - 2079.

Sadaghiani, S., Hesselmann, G., Friston, K. J, & Kleinschmidt, A. (2010). The relation of ongoing brain activity, evoked neural responses, & cognition, *Frontiers in Systems Neuroscience, 4,* 1 - 14.

Sadaghiani, S. & Kleinschmidt, A. (2013). Functional interactions between intrinsic brain activity and behavior. *Neuroimage, 80,* 379 - 386.

Sadaghiani, S. & D'Esposito, M. (2014): Functional characterization of the cingulo-opercular network in maintenance of tonic alertness. *Cereb Cortex, 25 (09),* 2763 – 2773, doi: 10.1093/cercor/bhu072.

Sadaghiani, S., Poline, J.B., Kleinschmidt, A., & D'Esposito, M. (2015). Ongoing dynamics in large-scale functional connectivity predict perception. *Proc Natl Acad Sci U S A, 112 (27),* 8463 - 8468.

Sala-Llonch, R., Bartés-Faz, D., & Junqué, C. (2015). Reorganization of brain networks in aging: a review of functional connectivity studies. *Front Psychol, 5,* (article 663).

Salat, D.H., Buckner, R.L., Snyder, A.Z., Greve, D.N., Desikan, R.S.R., Busa, E., Morris, et al., (2004). Thinning of the cerebral cortex in aging. *Cereb. Cortex, 14,* 721 - 730.

Salat, D. H., Williams, V. J., Leritz, E. C., Schnyer, D. M., Rudolph, J. L., Lipsitz, L. A., & Milberg, W. P. (2012). Inter-individual variation in blood pressure is associated with regional white matter integrity in generally healthy older adults. *Neuroimage, 59(1),* 181 - 192.

Salthouse, T.A. (1996). The processing-speed theory of adult age differences in cognition. *Psychol Rev, 103 (3),* 403 - 428.

Salthouse, T.A., (2011). Neuroanatomical substrates of age-related cognition. *Pychol Bull, 137 (5),* 753 - 784.

Santarnecchi, E., Galli, G., Polizzotto, N.R., Rossi, A., & Rossi, S. (2014). Efficiency of weak connections support general cognitive functioning. *Hum Brain Mapp, 35(9),* 4566 - 4582.

Schölvinck, M.L., Leopold, D.A., Brookes, M.J., & Khader, P.H. (2013). The contribution of electrophysiology to functional connectivity mapping. *Neuroimage, 80,* 297 - 306.

Seeley, W.W., Menon, V., Schatzberg, A.F., Keller, J., Glover, G.H., Kenna, H., Reiss, A.L., et al., (2007). Dissociable intrinsic connectivity networks for salience processing and executive control, *J. Cogn Neurosci, 27 (9),* 2349 - 2356.

Seghier, M.L., Fagan, E., & Price, C.J. (2010). Functional subdivisions in the left angular gyrus where the semantic system meets and diverges from the default network. *J Cogn Neurosci, 30 (50),* 16809 - 16817.

Seghier, M.L. (2013). The angular gyrus: multiple functions and multiple subdivisions. *Neuroscientist, 19 (1),* 43 - 61.

Shao, Z, Janse, E., Viser, K., & Meyer, A.S. (2014). What do verbal fluency tasks measure? Predictors of verbal fluency performance in older adults. *Front Psychol, 5 (772).*

Shapira-Lichter, I., Oren, N., Jacob, Y., Grubberger, M., & Hendler, T. (2013). Portraying the unique contribution oft the default mode network to internally driven mnemonic processes. *Proc Natl Acad Sci U S A, 110 (13),* 4950 - 4955.

Shaw, E.E., Schultz, A.P., Sperling, R.A., & Hedden T. (2015). Functional connectivity in multiple cortical networks is associated with performance across cognitive domains in older adults. *Brain Connect, 5 (8),* 505 - 516.

Sheffield, J.M., Repovos, G., Harms, M.P., Carter, C.S., Gold, J.M., MacDonald A.W., Ragland, J.D., et al., (2015). Fronto-parietal and cingulo-opercular network integrity and cognition in health and schizophrenia, *Neuropsychologia, 73,* 82 - 93.

Shen, X., Tokoglu, F., Papademetris, X., & Constable, R.T. (2013). Groupwise whole-brain parcellation from resting-state fMRI data for network node identification. *Neuroimage, 82,* 403 - 414.

Shirer, W.R., Ryali, S., Rykhlesvskaia, E., Menon, V., & Greicius, M.D. (2012). Decoding subject-driven cognitive states with whole brain connectivity patterns. *Cereb Cortex, 22,* 158 - 165.

Shulman, G.L., Fiez, J.A., Corbetta, M., Buckner, R.L., Miezin, F.M. et al. (1997). Common blood flow changes across visual tasks: II. Decreases in cerebral cortex. *J Cogn Neurosci, 9,* 648 - 663.

Simpson, J.R., Snyder, A.Z., Gusnard, D.A., & Raichle, M.E. (2001). Emotion-induced changes in human medial prefrontal cortex: I. During cognitive task performance. *Proc Natl Acad Sci U S A, 98 (2),* 683 - 687.

Singer, T., Verhaegen, P., Ghisletta, P, Lindenberger, U., & Baltes, P. (2003). The fate of cognition in very old age: Six-year longitudinal findings in the Berlin Aging Study (BASE*). Psychology and Aging, 18 (2),* 318 - 331.

Sonnen, J.A., Sata Cruz, K., Hemmy, L.S., Woltjier, R., Leverenz, J.B., Montinez, K.S, Jack, C.R., Kaye, J., et al., (2011). Ecology of the aging human brain. *Arch Neurol, 68 (8),* 1049 - 1056.

Sowell, E.R., Peterson, B.S., Thompson, P.M., Welcome, S.E., Henkenius, A.L., & Toga, A.W. (2003). Mapping cortical change across the lifespan. *Nat Rev Neurosci, 6 (3),* 309 - 315.

Spreng, R.N., Stevens, W.D., Chamberlain, J.P., Gilmore, A.W., & Schacter, D.L. (2010a). Default network activity, coupled with the frontoparietal control network, supports goal-directed cognition. *Neuroimage, 53,* 303 - 317.

Spreng, R.N., Wojotowicz, M., & Grady, C.L. (2010b). Reliable differences in brain activity between young and old adults: A quantitative meta-analysis across multiple cognitive domains. *Neurosci Biobehav Rev, 34,* 1178 - 1194.

Sridharan, D., Levitin, D.T., & Menon, V. (2008). A critical role for the right fronto-insular cortex in switching between central-executive and default-mode networks. *Proc Natl Acad Sci U S A, 105 (43),* 12569 - 12574.

Stafford, J.M., Jarrett, B.R., Miranda-Dominguez, O., Mills, B.D., Cain, N., Mihalas, S., Lahvis, G.P., et al., (2012). Large-scale topology and the default mode network in the mouse connectome. *Proc Natl Acad Sci U S A, 111 (52),* 18745 - 18750.

Stanley, M.L., Moussa, M.N., Paolini, B.M., Lyday, R.G., Burdette, J.H., & Laurienti, P.J. (2013). Defining nodes in complex brain networks. *Frontiers in Computational Neuroscience*, 7, 169.

Steffener, J., Barulli, D., Habeck, C., & Stern, Y. (2014), Neuroimaging explanations of age-related differences in task-performance. *Front Aging Neurosci, 8* (article 48).

St John, P.D. & Montgomery, R.P. (2010). Cognitive impairment and life satisfaction in older adults. *Int J Geriatr Psyciatry, 25,* (8), 814 - 821.

Strauss, E., Sherman E.M.S., & Spreen, O. (2006). A compendium of neuropsychological tests. (3rd ed.). Oxford: Oxford University Press.

Stoodley, C.J., Valera, E.M., & Schmahmann, J.D. (2012). Functional topography f the cerebellum for motor and cognitive tasks: An fMRI study. *Neuroimage, 59,* 1560 - 1570.

Tagliazucchi, E. & Laufs, H. (2014). Decoding wakefulness levels from typical fMRI resting state data reveals reliable drifts between wakefulness and sleep. *Neuron, 82,* 695 - 708.

Tomasi D. & Volkow N.D. (2012). Aging and functional brain networks. *Mol Psychiatry, 17 (5),* 549 - 558.

Turner G.R. & Spreng R.N. (2012). Executive functions and neurocognitive aging: dissociable patterns of neural brain activity. *Neurobiol Aging, 33,* 826e1-826e13.

Tzourio-Mazoyer, N., Landeau, B., Papathanassiou, D., Crivello, F., Etard, O., Delcroix, N., Mazoyer, B. et al., (2002). Automated anatomical labelling of activations in spm using a macroscopic anatomical parcellation of the MNI MRI single subject brain. *Neuroimage, 15 (1),* 273 - 28.

Uddin, L.Q. (2015). Salience processing and insular cortical function and dysfunction. *Nature Reviews Neuroscience, 16,* 55 - 61.

United Nations, Department of Economic and Social Affairs / Population Division. (2013). World Population Ageing 2013, ST/ESA/SER.A/348, United Nations: New York.

Van Dijk, K.R.A., Heeden, T, Venkataraman, A, Evans, K.C., Lazar, S.W., & Buckner, R.L., (2010). Intrinsic functional connectivity as a tool for human connectomics; theory, properties and optimization. *J. Neurophysiol, 103,* 297 - 321.

Vincent, J.L., Patel, G.H., Fox, M.D., Snyder, A.Z., Baker, D.C., Van Essen, D.C., Zempel, J.M. et al., (2007). Intrinsic functional architecture in the anaesthetized monkey brain. *Nature, 447,* 83 – 86.

von Aster, M., Neubauer, A., & Horn, R., (2006). Wechsler Intelligenztest für Erwachsene. Göttingen: Hogrefe.

Voss, M.W., Wong, C.N., Baniqued, P.L., Burdette, J.H., Erickson, K.I., Prakash, R.S., McAuley, E. et al., (2013). Aging brain from a network science perspective: something to be positive about? *PlosOne, 8 (11),* e78345.

Weidlich, S., Lambert & G., Hartje, W. (2001). Diagnosticum für Cerebralschädigung (DCS) – ein visueller Lern- und Gedächtnistest, Bern: Verlag Hans Huber.

Whitfield-Gabrieli, S. & Nieto-Castanon, A. (2012). Conn: A functional connectivity toolbox for correlated and anticorrelated brain networks. *Brain Connect, 2 (3),* 125 - 141.

Wig, G.S., Schlaggar, B.L., & Petersen, S.E. (2011). Concepts and principles in the analysis of brain networks. *Ann N Y Acad Sci, 1224,* 126 - 146.

Yarkoni, T., Poldrack, R.A., Nichols, T.E., Van Essen, D.C., & Wager, T.D. (2011), Large-scale automated synthesis of human functional neuroimaging data. *Nature Methods, 8 (8),* 665.

Yeo, B.T., Krienen, F.M., Sepulcre, J., Sabuncu, M.R., Lashkari, D., Hollinshead, M., Roffman, et al. (2011): The organization of the human cerebral cortex estimated by intrinsic functional connectivity. *J. Neurophysiol, 106,* 1125 - 1165.

Zalesky, A., Fornito, A., & Bullmore, E.T. (2010). Network-based statistic: Identifying differences in brain networks. *Neuroimage, 53,* 1197 - 1207.

Zalesky, A., Fornito, A., & Bullmore, E., (2012). On the use of correlation as a measure of network connectivity. *Neuroimage, 60,* 2096 - 2106.

Zhang, H., Chen, W., Jiao, Y, Xu, Y, Zhang, X, & Wu, J. (2014). Selective vulnerability related to aging in large scale resting brain networks. *PlosOne,* 9 (10), e108807.

Zöllig, J., Mérillat, S., Eschen, A., Röcke, C., Martin, M., & Jäncke, L. (2011). Plasticity and imaging research in healthy aging: core ideas and profile of the international normal aging and plasticity imaging center (INAPIC), *Gerontology, 57 (2),* 190 - 192.

8 Curriculum Vitae

PERSONAL DATA

Name	Angela Martina Müller
Date of Birth	09.07.1966
Place of citizenship	Hospental (UR)

EDUCATION IN NEUROPSYCHOLOGY

2013 - 2016	Doctoral Student in Neuropsychology, University of Zurich, Switzerland, Doctoral Thesis: *„The intrinsically active baseline configuration of the aging brain and how it relates to cognition and behavior“* Thesis Advisors: Prof. Dr. Lutz Jäncke (University of Zurich) and Prof. Dr. Klaus Oberauer (University of Zurich)
2007-2012	Master in Neuropsychology (*summa cum laude*), University of Zurich, Switzerland, Master Thesis: *”Sprache und das Gehirn in Ruhe - Gibt es ein Resting State Netzwerk für Sprache im Gehirn?”* [Language in the brain at rest – does the brain have a specialized resting state network for language?] Thesis Advisor: Prof. Dr. Martin Meyer (University of Zurich)

AWARDS

2013	Semester Award of the University of Zurich for the Master Thesis *”Sprache und das Gehirn in Ruhe - Gibt es ein Resting State Netzwerk für Sprache im Gehirn*?” [Language in the brain at rest – does the brain have a specialized resting state network for language?]

PUBLICATIONS

2016	Muller A.M., Mérillat S., and Jäncke L. (2016) Older but still fluent? Insights from the intrinsically active baseline configuration of the aging brain using a data driven graph-theoretical approach, *Neuroimage,* 127, 346 – 362.
	Muller A.M., Mérillat S., and Jäncke L. Small changes but huge impact? The right anterior insula’s loss of connection strength during the transition of old to very old age (*Accepted for publication by Frontiers in Aging Neuroscience*).

Muller A.M., Mérillat S., and Jäncke L. Successful functional compensation or age-related decline - What can we learn by looking at the intrinsically active baseline of the healthy aging brain? (*Manuscript submitted for publication*)

2014 Muller A.M. and Meyer M. (2014). Language in the human brain: Beyond the specialization of the left hemisphere for language. Evidence from intrinsic connectivity fMRI based graph theoretical analyses; *Frontiers of Human Neuroscience.*

POSTER PRESENTATIONS AT SCIENTIFIC MEETINGS

2016 Muller, A.M, Mérillat, S., and Jäncke, L.: "The healthy aging brain's potential to compensate for age-related functional decline - What can we learn by looking at the intrinsically active baseline?" *The Annual Meeting of the Cognitive Neuroscience Society, 2016, New York, New York USA, April 2016.*

2015 Muller, A.M, Mérillat, S., and Jäncke, L.: "How the ageing brain performs verbal fluency: Insights from task-free fMRI based graph analyses," *The 21th Annual Meeting of the Organization of Human Brain Mapping 2015, Honolulu, Hawaii, USA, June 2015.*

Muller, A.M, Mérillat, S., and Jäncke, L.: "Successful functional compensation or age-related decline - What can we learn by looking at the functional baseline?" *The 21th Annual Meeting of the Organization of Human Brain Mapping 2015, Honolulu, Hawaii, USA, June 2015.*

Muller, A.M, Mérillat, S., and Jäncke, L.: "The Importance of Staying Connected in Old Age Insights from the resting-state network perspective of the aging brain", *LiMaDoKo 2015, University of Zurich, Switzerland, May 2015.*

2014 Muller, A.M, Mérillat, S., Hirsiger, S., and Jäncke, L.: "The association of intrinsic connectivity networks and verbal fluency performance in healthy aging adults: Preliminary results of graph theoretical analyses." *Resting state and state dependent information processing in health and disease. Monte Verità, Ascona Switzerland, October 2014.*

Muller, A.M, Mérillat, S, Hirsiger, S., and Jäncke, L.: "LHAB-Data: The association of intrinsic connectivity networks and cognitive performance in the healthy aging brain: Preliminary results of graph theoretical analyses." *INAPIC Fall Workshop, University of Zurich, September 2014.*

Muller, A.M. and Meyer, M.: "Language in the human brain: "Beyond the specialization of the left hemisphere for language." *The 20th Annual Meeting of the Organization of Human Brain Mapping 2014, Hamburg, Germany, June 2014.*

2013 Muller, A.M. and Meyer, M: "Language in the human brain: Beyond the specialization of the left hemisphere for language Evidence from intrinsic connectivity fMRI based graph theoretical analyses." *International Conference on Basic and Clinical Multimodal Imaging 2013, Geneva, Switzerland, September 2013.*

EDUCATION IN CLASSICS

2006	PhD in Classics (*magna cum laude*), University of Zurich, Switzerland, Doctoral Thesis: *„Die Selbsttötung in der lateinischen Literatur bis zum Ende des 1. Jhr. n. Chr.“* [Suicide in the latin literature of the first century A.C.] Thesis Advisor: Prof. Dr. Hermann Tränkle (University of Zurich).
1993	Master of Art in Classics and History (*magna cum laude*), University of Zurich, Switzerland, Major: Latin Literature and Linguistics, First Minor: Greek Literature and Linguistics, Second Minor: Ancient History; Master Thesis: “Seneca in den Annalen des Tacitus” [Seneca in the annals of Tacitus] Thesis Advisor: Prof. Dr. Hermann Tränkle (University of Zurich)